TENDON AUGMENTATION WITH A NOVEL BIOMIMETIC POLYDIOXANONE PATCH: AN *IN VIVO* BIOCOMPATIBILITY STUDY

A THESIS SUBMITTED TO THE
UNIVERSITY OF OXFORD

IN PARTIAL FULFULMENT OF THE REQUIRMENTS FOR THE DEGREE OF MASTER OF SCIENCE IN MUSCULOSKELETAL SCIENCES

MARK E. MORREY, M.D., M.S.

WORCESTER COLLEGE

OXFORD
2013

Acknowledgements

First, and foremost, I would like thank God for the blessings, opportunities and grace that He has given me throughout my life. Not the least of these blessings is my family to whom I owe in spades. To my parents who have never wavered in their support of any and all my endeavors and to my children who have to put up with my antics on a daily basis, yet rarely complain…I thank you. I especially want to thank my loving, caring, thoughtful, kind, intelligent, beautiful, athletic, wonderful and gracious wife. I could go on indefinitely with the adjectives I could use to describe you and what you mean to me. You are a constant source of joy in my life. I could not have written this thesis without your support and thank God daily for bringing you into my life.

I want to thank the 'team' with whom I worked so closely with this past year for all of the advice, help, fun and the adventures that we shared together. Emilie, the Sarah's, Osnat, Pierre, Nasim-Joon, Tom, Michael and the Ben's- you are my life-long friends. I have loved every minute of my time at Oxford shared with you (except for when riding home in the rain on my bike). Your dedication, passion and light-hearted attitudes are contagious and made the dismal British weather bearable… as did looking forward to Pippin's doughnuts every other Friday.

Finally, to Andy, without whom none of this would be possible, thank you. Thank you so much for giving me the opportunity to come to Oxford and research not only an important topic, but one that I believe will ultimately change the way we treat musculoskeletal disorders. Thank you for being a friend as well as a role model. I am forever in your debt.

Abstract

Tendon Augmentation with a Novel Biomimetic Polydioxanone Patch:
An *In Vivo* Biocompatibility Study

Mark Morrey — Worcester College
Master of Science — Trinity Term 2013

Introduction and Aims: There is great interest in biomimetic devices to augment tendon repairs. Ideally, implants improve healing without causing adverse local or systemic reactions. Biocompatibility remains a critical issue prior to implantation into humans, as some implants elicit a foreign body response (FBR) involving inflammation, poor wound healing and even fistulae formation. Any implant should maintain its tensile strength while tendon healing occurs. Additionally, the effect on articular cartilage locally or systemically with placement of juxta-articular implants has not been examined. The aim of this thesis is to test the *in vivo* biocompatibility and tensile strength of a novel hybrid woven and electrospun polydioxanone patch in a rat tendon transection model.

Main Study Methods: Sixty Lewis rats were divided into 4 groups in which the infraspinatus was surgically transected 3 mm from its insertion. Tendons were repaired with a laminated woven and electrospun polydioxanone patch (PDOe) and 5-0 polypropylene sutures. Polylactic-coglycolic acid (PGLA) and silk patches or a simple polypropylene suture repair served as comparators. Animals were sacrificed at 1, 2, 4, 6 and 12 weeks to examine the biocompatibility of the implants. Immunohistochemistry was used to examine macrophage subpopulations and hematoxylin and eosin staining was used to assess foreign-body giant cells (FBGC) and both analyzed with a two-way ANOVA with significance set at $p<.05$. Articular cartilage was scrutinised with semi-quantitative analysis. Hind paw inflammatory indices were used to determine the systemic effects and biomechanical testing the tensile strength of the materials over time.

Findings and Results: The PDOe patch remained grossly quiescent at all time-points. There was a severe inflammatory reaction to Vicryl at one and 2-week time-points with a massive transudate. Silk patches were associated with larger fibrous capsules at each time point. There were no adverse systemic effects and articular cartilage remained normal with no differences between materials and controls. Immunohistochemistry showed a significantly higher ratio of inflammatory macrophages to total cells for the PGLA and silk patches compared to the PDOe patch and controls at each time-point except four weeks and no difference in regenerative macrophages across all time-points. Silk and Vicryl patches had a significantly greater number of FBGC's compared to the PDOe patch and controls($p<.05$) at all time-points, again with the exception of 4 weeks, suggesting incorporation rather than rejection and walling off of the biomaterial. Tensile strength of the PDOe patch remained around 20N until 6-weeks and then gradually declined from 6 to 12-weeks.

Discussion and Conclusions:

The novel PDOe patch appears to be biocompatible and illicit very little FBR in this rat tendon injury

model. Importantly, there was no joint reaction to the biomaterial, which has not been addressed previously. The electrospun component of the patch recapitulates native tendon architecture creating a tissue healing microenvironment directed by a regenerative macrophage subpopulation. These results corroborate earlier *in vitro* work that showed incorporation of tenocyte-like cells within the electrospun scaffold. The woven component of the scaffold provides tensile strength as the tendon heals and begins to degrade after healing is underway making it less likely to elicit a FBR. Based on these and earlier *in vitro* data we believe this implant shows excellent biocompatibility and is ready to proceed to human trials.

Table of Contents

Table of Tables

Figure Table of Contents

Abbreviations:

advanced glycation end-products (AGE's),

anterior cruciate ligament (ACL)

antigen presenting cell (APC)

deoxyribonucleic acid (DNA)

electrospun polydioxanone patch (PDOe)

extra cellular matrix (ECM)

fatty infiltration (FI)

fibroblast growth factor (FGF)

foreign-body giant cells (FBGC)

foreign body response (FBR)

general practitioner (GP)

haematoxylin-eosin (H&E)

immunoglobulin (Ig)

interferon gamma IFNγ)

interleukin (IL)

macrophage (mΦ)

macrophage/granulocyte colony stimulating factor (MG-CSF)

magnetic resonance (MR)

magnetic resonance imaging (MRI)

matrix metalloproteinases (MMPs)

Osteoarthritis Research Societies' histopathology initiative (OARSI)

natural killer (NK)

range of motion (ROM)

rotator cuff (RC)

Two-way analysis of variance (ANOVA)

platelet derived growth factor (PDGF)

polycaprolactone (PCL)

polydioxanone (PDO)

polylactic-coglycolic acid (PGLA)

poly-L-lactic acid (PLA),

poly(lactic-co-glycolic acid) (PGLA)

polymicrobial associated molecular patterns (PAMPs)

reactive oxygen species (ROS)

scanning electron microscopic (SEM)

t-cell (Tc)

t-helper cell (TH)

tissue inhibitors of metalloproteinases (TIMPs)

toll-like receptor (TLR)

transforming growth factor beta (TGF-β)

tumor necrosis factor (TNF)

vascular epidermal growth factor (VEGF)

Chapter One

1. Introduction and Background

Epidemiology and Economic Costs to Society

Complaints of shoulder pain account for nearly 4.5 million visits to physicians annually in the United States[1]. The rotator cuff is a group of muscles which originate on the scapula to insert onto the bony prominences, or tuberosities, of the humerus via tendinous attachments. These muscles are responsible for dynamically holding the humeral head against its articulation on the scapula, the glenoid (Figure 1.0).

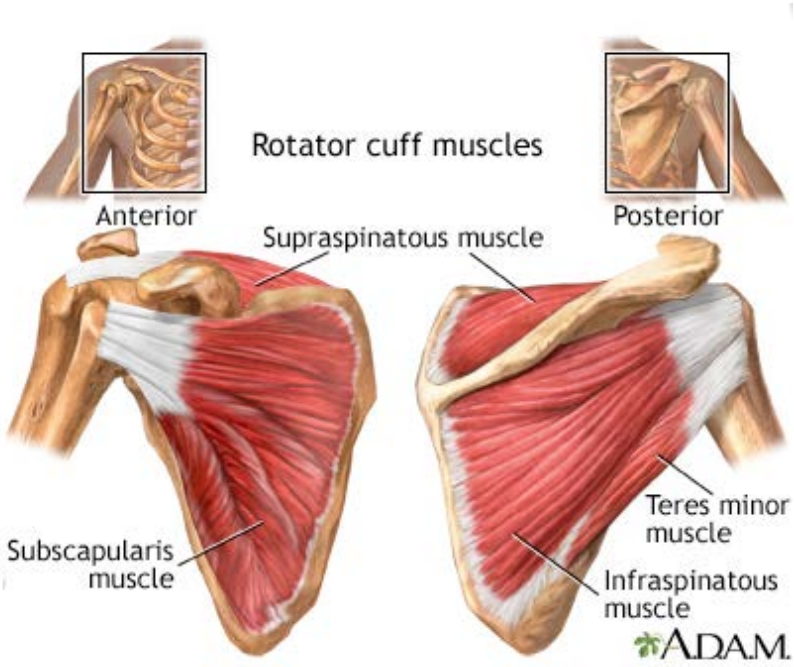

Figure 1.0 **The muscles and tendon attachments of the rotator cuff. Rotator cuff muscles include the subscapularis inserting on the lesser tuberosity of the humerus and the supraspinatus, infraspinatus and teres minor muscles which insert onto the greater tuberosity. Image from http://www.adamimages.com/**

Rotator cuff (RC) disease represents a substantial proportion of these visits and is the third most prevalent musculoskeletal disorder in the U.S. after low back and neck pain with tears

affecting nearly 50% of the population of those over the age of 50[2-4]. From these complaints nearly 300,000 surgical procedures are performed for RC pathology (tendinopathy, often referred to as impingement, and tears) of which 75,000 represent repairs of the RC annually [5,6].

Problems related to the RC are certainly not unique to the U.S. In the United Kingdom, visits to the general practitioner (GP) for shoulder pain is estimated to be 14%, with an incidence of 1–2% per year representing 2.4% of all GP visits annually[7,8]. RC tears and tendinopathy account for nearly 70% of these complaints[9]. In Japan, RC tears are also common, with a prevalence of 25% in those older than 50 in one study[10] and nearly 20% in those over 20 years of age in another[11,12].

The economic impact of managing the worldwide burden of RC pathology is substantial. In the U.S. alone it is estimated to be around $3 billion dollars annually[6]. Most of this economic drain comes from an impaired ability to work[13], however shoulder pain also prevents individuals from performing routine household tasks[14], recreational and competitive athletics[15].

Although the initial management of shoulder pain due to tendinopathy is conservative, approximately 40% will have continued pain, some of which will require surgery. Furthermore, traumatic ruptures virtually all lead to surgical repair [16,17]. RC repairs can be accomplished via open, mini-open surgeries in which a small incision is made and the repair is completed with special bone anchors or transosseous sutures which go through the tendon and then the bone. Alternatively, the procedure can be performed arthroscopically, a 'key-hole' surgery, in which a camera and surgical instruments are inserted into the shoulder through very small incisions. If this technique is chosen, bone anchors are utilised to repair the tendon to the bone. Figure 1.1

shows the different repair techniques. It is debatable whether one technique offers an advantage over the other. Furthermore, different repair strategies, anchor systems, postoperative immobilisation and rehabilitation protocols have been developed to prevent failures with mixed results[18-22].

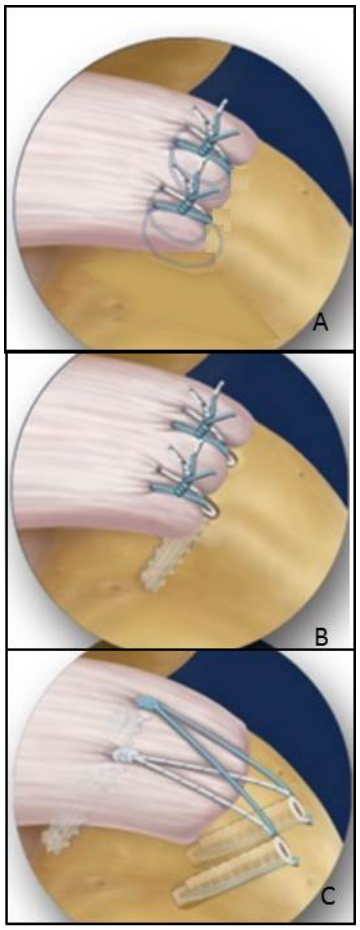

Figure 1.1 Different ways of performing RC repair. (A) A transosseous repair in which suture is passed through the tendon stump then through the bone and tied. (B) An single row anchor repair. Suture from the anchor that is placed in the bone are passed through the tendon and tied. (C) A double row repair. The medial row of anchors are used to pass suture through the tendon and are then tied down. A second laterally based anchor is used to reinforce the repair. (Image adapted from http://www.nottinghamshoulders.com/

Rotator Cuff Repair Failures

Even though the surgical management of RC tears continues to evolve and new anchors, sutures and techniques to increase repair strength have inundated orthopaedic practices, achieving a structural repair, with a demonstrably healed tendon, remains a significant problem. Despite

increasing awareness of the need to improve RC healing, the efficacy of RC repairs remains a challenge as between 20% to 94% are reported to fail[23-30]. In fact, the longer the time from operative intervention, the greater the likelihood that failure will occur. In the longest follow-up study of RC repairs to date, with a mean of 20 years follow-up, 94% had failed[30].

Reasons for Failed Cuff Repair

The reasons for failure are likely multifactorial, but several studies have shown correlations with certain parameters including tear size, patient age, tendon retraction, muscle atrophy and fatty infiltration (FI), synovial fluid infiltration at the bone tendon junction, and tissue quality both grossly and ultimately at the molecular level[31-36]. The roles of each of these in RC pathology are examined further below and highlight a very real need for increased focus on tendon biology to improve healing and reduce reruptures. Figure 1.1 gives an overview of the interactions between these factors and their relationship to the complex issue of failed RC repairs.

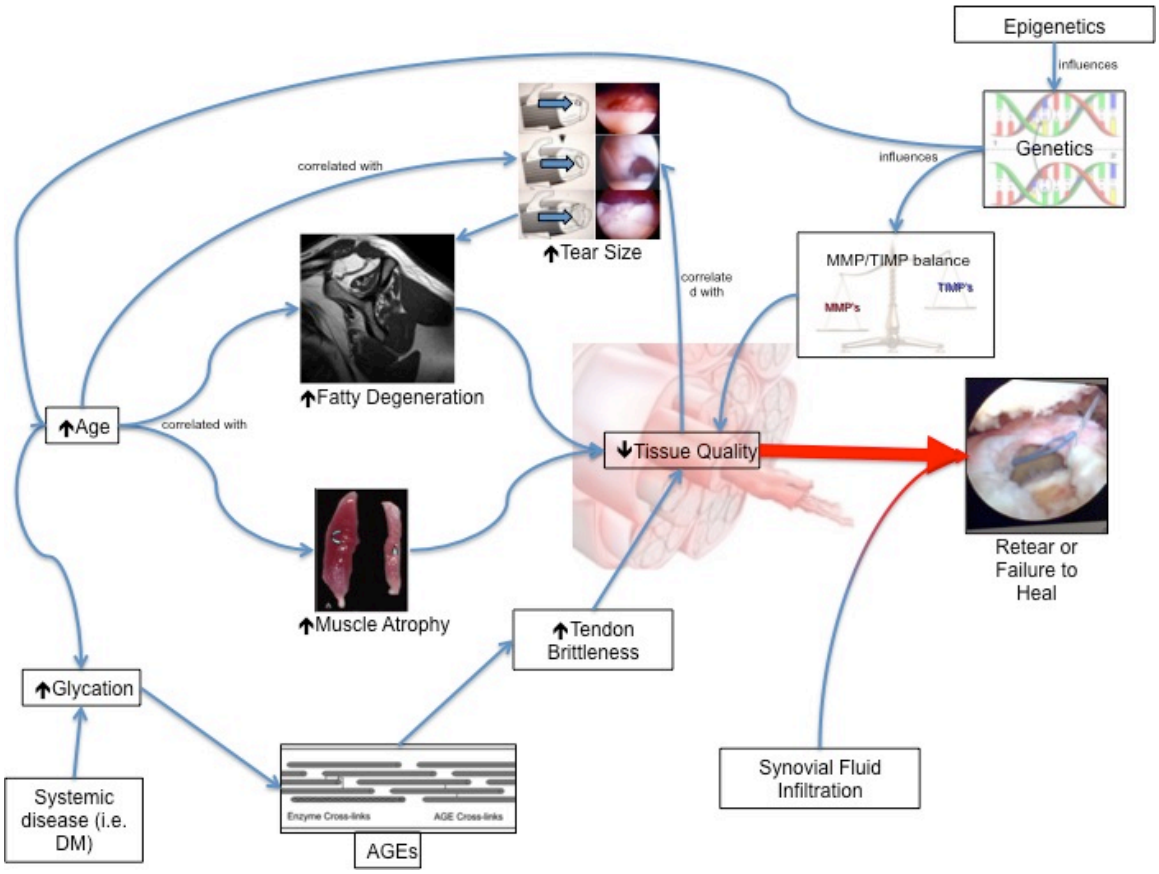

Figure 1.2 **Some of the factors affecting RC re-tears. The final common pathway leads to decreased tissue quality leading to high re-tear rates or an inability to heal repairs.**

Rotator Cuff Tear Size and Failed Repairs

Although often attempted, cuff tear size is sometimes difficult to quantify and compare between studies of RC repairs. Despite study heterogeneity, cuff tear size has been correlated with repair failures in numerous studies [24,27-29,37-49]. In contrast to large tears, good to excellent anatomic and functional results have been reported after repairing small and medium-sized full-thickness RC tears[24,25,50,51]. Furthermore, the re-tear rate is substantially lower for small and medium-sized tears when compared to large and massive tears [26,27,29,52-54]. Finally, Nho *et al*[55] were able to correlate increasing tear size with re-tear risk. These investigators found that for

every one-centimetre increase in original tear size, patients were 2.3 times more likely to re-tear. If multiple tendons were involved the odds ratio was even more dismal as re-tear risk increased 8.9 times.

Age and Rotator Cuff Tears and Repair Failures

Patient age has been positively correlated to RC tears in almost all investigations of primary tears, failures after repair and progression of tear size. It is well described that both symptomatic and asymptomatic RC tears increase with age [56-58]. In a study by Yamaguchi *et al*[59], the average age for patients with a painful unilateral partial- or full-thickness tear was 58.7 years, and it was 68.7 years for those with bilateral tears. This study also showed that patients with a painful unilateral full-thickness tear had a 35.5% prevalence of an asymptomatic tear on the contralateral side. This is significant as a proportion of individuals with asymptomatic tears do become symptomatic. Furthermore, this has been correlated to tear size progression after only short-term follow-up [60]. Finally, and significantly, higher rates of re-rupture occur with increased patient age [45]. Nho *et al*[55] also found that for every increased year of the patient's age there was an odds ratio of 1.08 for tendon defect after repair. This correlation is likely due to the underlying decrease in tendon quality as people age. As discussed below, age is positively correlated with increased advanced glycation end-products (AGE's), fatty infiltration (FI) and muscle atrophy, all of which have been independently associated with RC repair failure.

Fatty Infiltration, Muscle Atrophy and Rotator Cuff Healing

Fatty infiltration (FI), muscle atrophy and subsequent tendon retraction have also been associated with higher failure rates of RC repairs. In the first study to detail this association, Goutallier *et al*[61] found that failures were observed when muscle advancement had been

performed for atrophied muscles and retracted tendons. These authors developed a staging system for the severity of fatty change in the muscles of the RC based on CT scans which was later modified for MRI by Fuchs *et al*[62] and has become the standard means by which to assess the cuff musculature for FI (Table 1.1 and Figure 1.3).

Table 1.1

Original stages of FI by Goutallier as determined by CT scan

Goutallier Fatty Degeneration Staging
Stage 0 = completely normal muscle, without any fatty streak
Stage 1 = the muscle contains some fatty streaks
Stage 2 = the fatty infiltration is important, but there is still more muscle than fat
Stage 3 = as much fat as muscle
Stage 4 = more fat than muscle
(Goutallier D, CORR 1994;304:78)

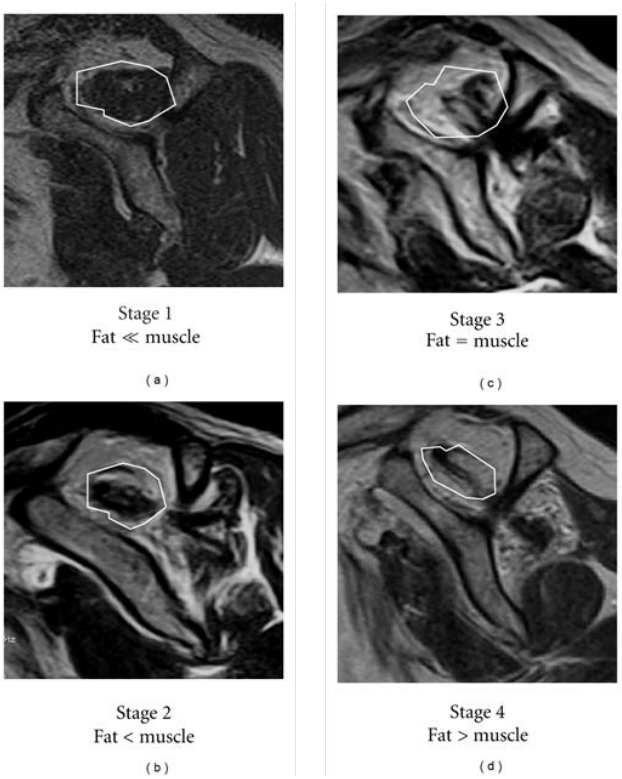

Figure 1.3 **Fuchs MRI modification to stages of FI with descriptions below each stage. Shown is the supraspinatus muscle on a sagittal oblique MRI used for staging. Stage 0 which is not shown is completely normal muscle. From reference** [63]

Significantly, the stage of FI was correlated with patients' function (as measured by ROM and strength). External rotation was the most significantly affected with fatty atrophy of the posterior portion of the supraspinatus and leading edge of the infraspinatus- a common tear pattern. The authors of this study concluded that if there was difficulty closing the defect due to significant retraction and atrophy, undue tension was placed on the repair site and it was at greater risk of failure. Because FI and retraction happen over time, authors recommended repairs of RC tendons prior to the presence of irreversible changes in the muscle. Melis *et al*[64] examined the rate of progression of FI of the infraspinatus and found that it was related to the number of tendons torn, a delay in the onset of symptoms and imaging studies and age of the

patients. Significant FI occurred 2.5 years after symptom onset and progressed to severe FI at 4 years post symptom onset. These authors also concluded that surgical repair should be done within 2.5 years after symptom onset if it is to be undertaken. Playing a significant role in the decision to operate is whether or not FI is reversible. Several studies suggest that FI is irreversible, however, operative intervention may prevent progression [65-68].

Ultimately, FI is a complex process in which the underlying biological mechanisms responsible for its etiology are unknown. Underscoring this fact is the recent finding that FI includes even untorn tendons [69,70]. Barry *et al*[70] showed that atrophy of the muscle and fatty degeneration were separate entities with different risk factors and prevalence. They showed that FI was related to increasing age, muscle tear severity, and sex, whereas muscle atrophy was only related to increasing age but not tear severity. Furthermore, even in patients without tears, FI and muscle atrophy increased independently with increasing age. It is safe to say that there is a lack of understanding of the biologic etiology of this process and more work is needed to uncover the relationship between age and the sarcopenic and fatty changes seen in RC tears.

Synovial Fluid Infiltration and Rotator Cuff Healing

In multiple preclinical studies, it has been demonstrated that synovial fluid infiltration affects the ability of the tendon to heal[34]. In anterior cruciate ligament (ACL) reconstructions of the knee, which rely on tendon to bone healing, the cytokines present and constituents of the synovial fluid, have been shown to be detrimental for tendon-to-bone healing[71,72]. It is for this reason that one of the goals of RC repair has been to create a watertight seal of the tendon to the footprint so that no synovial fluid penetrates this interface[73]J

Tissue Quality and the Underlying Molecular Changes in Rotator Cuff Pathology

Several studies have alluded to the quality of the tissue and its insufficient ability to heal quickly or normally as reasons for increased failures [55,74,75]. Nho *et al*[55] grossly described tendon tissue quality with arthroscopic or key-hole surgery. In their prospective study they were able to show that patients with thinned and difficult to mobilise tendons were 3.3 times more likely to have a defect on follow-up ultrasound with 2 year follow-up.

In the molecular realm, aberrant crosslinking with advanced glycation end-products (AGEs) has been associated with increased fibrillar stiffness, decreased tendon toughness and impaired matrix remodeling, leading to an overall decreased ability for tendons to heal and remodel[76]. It makes intuitive sense that AGEs may be partially responsible for an inferior tissue quality which predisposes patients to failure after repair. These AGEs form as collagen reacts with sugars in the process of glycation and ultimately lead to the formation of covalent bonds. The covalently bonded AGEs impair the ability for the normal enzymatic cross-links involved in fibrillogenesis[76]. Finally, AGEs can affect extra cellular matrix (ECM) interactions, which can lead to increased inflammation and poor tissue repair [77,78]. The onset of AGE cross-links is well characterised in aging and diabetes, both of which have been correlated to poor healing, increased re-tear rates and worse results after RC surgery [79,80].

Underlying molecular differences may predispose patients to tears from prior tendinopathy and weakened tissue. Although controversial, the typical proposed order of events is a tendonitis followed by tendinopathy and finally tendon failure. A lot of investigation has been done to describe the histologic changes including collagen disruption, increased ground substance, altered fibroblast (tenocyte) morphology and neovascularisation that occur in tendinopathy [81-84]. Fibrocartilaginous changes including an increased quantity of type III

collagen and glycosaminoglycan deposition further characterise the poor tendon quality in RC tears.[85] Collagen turnover is altered in these tendons, which is fueled by a disruption in the anabolic and catabolic balance between matrix metalloproteinases (MMPs), which promote collagen degradation, and tissue inhibitors of metalloproteinases (TIMPs) that inhibit it.[86]

Whether there is a 'tendonitis' or inflammatory disorder which leads to a tendinopathy and ultimate failure of the RC tendons is still highly controversial[87]. Certainly, several cytokines considered to be 'inflammatory' such as members of the interleukin family are increased in disease, but this is in contradistinction to histologic descriptions in tendinopathy in which there are reportedly a paucity of traditional inflammatory cells. Nevertheless, it has been postulated that inflammation may play a role in the evolution of tendinopathy and ultimately tendon failure [88]. Work done by Molloy *et al*[89] on a running rat supraspinatus tendinopathy model revealed upregulation of inflammatory cell receptors and immunoglobulins on microarray. In humans, Millar *et al* [90,91] examined matched intact subscapularis tendons from patients with full-thickness RC tears. Based on histologic appearance, and significantly increased levels of cytokines and apoptotic markers in these tissues, these researchers suggested it might serve as an early model for tendinopathy. Finally, human tissue biopsy samples from small RC tears, presumably tears at an earlier stage of degeneration than larger tears, showed significant inflammation with macrophages and mast cells[92].

Genetics, Host Variation and Tendon Pathology

There is little question that there is significant variation in the pathology of RC tears due to genetics. This 'host variation' was examined for the Achilles tendon by Abrahams *et al* [93] who found polymorphisms in the gene for collagen V which were independently associated with

chronic tendinopathy. Recent work by El Khoury *et al* [94] corroborated this link by showing an additional association between tendinopathy and tissue inhibitor of metalloproteinase 2 (TIMP2), which helps to regulate extracellular matrix remodeling within the tendon. Interestingly, an additional gene variant of A Disintegrin And Metalloproteinase with Thrombospondin Motifs 14 (ADAMTS14), which functions as a tendon homeostatic gene, appeared to be protective from tendinopathy.

Such links to genetics have long been suspected, particularly for tendinopathic individuals with multiple tendinopathies or ruptures. Clinicians have long since recognised the frequency with which patients with RC tendinopathy and tears also have concomitant tennis elbow or Achilles tendinopathy. Jarvinen *et al* [95] found that there was a 41% chance of developing a contralateral Achilles tendinopathy within an 8-year period if one side was affected. As genome wide association and epigenetic studies become increasingly available, it is possible that structural changes in the tendon may be due to changes in gene expression or cellular phenotype, caused by mechanisms in the underlying DNA sequence or in DNA methylation and histone modification. A number of recent studies have highlighted a link between epigenetics and wound healing [96]. Because failed RC repairs are an expression of failed wound healing, it is entirely reasonable to suggest that an epigenetic mechanism may at least partially be the cause of these failures.

Rotator Cuff Failures and Clinical Outcomes- Is There a Link?

There is some debate as to whether or not RC re-tears are associated with worse clinical results. While Knudsen *et al*[97] found no correlation between tendon integrity on postoperative MR images and functional outcome, other evidence favors improved function

with intact repairs. Harryman *et al*[29] and Thomazeau *et al*[53] showed that the clinical results of shoulders with a structurally successful repair were superior to those with RC re-tears. However these authors and Galatz[26] also found that pain was improved whether the repair remained intact or was associated with a re-tear. Gerber *et al*[28] reported improved shoulder function after surgery as compared with preoperative function, but importantly there was less improvement in patients with re-tear compared with those who had successful repair. Finally, in the longest follow up studies in the literature, and contrary to earlier reports on pain improvement, re-tears have been shown to correlate with decreased function in measures of strength and ROM[30,98].

Biologic Solutions to Rotator Cuff Repair

With such high failure rates, and the possibility that these failures are associated with increased morbidity, it is imperative that solutions to this complex disorder are sought. As alluded to earlier, one avenue that may offer, not only insight into the disorder, but novel solutions, is the study of the biology associated with normal tendon, tendon healing and the regenerative potential of damaged tissue. As the burden of evidence reveals poor quality scar tissue is laid down in an attempt at tendon repair, it seems intuitive that instead of a failure of technology, the reason most RC repairs break down is a <u>failure of biology</u>. Surgeons can tie tendons down with any of the 'latest and greatest' tools and techniques, but these will not ensure the tendon will heal to the bone. This situation is analogous to planting a garden. The gardener can have the newest rakes, tillers, spades and even automated seed planters, but without the right seeds, soil and time-of-year, the plants will not grow. It may not matter how many sutures, or in what configuration the surgeon places them in the tendon, if the tendon biology is not restored, the repair will fail.

As discussed earlier, disordered healing occurs after ruptures. Abnormal cells, which are morphologically distinct from normal tenocytes, display chondroid metaplasia with round cells resembling chondrocytes rather than the long thin tenocytes of normal tendon (Figure 1.4).

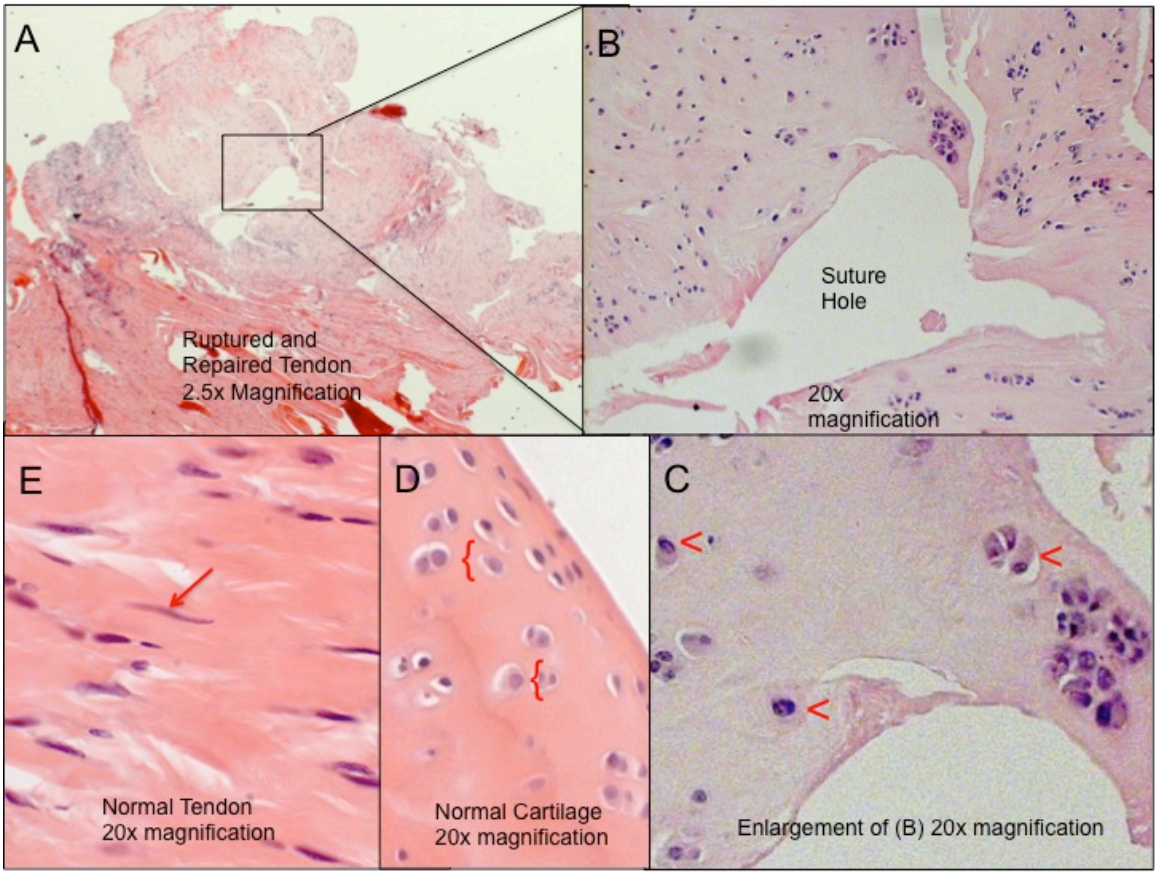

Figure 1.4 **Comparison of normal tenocyte morphology to damaged rat tendon displaying chondroid metaplasia. (A) 2.5x magnification of damaged and repaired tendon. Note the suture hole and orientation for (B) and (C) which reveals cells with chondrocyte morphology (<) compared to normal cartilage cells ({) in (D) and tenocytes (red ←) in (E). Cells with chondroid metaplasia occur in areas without mechanical tension or architectural cues for differentiation toward a tenocytic phenotype.**

Why should this be the case? One possibility is that these changes may be the result of cells lacking normal mechanical or architectural cues from the surrounding environment- they lack the right soil. Cells therefore do not display tenocytic phenotype, and instead of assuming the characteristic elongated shape and function, change as a result of the altered environment.

Several investigators have demonstrated the role of mechanical loading in this environment, which activates mechanotransduction and stimulates tenocyte/fibroblast density and differentiation[99-103]. In addition to load, micro-environmental cues, such as shape, size and orientation have also been shown to play a role in differentiation of cells around implants, as well as the acceptance of the implant by the host[100]. If failed biology is the critical factor behind failed repairs, regenerative strategies must capitalise upon, optimise and be able to deliver enhanced biology to healing tendons.

Engineered tissue scaffolds have the potential to not only provide the correct micro-environment, but can also be vehicles of delivery for critical factors needed to restore the natural biology and promote healing of RC tendons. The next section will examine the development and biocompatibility of biomaterials, and specifically tendon scaffolds, to aid tendon healing.

Chapter 2

2. Tendon Scaffolds and Biocompatibility

The Development of Tissue Engineered Tendon Scaffolds

As basic science research has informed our understanding of the changes in diseased tissue, an effort to develop scaffolds to supply these cues to fibroblasts has progressed. Biomaterials have been sought which not only strengthen tendon repair but also, importantly, give the correct signals to the healing tendon; they offer the right soil. It is hoped that these cues will improve the biology and help cells to assume a more tenocyte-like phenotype and consequently develop into a competent scar tissue, which more faithfully recapitulates normal tendon. Recently there has been an explosion in the use of biosynthetic devices to augment tendon repair. In fact, tissue engineering and polymer scaffold research publications have increased over 800% in the last 10 years (PubMed search 'tissue engineering' and 'polymer' and 'scaffolds' Figure 2.1).

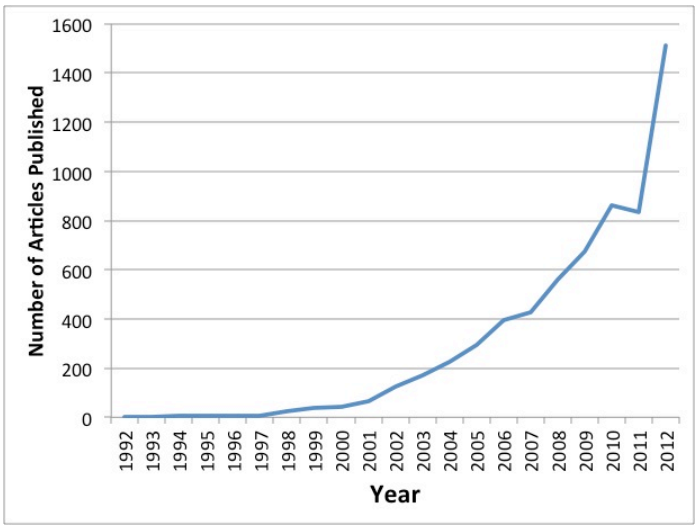

Figure 2.1 **Number of publications on tissue engineering and scaffolds from 1992 through 2012.**

Scaffolds play an essential role in tissue engineering, by providing a substrate for cells to migrate into, attach, differentiate and proliferate (Figure 2.2).

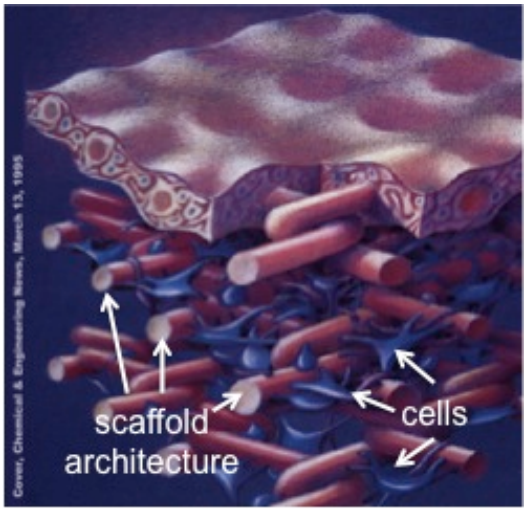

Figure 2.2 **Scaffold architecture allows for cell ingrowth, differentiation and proliferation depending on the type of tissue to be engineered (Image adapted from http://www.quora.com/Bioengineering/What-is-the-scope-of-bioengineering).**

To improve tendon healing, scaffolds must have the right architecture and chemistry that preferentially attracts the purported repair cells, fibroblasts, and allows them to assume the correct morphology of normal tenocytes. Furthermore, scaffolds must have the strength to withstand the mechanical stresses that the tendon undergoes during healing [104]. For degradable implants this means that the scaffold degradation rate should complement the wound repair rate and the regenerate tissue which is left behind assumes the proper orientation and morphology of normal tendon [105] (Figure 2.3).

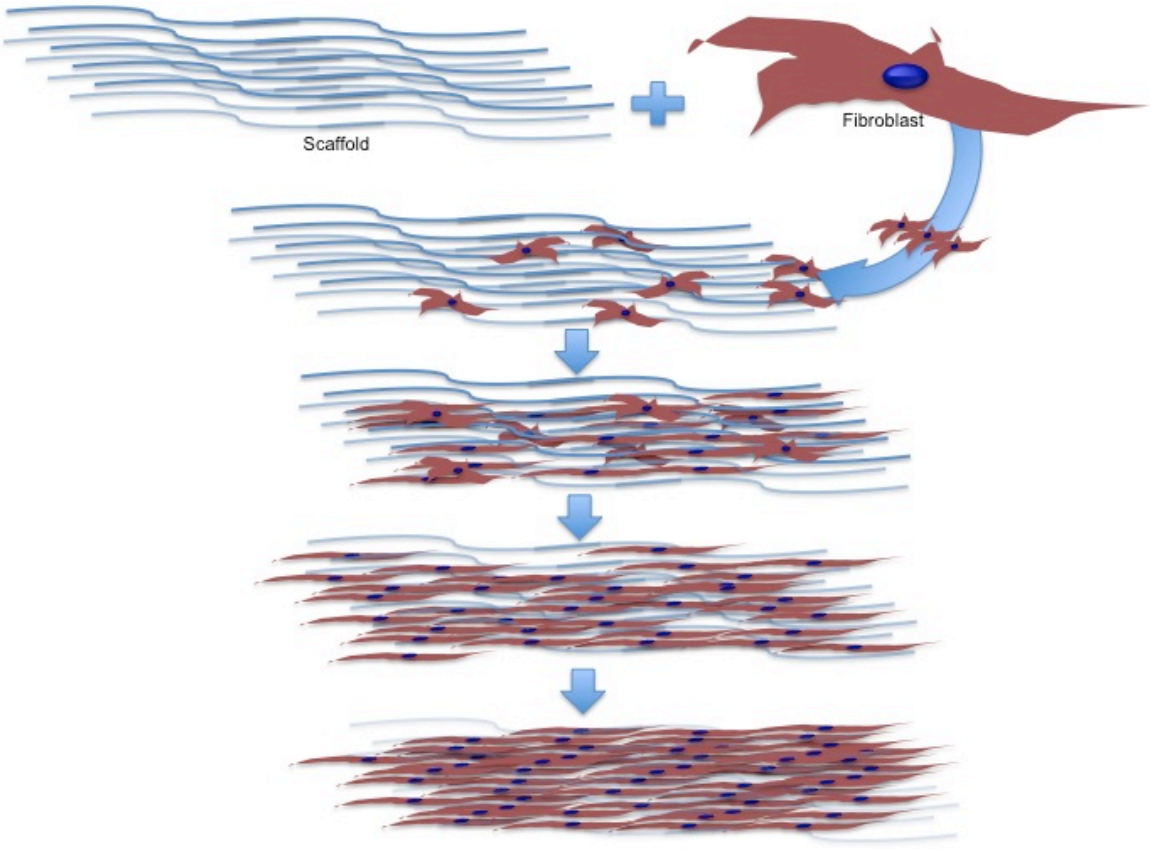

Figure 2.3 **A schematic representation of scaffold degradation and repair. Cells migrate into the scaffold, attracted by the orientation and chemical composition of the fibres. Cells progressively and preferentially differentiate toward the desired phenotype while the scaffold degrades leaving behind only regenerated tissue in the correct orientation and morphology of a normal tendon.**

Electrospinning of Scaffolds

There are multiple methods of fabricating scaffolds including bioprinting, template synthesis, phase separation, drawing, self-assembly, and electrospinning among others [106,107]. Electrospinning utilises a voltage gradient between a polymer solution and collector to create a variety of micro- and nano-scaled fibres from natural or synthetic polymers[108-114](Figure 2.4).

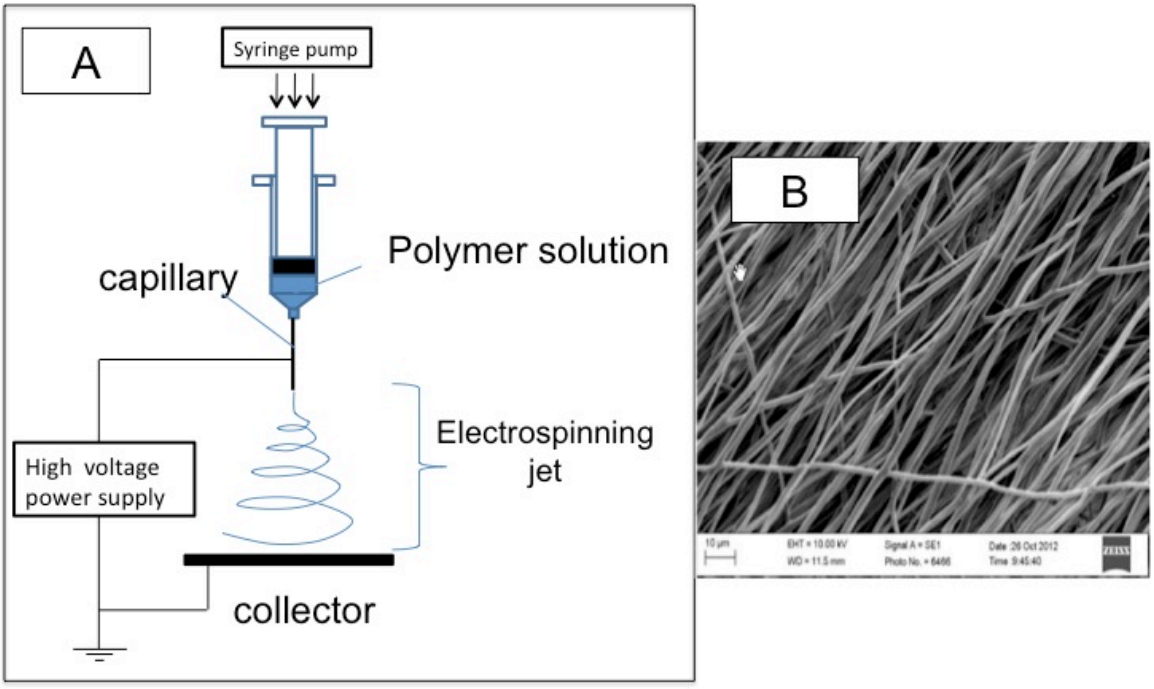

Figure 2.4 **Electrospinning diagram. (A) A melted or liquid solution of natural or synthetic polymers is placed in a syringe and forced through a capillary nozzle where the micro or nano-scaled fibres are gathered on a charged collector plate. (B) Representative example of the scale and orientation of fibres that can be assembled with electrospinning. Scale bar in the bottom left hand corner is 10µm. (Electrospinning diagram and image courtesy of Pierre-Alexis Mouthuy)**

The ability to control fibre size, morphology, and alignment pattern makes electrospinning an attractive method for the fabrication of scaffolds [115,116]. Because of these properties, electrospinning has been utilised in a wide range of tissue engineering applications for the musculoskeletal system including skin[117,118], nerve[119], muscle[112], bone[120], ligament[121] and tendon[115,116,122].

For tendon regeneration, these implants are commonly referred to as patches and provide for the possibility of augmentation of the repair while imparting strength and directing the course of healing of the damaged tissues (Figure 2.5).

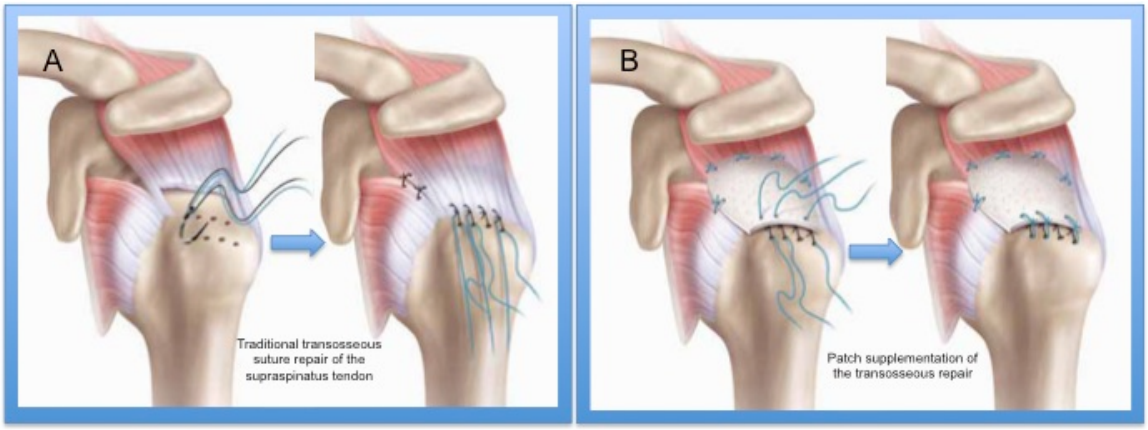

Figure 2.5 **Engineered tendon patch repair diagram. (A) Traditional transosseous suture repair of the supraspinatus. (B) The same repair augmented with a tendon patch (Image adapted from http://www.atlasklinik.de/stuttztg_061011.html).**

Natural and synthetic, degradable and non-degradable polymers have all been proposed as patches to repair tendons. All natural polymers, such as collagen, alginate, and chitosan eventually degrade and have been investigated for use in tendon repair with varying success[123-125]. However, greater interest in synthetics has developed due to their superior mechanical properties, consistency and availability. Unfortunately, because they are non-degradable, synthetics, such as polypropylene mesh, polytetrafluoroethylene (PTFE) or poly(ethylene terephthalate), can harbor infection and elicit an ongoing foreign body response (FBR) which may diminish their effectiveness in the long-term[126-128]. Degradable synthetic polymers such as poly-L-lactic acid (PLA), poly(lactic-co-glycolic acid) (PGLA), polycaprolactone (PCL) and polydioxanone (PDO) among others, may offer a better solution by combining sound mechanical properties while minimising the risk of infection or tissue reaction by resorbing

over time. For these reasons, synthetic degradable polymers are often considered favorable scaffolds for tendon repair.

Biocompatibility of Implants

Despite the promise that degradable scaffolds can minimise potential risks to humans, the critical issue that remains is safety, or biocompatibility. Biocompatibility is defined as the following:

"the ability of a biomaterial to perform its desired function with respect to a medical therapy, without eliciting any undesirable local or systemic effects in the recipient or beneficiary of that therapy, but generating the most appropriate beneficial cellular or tissue response in that specific situation, and optimising the clinically relevant performance of that therapy"[129].

Several factors have been shown to affect an implant's biocompatibility. These include size, shape, porosity, chemical composition and its constituent degradation products, and all of these factors may affect implant integration or rejection.

Polymer Size

The size of the fibres of the scaffold affects both performance and biocompatibility. Nanofibres, such as those produced from electrospinning, are of particular interest, as they can be used for directing cell adhesion, proliferation and differentiation [115,130]. Recently, Saino *et al* [115] showed that the size of the fibre was correlated to one important aspect of biocompatibility- the inflammatory foreign body response (FBR). They found that smaller diameter fibres in electrospun scaffolds resulted in a fewer number of activated macrophages and foreign body giant cells (FBGCs). This corroborated earlier work on fibre size being an important factor in the FBR [131,132].

Implant Shape

Implant topography can also affect the integration or rejection by the host. Nanofibres created by electrospinning or bioprinting are able to mimic the structure and biology of the extracellular matrix (ECM) and they have been shown to exhibit excellent cellular response and biocompatibility[107]. *In vitro* evaluation has demonstrated that electrospun materials are likely to cause a lower immune response than sheets or films of the same materials [115].

Scaffold Porosity

Biocompatibility and cell ingrowth can also be greatly affected by the porosity of the material [107,133]. Work by multiple researchers utilising porous scaffolds has shown that micro-porous structures in the 30-40 micron range have excellent biocompatibility. Furthermore, these researchers suggest that perhaps the pore size may be a definitive factor driving a 'regenerative' macrophage subtype. They were consistently able to show that at the 30-40 micron range there was rich macrophage infiltration followed by normal and robust healing[107].

Chemical Composition

Finally, chemical constituents and more importantly their degradation products can have an effect on biocompatibility. Hakimi *et al*[134] showed that there was differential growth on sutures of various chemical compositions. These investigators hypothesised that the acidic nature of some rapidly absorbable sutures are toxic to cells *in vitro*. Furthermore, one commonly used agent, polylactic-coglycide acid (PGLA) has also been shown to have significant inflammatory responses and FBRs to the breakdown products of bioabsorbable screws, anchors and other fracture fixation implants [135,136].

Reactions to Implanted Biologic Materials

It is well known that biologic implants can elicit a FBR that involves inflammatory cells which has a characteristic pattern over time[137]. This FBR can cause problems with wound healing and wound contracture to varying degrees depending on the material used and the host's immune response to non-host constituents of the implanted material. For example, clinical studies utilising porcine intestinal submucosal collagen scaffolds have reported reactions resembling infection [138,139]. Clinically these implants have resulted in hallmarks of inflammation including swelling, pain and even fistula formation[140].

Vroman Effect

The ability for inflammatory cells, whether neutrophils or macrophages, to adhere to and interact with the surface of an implanted material and to elicit an inflammatory or healing response is dependent on which proteins have adsorbed to an implant. Protein adsorption is dependent on the 'Vroman effect', or local proteins' mobility and affinity for the implant. Certain proteins have a high mobility and concentrations and low affinity to the implant and will attach quickly at the outset of implantation. Later the higher affinity proteins will replace the initial higher mobility proteins. The types of proteins that adsorb to the material affect which cells will be attracted, and have the ability to bind, and survive, which consequently affects the biocompatibility of the implant (Figure 2.6)[141-143].

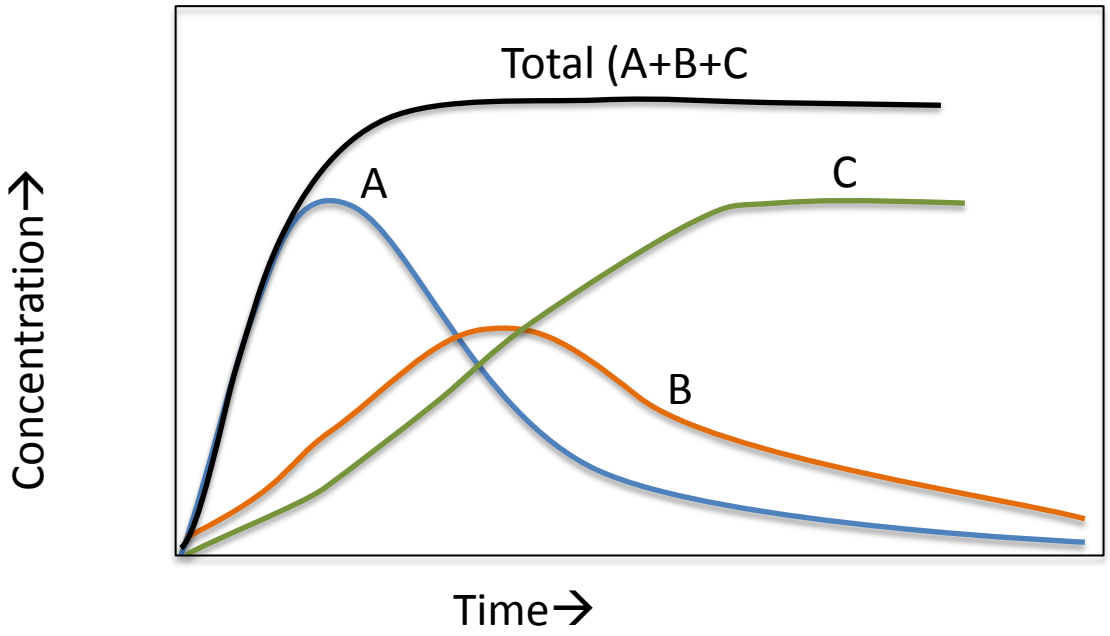

Figure 2.6 **Graphical representation of the Vroman effect. Lines A, B and C represent different proteins which adsorb to a biomaterials surface. While protein A has the highest mobility for the material and adsorbs quickly, protein B is in the middle and protein C has the highest affinity and ultimately replaces A and B on the surface. A proteins' mobility and concentration determine the overall adsorption kinetics (Image created from sources [141,142,144]).**

An example of this occurs with orthopaedic implants that require osteoblastic spreading. This phenomenon is dependent upon macrophages binding to vitronectin and fibronectin at the interfaces between the implant and the host. If conditions aren't right, and the requisite proteins are not bound to the surface of the implant, an inflammatory FBR ensues, highlighting the importance of the local environment to implant biocompatibility[145].

Macrophages in the FBR

As discussed above, the immune response to biomaterials is based upon the interaction of the cells with adsorbed proteins on its surface. Both innate and acquired immune responses can be activated with concomitant production of cytokines and chemokines from effector cells, which determine how the organism responds to the biomaterial [107,146,147]. While neutrophils

predominate early, and may result in reactions resembling acute infection and rejection of implants, macrophages are increasingly recognised as key effector cells mediating the response to biomaterials occurring weeks, months and years after implantation[148].

The FBR to biomaterials plays a major role in wound healing and tissue regeneration. Clearance of wound debris, release of matrix metalloproteinases (MMP's-important for tissue remodeling), cytokines, chemokines and growth factors (which induce migration and proliferation of fibroblasts and other cells) are signaled by macrophages which are the crucial directors of tissue regeneration[149]. These different functions are governed by different subpopulations, referred to as M1 (classically activated) and M2 (alternatively activated) macrophages [150]. Although it is likely more complex than these simple designations, based on their principal functions, these subpopulations have been further subdivided into classically activated, regulatory, and wound-healing macrophages based upon their roles in host defense, immunoregulation and tissue repair respectively (Figure 2.7)[151].

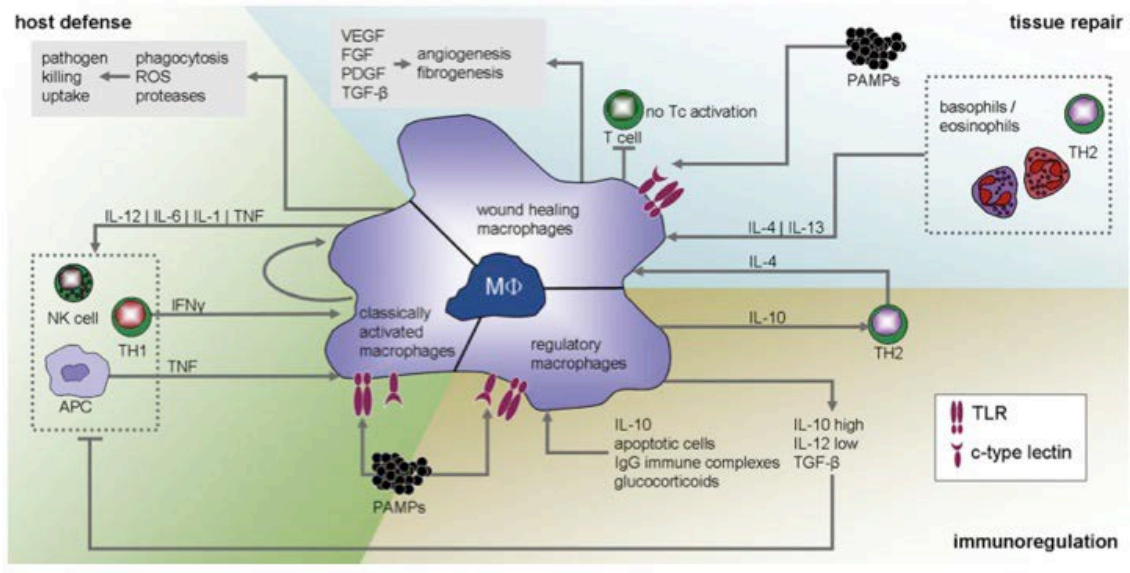

Figure 2.7 **Macrophage subpopulations. Macrophage heterogeneity and plasticity allows them to exert a number of effects and functions based on environmental cues which drives differentiation into different subpopulations. (ROS= reactive oxygen species; VEGF=vascular epidermal growth factor; FGF=fibroblast growth factor; PDGF=platelet derived growth factor; TGF-β= transforming growth factor beta; TNF=tumor necrosis factor; IFNγ=interferon gamma; APC = antigen presenting cell; PAMPs= polymicrobial associated molecular patterns; TH= t-helper cell; Tc=t-cell; NK=natural killer; IL=interleukin; Ig=immunoglobulin; TLR= toll-like receptor; mΦ=macrophage) (Image from reference[152] Franz *et al*.)**

In general, M1 cells have decreased phagocytic capability and secrete pro-inflammatory cytokines, such as IL-1, IL-6, IL-12, IL-23 and TNF[153]. They also have anti-proliferative functions, and induce the T-helper subpopulation TH1 responses [154]. M2 macrophages, by contrast, are important in tissue remodeling after inflammation [155]. Macrophages can be stimulated to release a host of cytokines, including interleukins (IL), interferons (IFN), and tumor necrosis factor alpha (TNF-α), which in turn mediate other processes, including chemotaxis and cell activation, tissue repair, and angiogenesis[156].

It has been demonstrated that when monocytes bind to, and interact with, different biomaterial surface architectures their differentiation into the various macrophage subpopulations is affected. Ultimately, the type of macrophage subpopulation that

predominates determines whether a material will be accepted or rejected by the host. [115,155]. This phenotypic heterogeneity in macrophage subpopulations explains, in part, the varying responses to biomaterials. In other words, the macrophage has been implicated as the director of the FBR and a critical determinant of implant acceptance or rejection (Figure 2.8)[152].

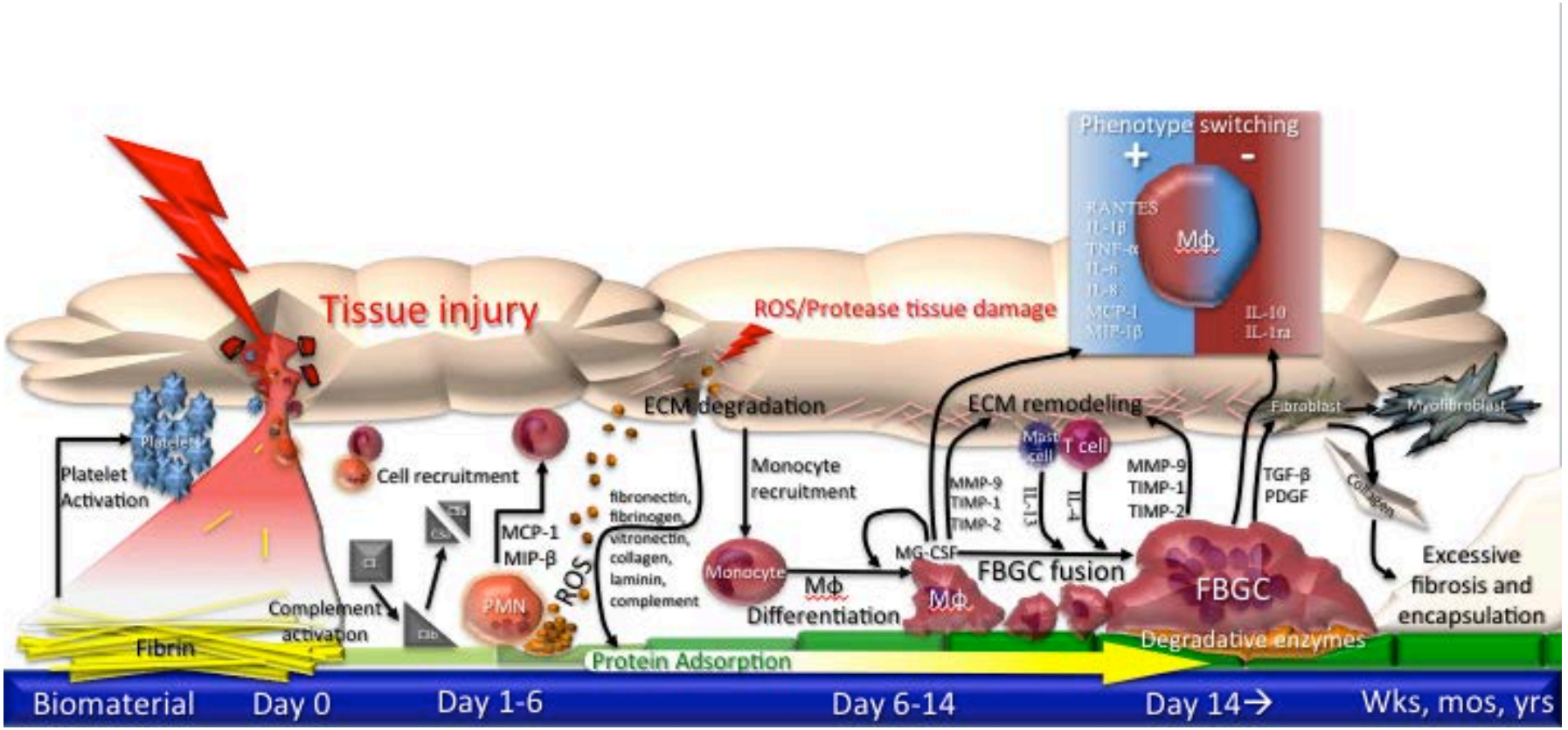

Figure 2.8 **Characteristic response to a biomaterial adapted from references[146,152,157]. On day 0, tissue injury allows blood products including platelets, blood proteins and white blood cells to enter the area of injury. The first protein to adhere is fibrin after cleavage from its blood protein form fibrinogen. Fibrin activates platelets which release products for chemotaxis and cleavage of complement. One complement product binds to the surface of the implant and the others recruit cells including PMN's and monocytes to the site. PMN's bind to the proteins which have already been adsorbed to the surface of the biomaterial and release cytokines MCP-1 and MIP-B which recruit monocytes, and ROS, which start a non-specific degradation of surface proteins, biomaterial, and ECM. The ECM degradation leads to release of other proteins which adsorb to the surface of the biomaterial and are chemotactic for monocytes. Monocytes entering the injury zone from days 1-6, adhere and differentiate into macrophages which release a host of cytokines and direct the response to the biomaterial. As time goes on the macrophages and other cells signal the fusion of macrophages into FBGC's via IL-4, IL-13 and MG-CSF. FBGC's also release degradative enzymes and a host of other cytokines including IL-10, IL-1B which feedback to other macrophages to inactivate and suppress the response and MMP-9, TGF-B which signal fibroblasts to activate and differentiate into myofibroblasts, both of which can contribute to excessive fibrosis, scarring and implant failure or rejection.**

Foreign Body Giant Cells and the Foreign Body Response

One of the possible consequences of macrophage interaction with biomaterials is fusion to form foreign body giant cells (FBGC). Formation of these cells is the hallmark of the FBR. The number or density of these cells within and around implants is typically used to determine the severity of the reaction to the biomaterial [146]. The fusion of macrophages into FBGC's is stimulated by cytokines such as IL-4 and IL-13 released from TH2-cells and mast cells and INF-gamma plus IL-3 or macrophage/granulocyte colony stimulating factor (MG-CSF) released from antigen presenting cells (APCs), macrophages, mast cells and TH1 cells [158]. Interestingly specific FBGC subtypes are formed based on the predominant stimulus (Figure 2.9).

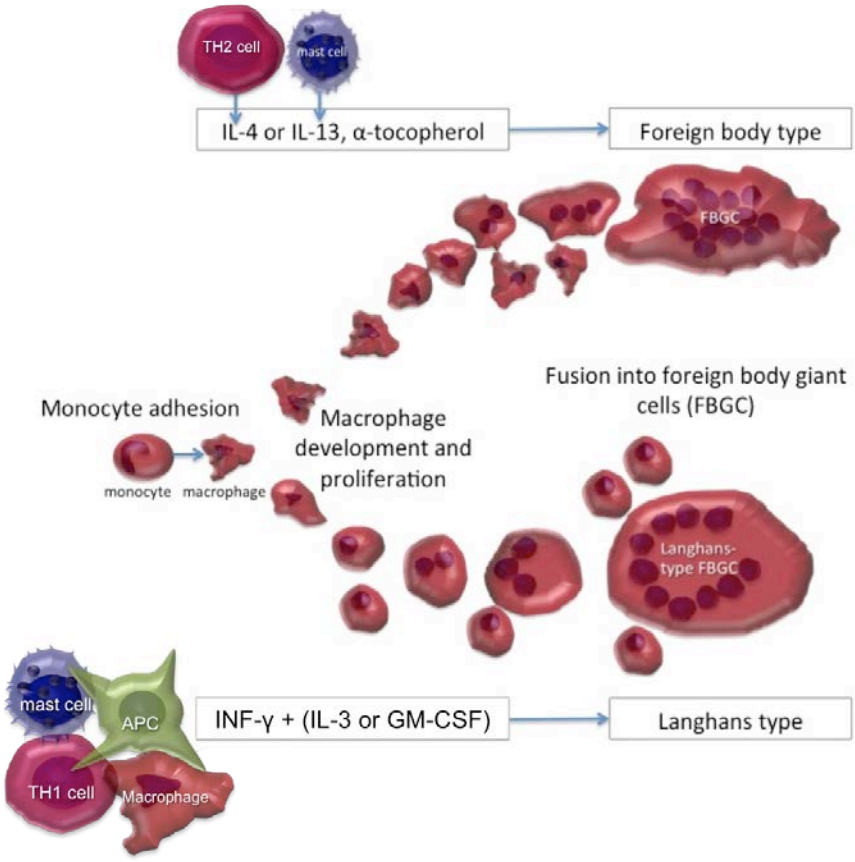

Figure 2.9 **The development of different foreign body giant cell (FBGC) types is based on different growth factors and cytokines released from different cell types which have responded to the biomaterial in different ways. The significance of the differences is not yet appreciated but the surface topography of the implanted material likely plays a role. Image modified and adapted from reference [158].**

Similar to the different macrophage subtype activation based on surface type, topography and constituents, recent studies have suggested that FBGC fusion and formation may also differ according to surface roughness, geometry and size. Particularly interesting are two studies by Sanders *et al*. [131,132] and studies by Garg [159], and Saino [115] which have demonstrated a dependence of the macrophage response to the diameter and pore size of fibrous implants. Therefore, the surface of the biomaterial in question plays a role in whether or not fusion to FBGC's occurs and the subsequent intensity of the FBR.

Animal Models for Biocompatibility

To determine the biocompatibility of implants in humans necessarily requires an intermediate study in lower species for safety reasons. Recent articles by Seok *et al* [160] and van der Worp *et al* [161] highlight the unique problem of applying findings in animal models to human clinical pathologies. It is well known that commonly used animal models heal more robustly than humans, making one-to-one correlations of treatment efficacy difficult [162]. The time scale of healing, for instance may be altered in different mammalian species as Ni *et al* [163] have pointed out in their recent review of stem cell viability over time in a rat patellar tendon injury model. Nevertheless, prior to using these treatments in humans it is prudent to test the safety and perhaps limited elements of efficacy and mechanisms of repair to help inform the human condition.

Unfortunately, the current guidelines on biocompatibility studies are vague and offer little concrete guidance. The ISO or International Organisation for Standardisation is a worldwide federation of national standards who have attempted to develop standards for such testing called the ISO 10993 [164]. The work of preparing Standards is normally carried out through ISO

technical committees, of which, part six is the most applicable to the testing of local reactions to implantable materials. ISO10993-6 covers the majority of orthopaedic implants including tendon augmentation scaffolds or patches. This standard outlines the species to be tested, appropriate controls and the types of biocompatibility testing that may be performed. For example, studies must have an inert negative control implant such as polypropylene, polyethylene or stainless steel for comparison. In addition, in some cases where a class of materials is expected to show a reaction, such as a polyester graft or patch that may cause significant FBR, it is advisable to implant an additional reference material to serve as another control. Unfortunately, most current biocompatibility studies fail to use such controls when reporting biocompatibility data.

Despite the best intentions of the standards, there are limitations with regards to the protocols designed for local implantation. In the case of tendon patches, implants are placed in a juxta-articular position that may have potential ramifications for the joint. Unfortunately, the current standards do not take this into account and instead recommend that devices be placed in the paravertebral muscles rather than the anatomic location in which they will be used.

For the practicing orthopaedic surgeon, this translates into the question of whether or not such devices affect the joint surfaces when implants are placed near the articular surface as in RC tears. This question is of utmost importance when determining safety of the implant, as adjuvant induced arthritis models have been shown to have innate and humoral responses to foreign materials[165]. Therefore, biocompatibility studies evaluating juxta-articular implants should be placed in their intended anatomic locations to test whether or not any adverse

reactions to the articular cartilage occur. This necessity has been highlighted by recent failures in metal on metal hip implants where a proportion of patients have exhibited exuberant immune and tumor-like responses[166].

Another significant problem with the standards is that the animals that are recommended for this testing are White New Zealand Rabbits, which are genetically heterogeneous. The choice of this species allows too much variability when trying to draw firm conclusions on whether an implant is biocompatible. As Festing [167] has pointed out, effective animal models, "should be sensitive to the experimental treatments by responding well, with minimal variation among subjects treated alike. Uncontrolled variation, whether caused by infection, genetics, or environmental or age heterogeneity, reduces the power of an experiment to detect treatment effects." In other words, isogenic strains should be utilised for biocompatibility testing because they are more uniform than outbred stocks. A recent review of animal testing reveals that this has not been the case and many studies purporting to be testing biocompatibility have actually used Sprague Dawley or Wistar rats[168]. The genetic differences between individual animals within these groups are considerable and are inappropriate for biocompatibility testing [167].

Finally, many studies that claim to be studies of biocompatibility, have used only a limited number of histological evaluation parameters or purely *in vitro* tests to determine whether or not an implant is biocompatible. Aurora *et al*[169] used only one animal at each time-point for their biocompatibility studies. Zhou *et al*.[170] and Zhou *et al* [118] used *in vitro* designs to test biocompatibility of electrospun polymers on the differentiation of bladder endothelium and wound healing dressings respectively with cytotoxicity studies. While some aspects of the

response can be measured, the full reaction can only be done in an *in vivo* system such as an animal model due to the vast interconnections with multiple components of the innate and acquired immune systems[171].

One Approach to Biocompatibility and Efficacy

We have recently designed a novel polydioxanone (PDO) monofilament patch [116]. The patch consists of an electrospun and a woven component laminated in a proprietary way to one another creating a scaffold with an electrospun component on one side (PDOe) (Figure 2.10).

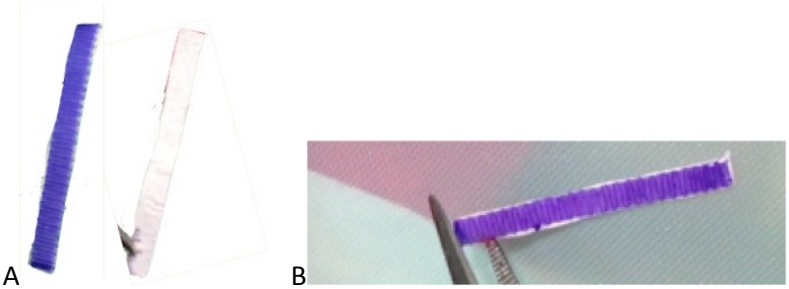

Figure 2.10 **Woven and electrospun components of the PDOe patch are laminated (A) to create a single patch construct (B).**

This patch has shown very favorable design qualities in that it has the ability to support tenocyte and stem cell proliferation on the electrospun component and recapitulate the crimp of normal tendon in *in vitro* experiments (Figure 2.11).

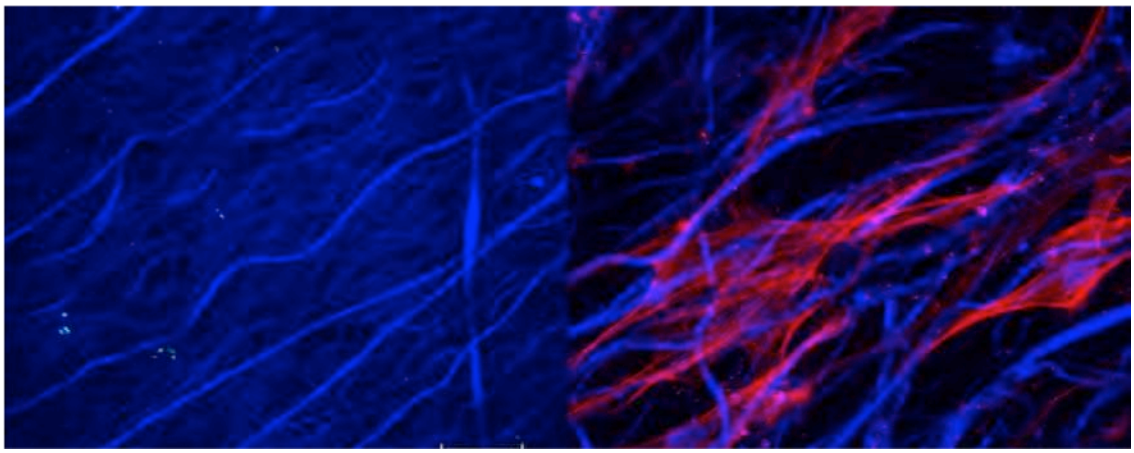

Figure 2.11 **Left panel shows electrospun components in the characteristic crimp and aligned orientation of normal tendon fibrils while the right panel shows the cell ingrowth (red fluorescence) (Image courtesy of Clarence Yapp and Osnat Hakimi).**

Importantly, tests have indicated that it is non-toxic to cells even after long periods *in vitro* [116]. Furthermore, the woven component of the patch has shown excellent ex-vivo degradation and strength characteristics, which should provide sufficient tensile strength to the repair while the tendon regenerates. The patch is flexible and has the ability to hold sutures. Finally as a degradable implant, any FBR is finite and as long as there is no large-scale acute inflammatory reaction, the patch should be relatively biocompatible.

Questions, purpose and hypotheses

Key questions remain prior to implantation in humans. One is whether or not this novel PDOe patch elicits any immune FBR which would preclude its use in humans. Secondly, are there other adverse effects to the joint or surrounding tissue which would make implantation unsafe? Thirdly, does the patch provide for, and maintain, adequate strength *in vivo* while the tissue heals before degradation? Such work, as discussed above, necessarily involves an intermediary such as an animal model in order to carry out *in vivo* biocompatibility testing. Therefore, the purpose of this thesis was to test the biocompatibility and biomechanical

characteristics of the PDOe patch in an *in vivo* model. As such, the hypotheses tested in this thesis were threefold:

1) That the novel woven and electrospun laminated PDO patch (PDOe) would be biocompatible and show little FBR.

2) The patch would not induce a systemic or local inflammatory arthropathy and

3) The patch would maintain tensile strength in the critical first 6 weeks of healing, in order to mechanically support neo-tissue formation prior to complete degradation.

Chapter Three

3. Experimental Design, Materials and Methods

In Vivo experimental design

The ethics review, animal care committee, and the UK Home Office approved the animal experiments. A randomised, block, factorial design was used to determine the biologic response to an infraspinatus tendon transection repaired with three different materials (PDO, PGLA and Silk patches) and a control repair with polypropylene (Prolene® Ethicon USA) suture at 5 different time points (1, 2, 4, 6 and 12 weeks post injury- Table 3.1). Time-points were chosen based on a typical inflammatory, regenerative and remodeling response to traumatic injury in addition to the adverse reactions to prior rotator cuff implants[139,148].

Table 3.1

***In Vivo* design- Randomised, block, and factorial design.**

Time-points represent separate blocks and repair patch constructs different experimental treatment conditions. The proposed number of animals sacrificed in each patch group and time-point is depicted in each cell. Two animals in the 12-week group were sacrificed early during at the outset of the project due to surgical complications, leaving only two animals in the PGLA and Silk groups after randomisation.

	Repair Constructs			
	Control Polypropylene	PDOe	Silk	PGLA
Time points	n=15	n=15	n=15	n=15
1 week	3	3	3	3
2 week	3	3	3	3
4 week	3	3	3	3
6 week	3	3	3	3
12 week	3	3	3	3

This design structure was chosen to increase the precision of the experiment while reducing the number of animals utilised in this experiment[167,168,171-177]. The negative control was chosen

because of its previously documented and relatively inert foreign body biological response to polypropylene suture [178,179]. The positive controls of silk and PGLA were also chosen for their known inflammatory reactions. We assumed there would be a difference in the degree of inflammatory cell response based on this prior work[134].

Blocking was employed as the logistics of operating on sixty animals in the same session was unreasonable, and this technique would help to reduce unwanted variation due to time and operational conditions when performing the procedure on different days[167]. Therefore, twelve animals per session were allocated for the surgery. Animals were physically randomised by blindly drawing numbers out of a box at the time of the surgery to receive one of three implants or control surgery without an implant.

A factorial component to the design was used to test the two independent variables of implants and time of termination to the dependent variable, or biologic response, to the implants. Factorial design was utilised as this experiment consists of two factors (implant material and time), each with discrete possible values (histologic response in number of foreign body and inflammatory cells), and because these experimental units take on all possible combinations of these levels across all factors. This experiment allowed us to study the effect of each factor on the response variable, as well as the effects of interactions between factors on the response variable allowing statistical comparisons. Therefore, this design allows for a much more powerful assessment of the interaction of these factors and reduces the number of animals without decreasing the power.[175,180]. The biologic response was measured as described below and consisted of quantitative counts of foreign body giant

cells (FBGC's) and macrophage subpopulation ratios treated as continuous rather than discrete variables.

Finally a sample size calculation was completed using the resource equation of Mead which revealed 3 animals per group would be a sufficient number to allow analysis with a two-way ANOVA[167] (Equation 1).

$$E = N-T-B$$

Equation 1: The resource equation. E is the error degrees of freedom, N is the number of animals-1, T is the number of treatment combinations-1 and B is the number of blocks-1 (In our experiment N=59, T=19 and B=4 which gives 59-19-4=36).

Normally, this calculation would have allowed for further reduction of animals to 2 per group. However, because the treatment effect size was unknown, this was the first time this protocol was used and the study complex, with analysis of both treatment and time on biologic response, an additional animal per group was chosen to ensure data analysis would be possible.

It could be argued that when studying the effects of an implant on biologic response, implantation of the material itself without injury to the tendon may be enough to measure a response with less pain to the animals. This was considered in the design of the experiment. However, for several reasons, the transection model was selected over implantation alone. First, the clinical situation in which these implants are placed necessarily involves disruption and debridement of the tendon in order to effect a repair. Therefore, we felt the original model would provide a more representative picture of the processes involved in the FBGC response as the role of inflammation due to surgical insult would be minimal in a purely subcutaneous location. Finally, these implants are placed on RC tendons that have direct

communication with the joint. To allow exposure of the underlying joint to the material, the tendon must be cut. This gives the most faithful representation of the clinical situation encountered in humans.

Animals

Sixty white female LEW/SsNHsd strain isogenic rats aged 10 weeks and weighing between 170 and 180 grams were used for the *in vivo* animal studies (weights taken immediately before surgery). Female animals were chosen for practical reasons given their lower cost and docility. Animals were obtained from Harlan UK and were kept four rats to a cage in isolation cages (as opposed to open to air) to avoid any contamination from others, which might increase variation and confound results (Figure 3.1).

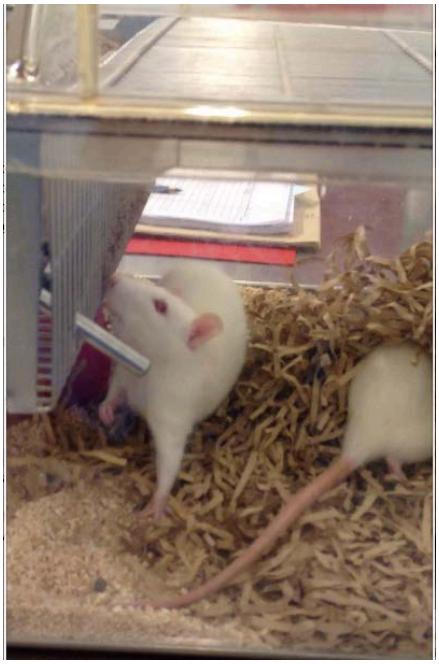

Figure 3.1 **Typical animal housing in an isolation cage with ad libitum food and water and sterile bedding.**

Bedding was Eco-pure chips 1-2.8 mm premium wood granules and was changed daily by a single technician who was also responsible for feeding the animals. Animals were given sterile

feed (SDS rm3 cubed diet with 22% protein irradiated at 25 kGy) and water ad libitum at all times prior to and after surgical procedures. The animals were housed with a 12-hour alternating light and dark cycle in a temperature and humidity controlled room (19-23°c and humidity 55% plus or minus 10%) throughout the experiment. Animals were certified to be free from infection upon arrival according to FELASA guidelines and showed no signs of infection locally or systemically throughout the *in vivo* experimentation. The animals were acclimated for one week prior to any surgical intervention.

The LEW/SsNHsd animals were specifically chosen for several reasons. First, the rat is thought to have an immune system that is highly responsive to antigens and is used for many immunologic studies [181-183]. Furthermore, this strain of rat is a commonly used animal to study RC healing[184] and tissue response to biomaterials [185,186]. Importantly, the LEW rat has been used in models of inflammatory arthropathy as it has a predisposition to developing joint changes after injections of adjuvants[187]. It was felt this unique property of the LEW rat would provide a high level of confidence that there would not be an unwanted response in humans if there were NO joint reactions to the materials implanted juxtaposed to the joint in rats. Finally, while other studies of biocompatibility have used Sprague-Dawley or Wistar rats, the genetic differences between individual animals within these groups introduce significant variability and the use of these animals requires greater numbers of animals to be utilised, may miss smaller treatment effects, and is inappropriate for biocompatibility testing[167]. In contrast, the isogenic strain of this LEW animal allows for more control of the variation and indirectly allows for a reduction in the number of animals.

Surgery

The surgical procedure was completed on greater than 30 cadaveric animals prior to operations on live animals to minimise the learning curve and any suffering to the animals. Both rats and mice were utilised in the training to provide an even greater degree of facility with the size of the tissues prior to any live surgeries. One complete surgery was performed on a cadaver and live animal in the presence of a veterinarian to further ensure proficiency with the surgical procedure and ensure animal safety. All surgical procedures were performed by one fully trained orthopaedic surgeon (MEM).

Animals were premedicated with .05mg/Kg Buprenorphine subcutaneously for analgesia both pre- and post-operatively which was re-dosed every 6-12 hours as needed for pain. Non-steroidal anti-inflammatory drugs (NSAIDs) were not used, as inflammatory markers were key endpoints in this experiment. Animals were monitored for temperature, pain and respiration rate throughout the procedure.

Surgical Procedure and postoperative protocol.

Animals were induced with 5% Isoflurane in an anesthetic box with a 5L/minute flow rate of oxygen. The animal was immediately weighed and a pre-surgical dose of the long-acting analgesic Buprenorphine (.01mg/Kg) was given subcutaneously in the scruff of the neck [Buprenorphine/Vetergesic .3mg/ml diluted 1:30 in sterile saline to give .01 mg/ml of solution. Formula Calculation = .01mg/kg * (x kg) divided by the concentration of the drug (mg/ml)]. The fur overlying the right shoulder surgical site was then shaved and the animal given 8 mg/Kg subcutaneous injection of 0.25% Bupivacaine for local analgesia in the area of the planned incision [Formula calculation = (8 mg/Kg x wght of animal in Kg)/2.5 mg/ml)]. The animal was then immediately placed on a nose cone in the left lateral decubitus position for

operation on the right shoulder, lacrilube placed in the eyes to prevent drying, temperature probe inserted rectally and the animal secured with flexible Coban©(3M United Kingdom) for the procedure (Figure 3.2).

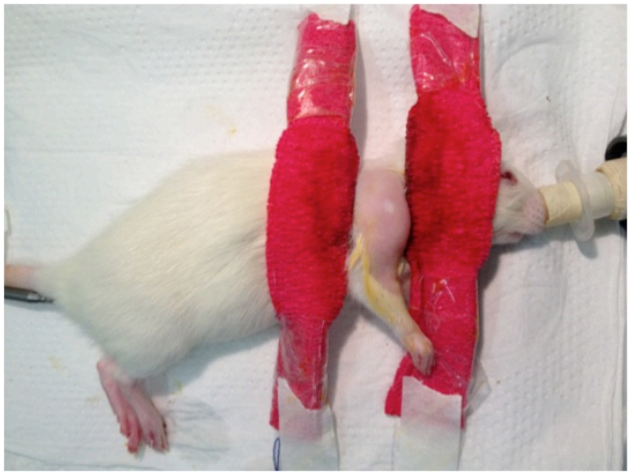

Figure 3.2 **Animal prepped for surgery. Right shoulder is shaved and animal secured with Coban to the operating table to allow exposure to the shoulder.**

Anaesthesia was maintained at 1.5%-2% Isoflurane with an oxygen flow rate of 1L/minute for the duration of the procedure. For skin preparation, the right shoulder was cleansed with 80% alcohol followed by Betadine and then completed with a second alcohol wash. The right forepaw was covered with sterile Coban wrap and the animal draped sterilely. A 1-2 cm incision was centered over the spine of the scapula and carried from the medial border of the scapula out to the acromion laterally (Figure 3.3).

Figure 3.3 **Incision centered over the spine of the scapula exposing the underlying musculature. The raphe between the posterior deltoid and trapezius is just visible.**

After blunt dissection, the underlying shoulder musculature was exposed. This dissection exposed the spine of the scapula and the fascial raphe between the scapular portion of the deltoid and the trapezius (Figure 3.4).

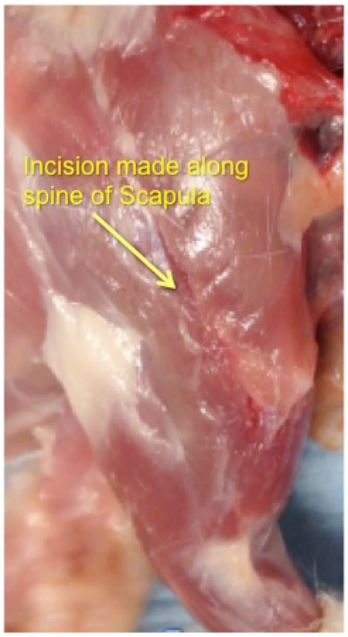

Figure 3.4 **Cadaver dissection of the incision made in the spinal raphe between the trapezius and the posterior part of the deltoid.**

This raphe was incised along the length of scapular spine to the acromion taking care to stay below the spine and above the infraspinatus tendon. The infraspinatus tendon was then exposed out to its insertion to the humerus by releasing the posterior deltoid from the acromion, which allowed visualisation of the entire infraspinatus tendon. Patches were then sutured to the distal insertion of the tendon with 5-0 polypropylene (Prolene™ Ethicon Blue Ash OH, USA) sutures. After control of the distal portion of the tendon was achieved, the tendon was then transected 3 mm from the insertion over the glenohumeral joint exposing the joint (Figure 3.5).

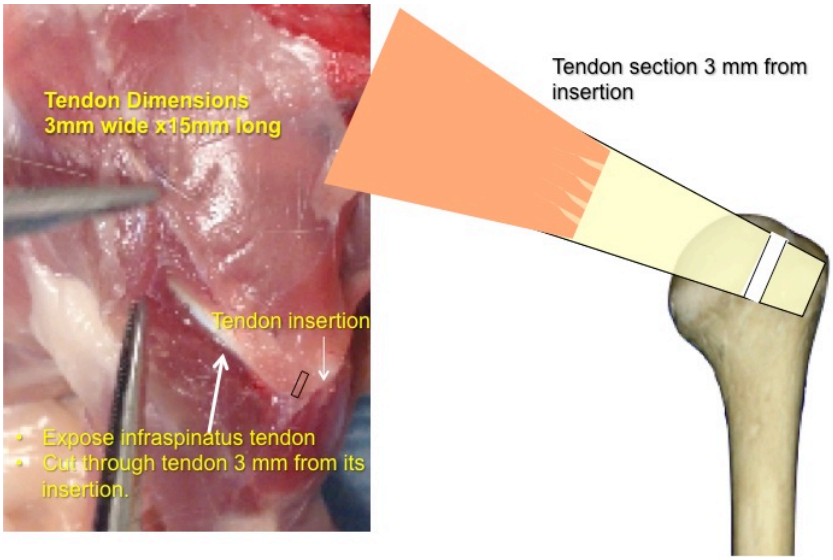

Figure 3.5 **Exposure of the infraspinatus tendon and transection of the tendon. Approximate location of the transection overlying the joint is marked with a rectangular box and shown to the right in the illustration. Key anatomic relationships and tendon dimensions are labeled.**

The proximal end of the tendon was then repaired with repair patches with a modified Mason Allen stitch with 5-0 polypropylene sutures maintaining a 3 mm gap between tendon ends (Figure 3.6).

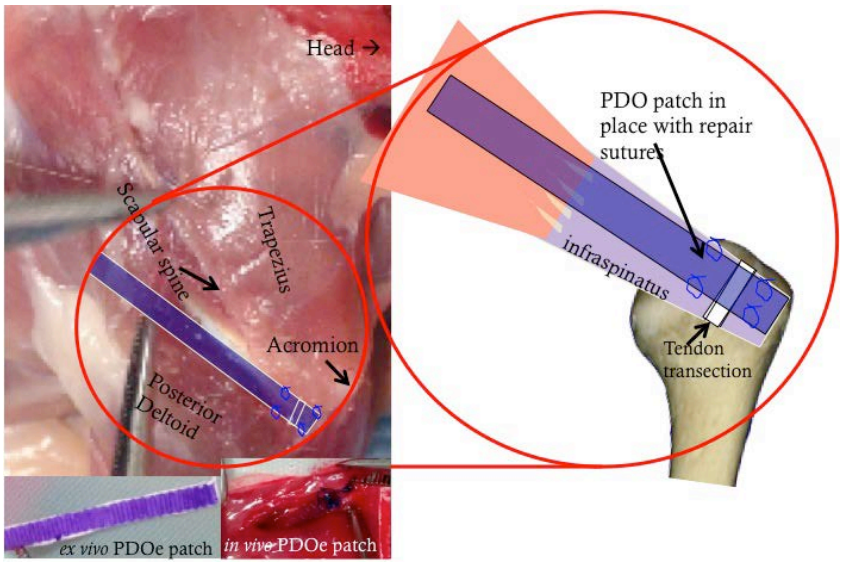

Figure 3.6 **Surgical procedure for patch placement. After the tendon was transected 3 mm from its insertion into the humerus over the joint, the repair patches (in this case the PDOe patch) were placed over the defects and sutured in place with polypropylene sutures. Insets in the bottom of the photo illustrate the PDOe patch and show its *in vivo* position once the repair has been completed.**

The remainder of the PDOe or other patches were placed overlying the muscular portion of the infraspinatus. The deltoid was closed over the patch and sewed back to the upper trapezius with 5-0 Prolene sutures completely covering the patch. The skin was closed with 5-0 Prolene and the animal was taken off anesthesia and placed on 2 L of oxygen per minute until recovery. The animal was then transferred to a warming box and then a housing cage when fully recovered and allowed to feed ad libitum. Sutures were removed on postoperative day 10.

Assessment of the Biocompatibility of PDOe

For the *in vivo* biocompatibility experiment, the PDOe patch was compared to a non-dyed silk and multifilament Vicryl® (polygalactin 910, a particular formulation of PGLA; made by Ethicon a subsidiary of Johnson & Johnson) suture (positive controls) hand woven with a plain weave configuration in the same way as the PDOe patch, but without electrospun

components (Figure 3.7). The patch design of the PDOe is proprietary but utilises a 7-0 plain weave configuration that is then laminated with an aligned electrospun component.

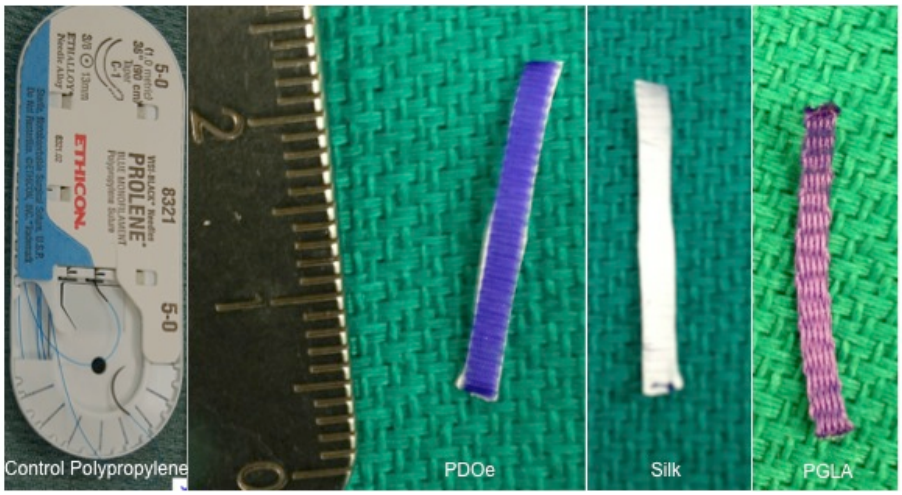

Figure 3.7 **Control suture and the three patches utilised in the thesis. Patches were woven to dimensions of 2mm wide x 2cm long in a plain weave configuration.**

Patches were 2 mm wide by 2 cm long. Simple suture repairs with non-absorbable monofilament Prolene sutures and modified Mason-Allen stitches served as negative controls. This suture material has been shown to be biologically inert [178,179]. The number of animals and time-points for sacrifice for each patch material and controls are depicted in Table 3.1 above.

Sterilisation of the patch material

Sterilisation procedures were carried out in a sterile hood. Sterile molecular grade ethanol (Sigma-Aldrich Co. LLC.) was filtered through a 20-micron filter. This sterile wash was then used to aliquot 10 ml into sterile test tubes with the patches. These were then agitated and ethanol washes changed every 10 minutes. This was repeated six times over one hour, after which patches were placed in sterile 5-mL tubes in a drying chamber for 24 hours until completely dry and prepared for implantation.

Animal Sacrifice

Animals were sacrificed according to Home Office regulations with a rising concentration of carbon dioxide in a clean euthanasia chamber. Animals' hind limbs were photographed immediately after sacrifice to determine hind paw inflammatory responses with a scoring system[188] as compared to 1-week suture removal pictures (Figure 3.8) and Table 3.2.

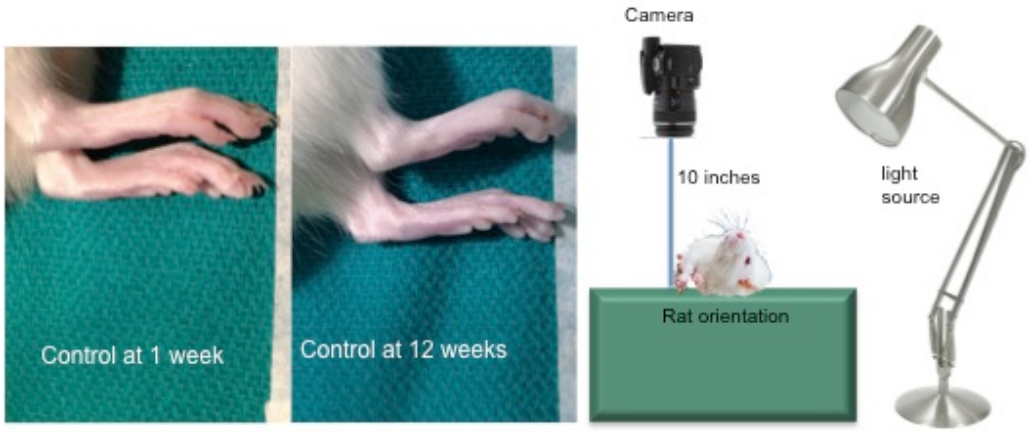

Figure 3.8 **Animal photographs for hind paw indices. The camera is placed in the same orientation and same distance with a consistent light source for photographic comparison between one and 12-week time points.**

Table 3.2

Inflammatory index scoring system from [188].

Score	Severity of induced arthritis
0	No arthritis
1	Swelling and/or redness of one to two interphalangeal (IP) joints
2	Involvement of three to four IP joints or 1larger joint
3	More than four joints are red/swollen
4	Severe arthritis of an entire paw

Animal photographs were taken in a standardised manner (Figure 3.8). The light source was placed 18 inches behind and 18 inches above the animals and photography source was 12 inches above the animals to allow for comparisons. After sacrifice the rats were immediately taken to a clean work surface for dissection of the shoulder tendons and bone (Figure 3.9).

Figure 3.9 **Dissection area, instruments and arrangement. Tissue was immediately placed in labeled cassettes and then 10% buffered formalin for fixation and tissue processing.**

Photographs and videos of the gross dissections were also obtained for gross descriptive purposes.

Tissue preparation, processing and sectioning

The entire patch, infraspinatus muscle and tendon were removed in their entirety from the infraspinatus fossa immediately after sacrifice and sectioned into two pieces just proximal to the repair sutures. A 1.5-cm portion of the patch was then dissected free of any surrounding tissue and sent for immediate biomechanical testing and electron microscopy as outlined below. The distal portion, encompassing the injury site, was placed into a labeled processing cassette and then into 10% buffered formalin. The tissue from the shoulder tendons was placed between two sponges to orient the tendon lengthwise for proximal distal superior and inferior landmarks of the tendon for later sectioning (Figure 3.10).

Figure 3.10 **Tendon is placed into the cassette with a specific orientation. The proximal end of the tendon, which was cut just proximal to the suture repair site (sutures just visible), was oriented toward the back of the cassette while the distal end was oriented toward the front labeled part of the cassette. A second sponge was added on the top to maintain orientation prior to immersion in 10% buffered formalin.**

The tendon tissue remained in the formalin for 2 weeks and then was removed and processed using a Leica™(Wetzlar, Germany) tissue processor and embedded in paraffin wax (Figure 3.11).

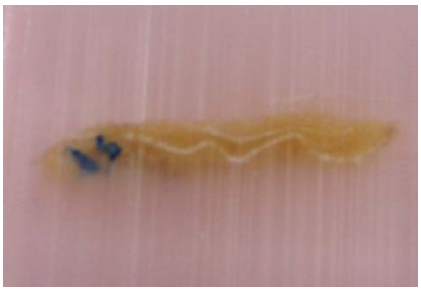

Figure 3.11 **Paraffin embedded section of a patch. Blue, repair suture is seen to the left of the image and the patch material is seen as a wavy line within the bulk of the tan colored tissue.**

During the embedding procedure, it was important to align the tissue for sectioning in order to obtain uniform sections. The tissue was placed into the molds after a longitudinal cut was made through the centre of the patch in this longitudinal orientation. This was done to ensure visualisation of the patch material and the tissue implant interface during longitudinal sectioning with the microtome (Figure 3.12).

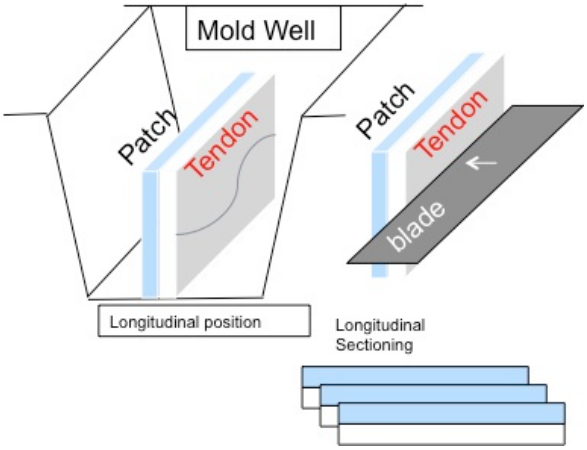

Figure 3.12 **Orientation of patch tendon tissue in mold well for subsequent tissue sectioning.**

The bone of the bilateral humeri and glenoids were also removed en bloc and also placed into a tissue cassette and 10% formalin for 3-10 days. This was followed by decalcification in 5% formic acid for 11-12 days. This method of decalcification is the preferred method for rat cartilage examination recommended by the Osteoarthritis Research Societies' histopathology initiative (OARSI) [189]. Prior to paraffin embedding, bone was also sectioned transversely to obtain a cross section through the centre of the glenoid or humeral head for later visualisation with H&E staining. The bone was then embedded in paraffin with the cancellous portion of the bone toward the bottom of the wax mold for proper orientation and sectioning (Figure 3.13).

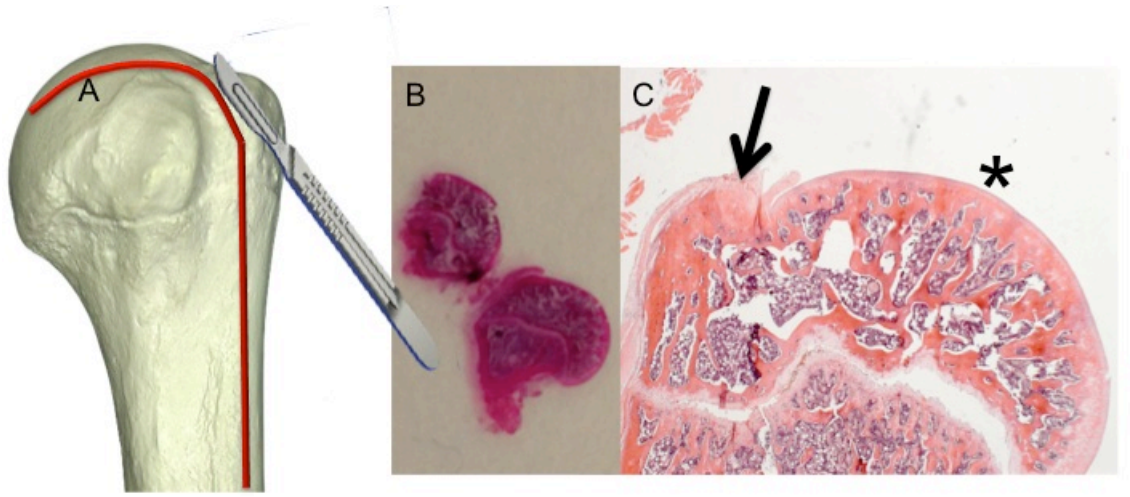

Figure 3.13 **Protocol for paraffin embedding of the bone after tissue processing. (A) The bone is sectioned in the coronal plane through the greater tuberosity and book-ended open. (B) The cut surfaces placed face down in the mold for H&E staining. (C) After removal and sectioning, the orientation is clear and allows easy visualisation of the, enthesis (→) and cartilage surface (*).**

Tissue blocks for both tendon and bone were placed on ice for 15 minutes and sectioned to 4µm using a Leica RM-2135 (Wetzlar, Germany) microtome. They were placed onto labeled Leica extra sticky glass slides. The specimen was then heat melted onto the slide using heat platforms of 60°C for thirty minutes followed by 37°C for one hour. The slides were stored at room temperature before staining.

Histology and Immunohistochemistry

General histological examination for cartilage surfaces and FBGC counts were performed using haematoxylin-eosin (H&E) staining. Cartilage surfaces were then examined and graded according to the OASRI grading scale as seen in table 3.3[189].

Table 3.3

Cartilage Degeneration Scoring

Parameter	Grade	Description
Cartilage degeneration	0	No degeneration
	1	Minimal degeneration; 5–10% of the total projected cartilage area affected by matrix or chondrocyte loss
	2	Mild degeneration; 11–25% affected
	3	Moderate degeneration; 26–50% affected
	4	Marked degeneration; 51–75% affected
	5	Severe degeneration; greater than 75% affected

Specific cell markers for macrophages (iNOS for M1 and mannose receptor for M2) were stained for immunohistochemistry. Prior to staining for IHC, all slides were baked at 60°C for an additional hour. The automated Dako PT Link machine performed de-paraffinisation and target retrieval. All immunostaining was performed on the Dako Autostainer Link 48 machine. The Autostainer slide racks were transferred from the wash buffer to the Autostainer Link 48 and further wash buffer applied to the slides in the machine prior to staining. The immunostaining protocols and dilution preparation varied according to the antibody used. The details of the antibodies are described in Table 3.4 which delineates the dilutions used for each particular antibody.

Table 3.4

Stains and dilutions used for IHC.

Subject	Stain	Method/Dilution
M1 macrophage (activated MΦ)	iNOS	1:5000 no linker
M2 MΦ	mannose receptor	1:1000 c/ linker

Microscopic Assessment and Image Analysis

The assessment of the microscopic appearance of the slides stained for Haematoxylin/Eosin was performed by one blinded investigator. Images were also sent to a trained histopathologist, who was also blinded, for confirmation of the findings. Images were taken with a systematic approach. After identifying the area of the patch material, or suture holes for controls, on 2.5x magnification the tissue was photographed at 10x and 20x magnification to get the overall area next to the patch material. Patch material and sutures were frequently cut out of the tissue, in which case residual imprints were left in the tissue allowing orientation to the patch materials. Then the microscope was refocused to 100x power under oil immersion. From the distal extent of each patch/tissue interface images were taken sequentially of different fields next to the interface. A minimum of 5 images and a maximum of 20 per slide, depending on the size of the tissue section were taken (Figure 3.14).

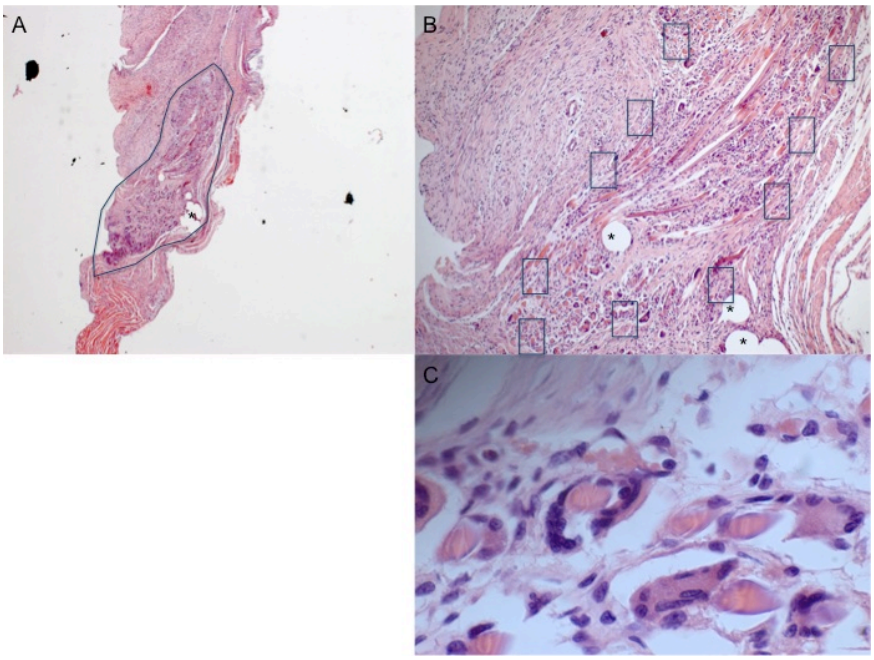

Figure 3.14 **Slide examination method. (A) shows the overview of the tissue section with the patch material outlined. (B) shows an example of where patch/tissue interface images might be taken from after zooming to 100x power with oil immersion as shown in (C). The (*) represent areas of sutures which have been cut out of the slide block.**

The images were then analyzed using ImageJ® in order to quantify the total number of cells and the amount of DAB stained cells present in each image in addition to manual counts for every image. A second investigator confirmed the results by repeating selected image counts. The details of the image analysis are described in Appendix 1.

H&E staining

After baking as described above, specimens were stained on a Bayer Tissue-Tec DRS 2000 autostainer with the following procedure. Slides were washed in distilled water and then stained for 5 minutes in Mayer's hematoxylin. Slides were then washed in tap water and blued in 2% sodium hydrogen carbonate for a few seconds followed by another wash in tap

water. Slides were then stained in 1% eosin for 5 minutes, rinsed with tap water and dehydrated using alcohol, cleared in xylene and mounted in D.P.X. Finally, coverslips were placed over the sections and imaged according to the microscope protocol as described above.

Biomechanical Tests

For each type of patch, 3 separate specimens were used, measuring 15 mm in length and 2 mm in width. The testing protocol was based on a modified version of previously published studies of the mechanical properties of other tendon patches [190,191]. Modified clamps were used to grip the ends of the patches, leaving a nominal grip-to-grip gauge length of 10 mm. Specimens were tested to failure in tension using Deben machine at a rate of 0.3 mm/min until failure (150 N load cell). We assessed load to failure (N), which was defined as a decrease in load of more than 20% during tensile testing. Scanning electron microscopic (SEM) images were taken during the test using SEM Carl Zeiss™ (Oberkochen, Germany) microscope.

Statistics

Data were analyzed with Prism© (GraphPad Software, Inc. USA) statistical software. Values were expressed as means and standard deviations with 95% confidence intervals. Two-way analysis of variance (ANOVA) was conducted to test the significance of differences between the different patch materials, controls and time-points (independent variables) with respect to counts of FBGCs, inflammatory macrophages (M1) and regenerative macrophages (M2) (dependent variables). Two-way ANOVA was utilised after discussion with statisticians. This test examines the influence of the different independent variables utilised of patch material

and time on the dependent variable of biologic response (inflammatory cell counts). The two-way ANOVA assesses the main effect of each independent variable and also if there are interactions between them. These results were plotted as cell number over time with 95% confidence intervals for each time-point. Significant differences between biomaterials at the different time-points were those without overlapping confidence intervals corresponding to a p value of $<.05$).

4. *In Vivo* Biocompatibility Results

Systemic Reactions to Implants

There were no systemic reactions to any of the implants at any time-point as measured by hind paw inflammatory indices (Figure 4.1).

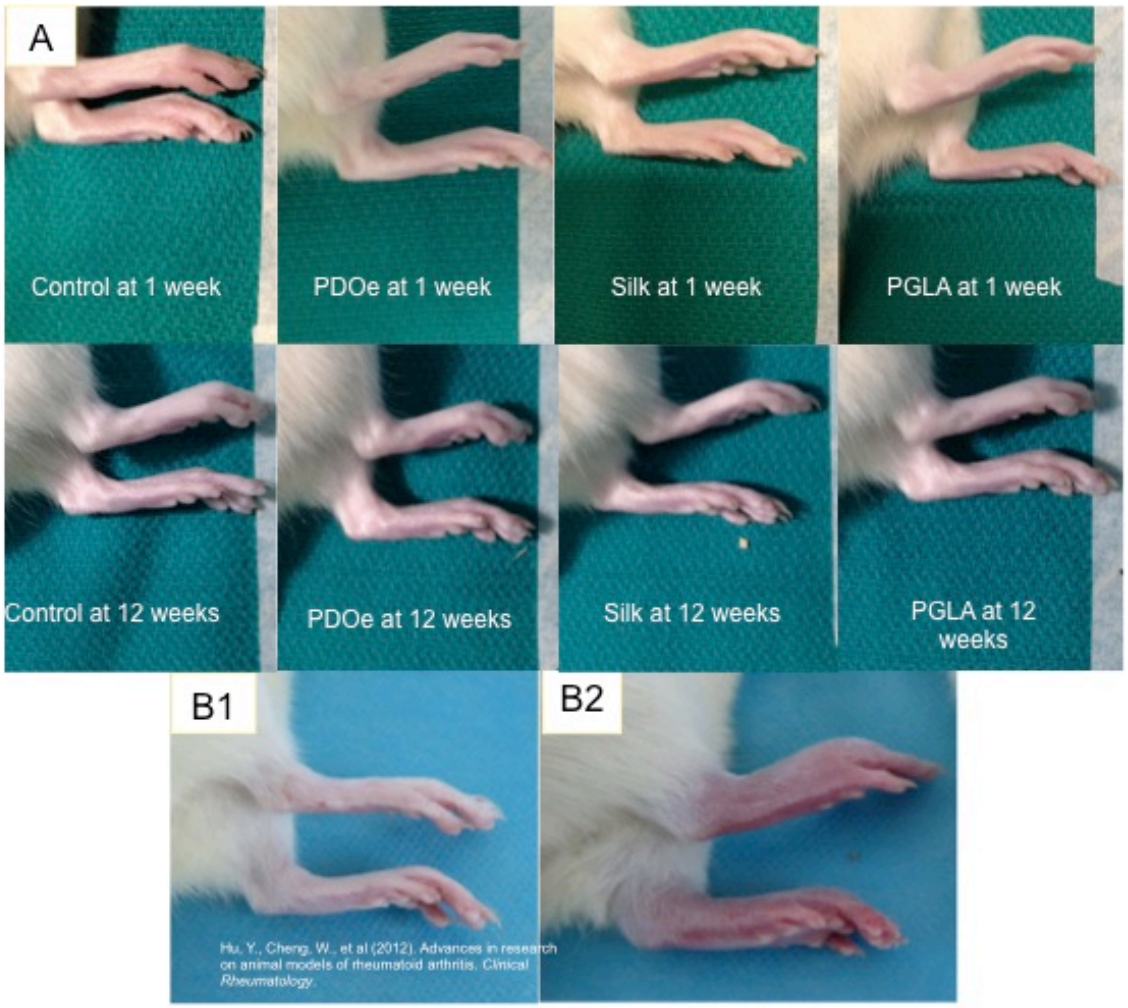

Figure 4.1 **Hind paw inflammatory indices. (A) Representative hind paws show no swelling or erythema at 1 and 12 weeks or any intervening time-point (data not pictured) for any of the biomaterials. (B) A representative figure displaying (B1) normal and (B2) hind paw swelling and erythema from Lewis rats with adjuvant induced arthritis with collagen (Image taken reference [188]). The loss of normal bony landmarks in B2 signifies significant swelling.**

The wounds themselves remained benign and there were no cases of wound dehiscence, draining seroma, fistula formation or infection. Animals did not aggressively attempt to scratch or eat out their sutures for any of the materials used. There were 2 cases of scratches next to shoulders with PGLA and one case of scratching next to silk and none for the PDOe or control materials, although these seemed to be isolated or incidental and not due to undue irritation to the sutures or patch material (Figure 4.2).

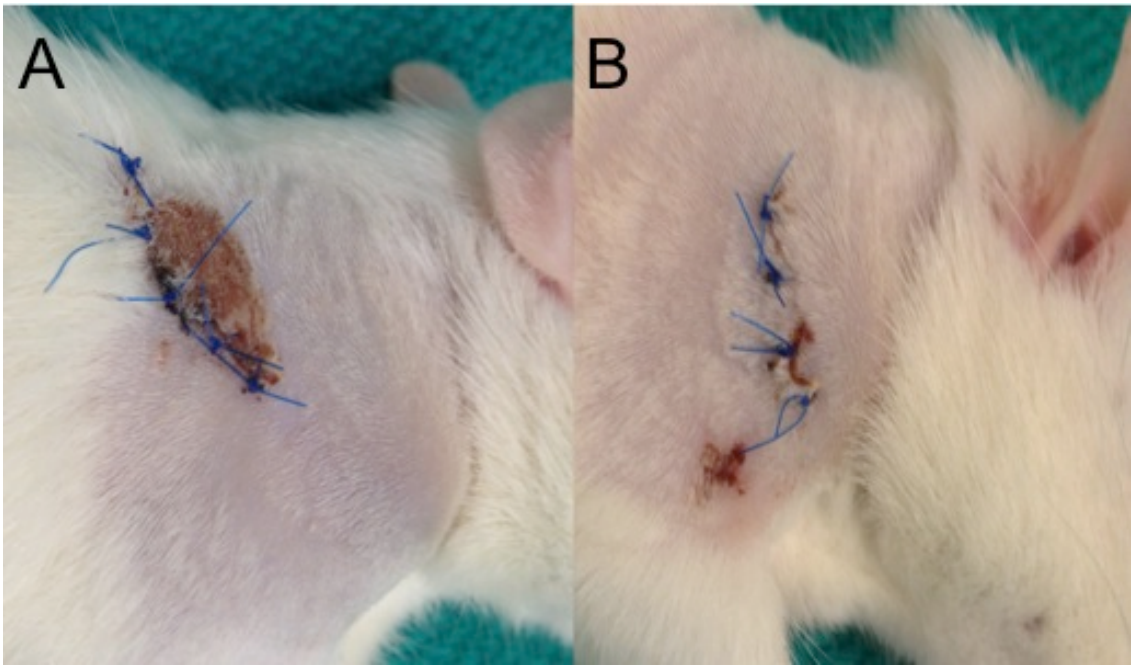

Figure 4.2 **Cutaneous reactions at 1 week. (A) Silk and (B) PGLA. Note the abrasion and superficial scratch near the wounds. There were no other cases of injury around incisions and all superficial scratches had healed by postoperative day 10.**

Local Responses

On gross dissection, control animals had mild adhesions to the subcutaneous skin. These adhesions became less prominent at 4 weeks and were virtually nonexistent at 6 and 12 weeks. The control transections were grossly bridged with robust scar tissue at one-week even in the single case where the suture had pulled through the proximal tendon and the

repair failed (Figure 4.3). Over each time-point the scar matured and was less bulky at 12 week time-points, but visibly more amorphous and grey in contrast to the bright white and aligned striations of normal tendon.

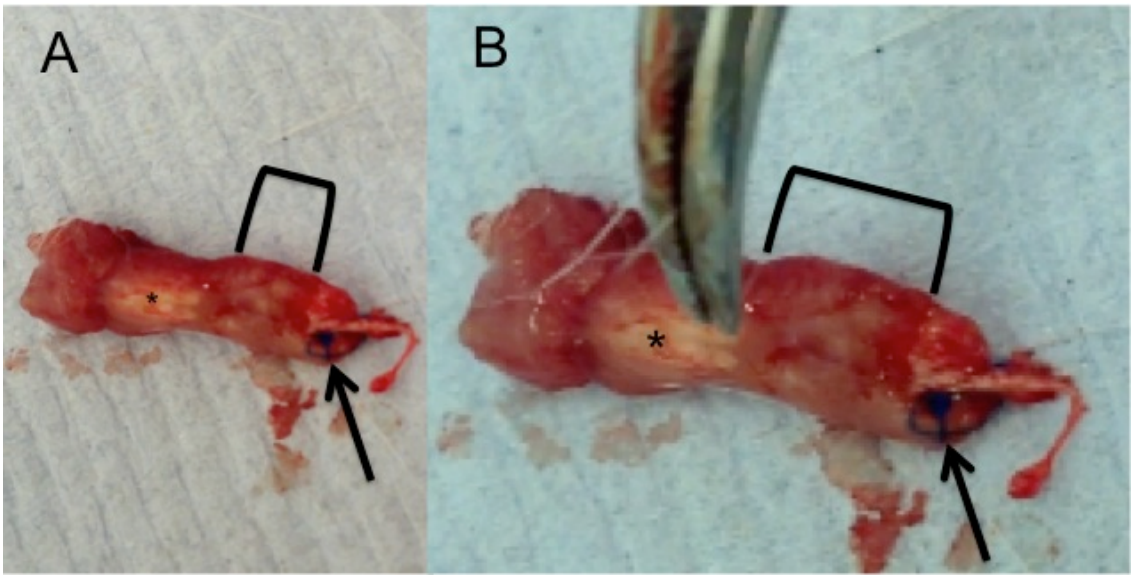

Figure 4.3 Scar tissue formation in a control failed repair after one week. (A) The tendon (*) is in continuity with scar tissue (bracket) area even with suture pullout and failure. The suture knot and loop (→) are seen to the right of the area of scarring (bracket). (B) Close up of the same tendon. The forceps denotes the distal portion of the tendon, which is lighter in color. The longitudinal area of suture pullout can be seen immediately below the forceps to the right of the (*) on the image.

There was a large transudate at the one- and two-week time points for the PGLA implanted animals (Figure 4.4).

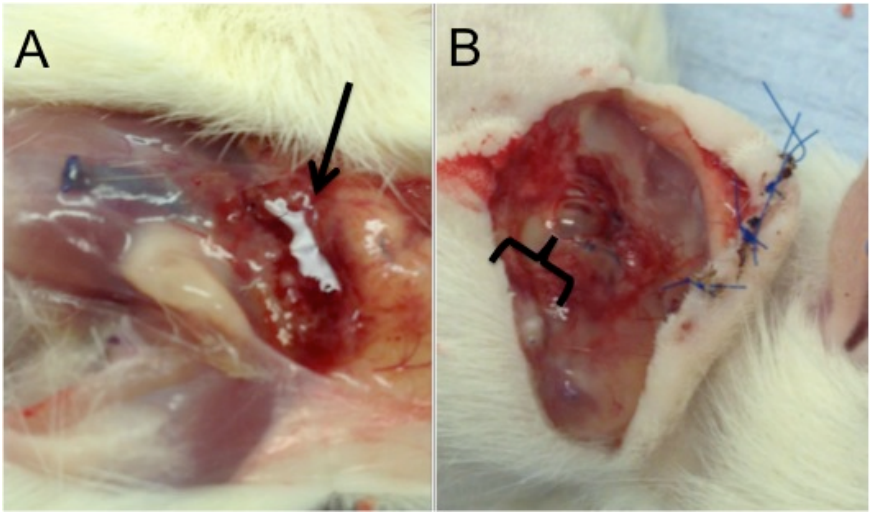

Figure 4.4 **PGLA transudate encountered at (A) 1-week (→) and (B) a seroma (}) at 2-week time-point. This fulminant serous fluid was not present at 4, 6 and 12 weeks.**

The PGLA capsules contained serous fluid and the patch material degraded visibly over time and was not grossly identifiable at 12 weeks. Scar tissue was soupy and amorphous at 1 and 2-week time-points and congealed at later time-points with a more robust thicker scar tissue at 6 and 12-week time-points.

Silk implanted animals had a large capsule surrounding the implant which increased in size over time. This capsule was readily identifiable after initial subcutaneous dissection as a bulging mass beneath the muscle (Figure 4.5).

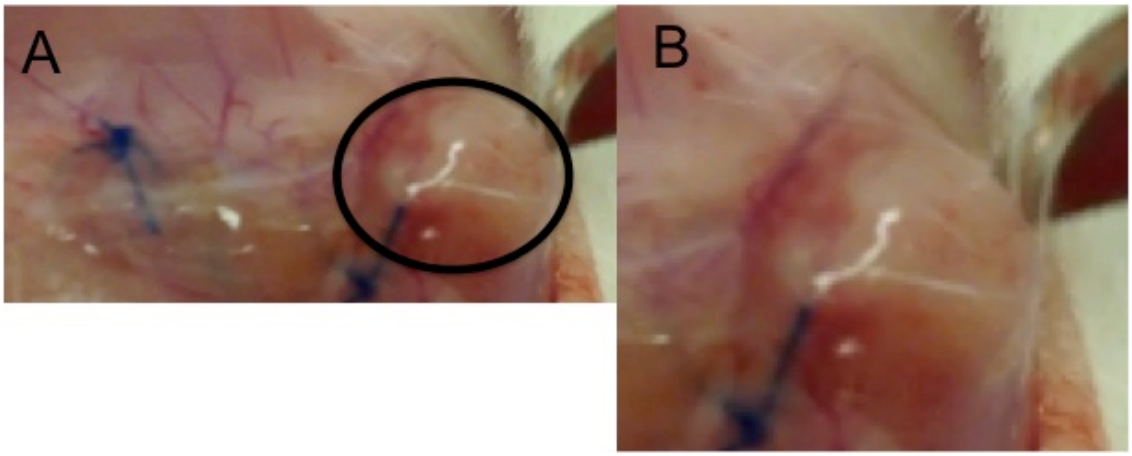

Figure 4.5 **Fibrous capsule of Silk after subcutaneous dissection. (A) outlines area of capsular thickening bulging below muscular repair (O). (B) is an enlargement of the same image.**

The fibrous capsule extended the length of the patch and although very thick was easily peeled away from the patch showing little incorporation (Figure 4.6).

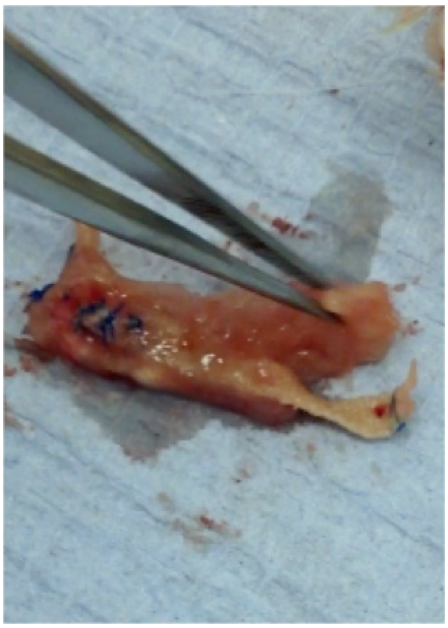

Figure 4.6 ***Ex vivo*** **dissection of the silk patch. Large fibrous encapsulation of the silk patch (in forceps) with little incorporation at 1-week time-point.**

Although encapsulation was present in PDOe and PGLA patches, grossly it was not as robust as that seen with the silk patches.

PDOe and control repairs had fibrous capsules around repaired tendons which seemed to increase in size up to 2-weeks and then gradually decrease in size up to 12-weeks (Figures 4.7 and 4.8). Animals implanted with PDOe showed a similar response when compared to controls.

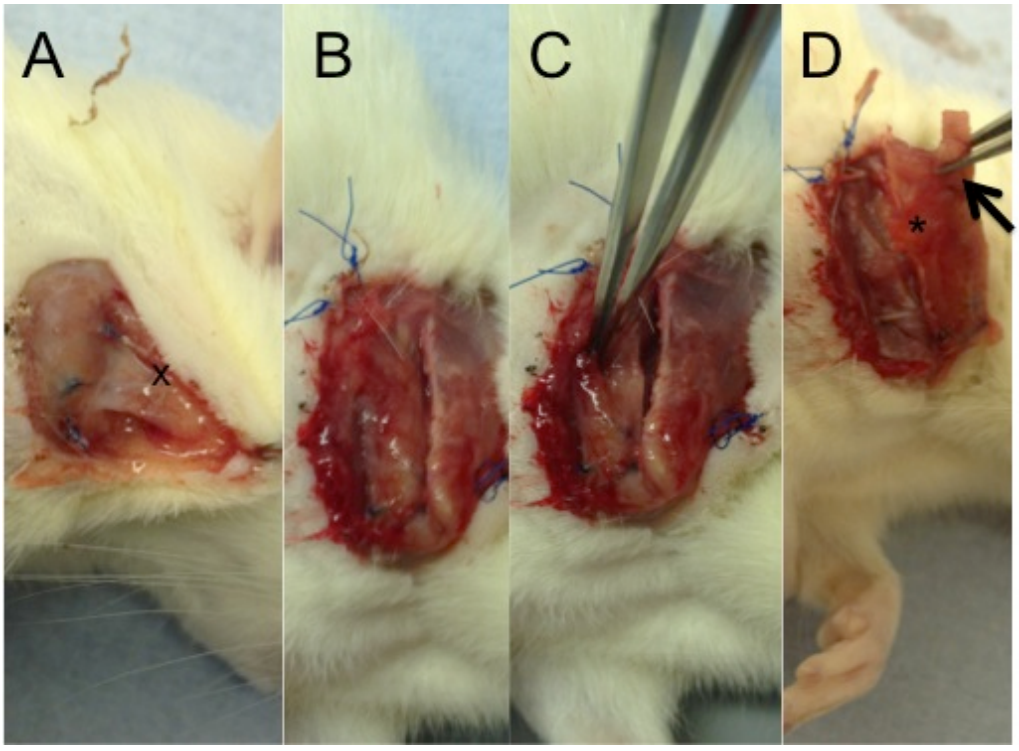

Figure 4.7 **In situ dissection of PDOe patch at 1 week. (A) Small adhesions (x) to the skin were most prominent at the 1-week time-point and diminished over time. (B) and (C) show patch dissection out of the infraspinatus fossa. (D) shows the patch being removed along with underlying muscle (*). The fibrous capsule around the implant is clearly visible (→).**

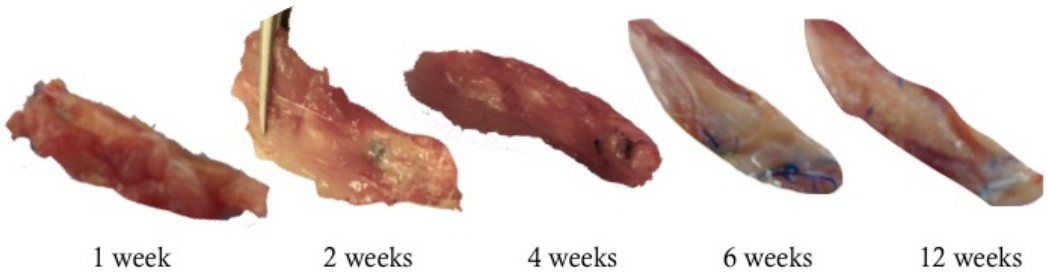

Figure 4.8 **PDOe patch dissection over time. There was an initial increase in fibrous capsule thickness between 1 and 2 weeks followed by gradual decreasing size from 4 to 12 weeks.**

Electron Microscopy

Electron microscopy was undertaken in order to visualise the interface between the patch and host during tensile testing. Images revealed a coating of homogenous material within 2 weeks of implantation. This layer appeared to become thicker over time with all implants. However, even though this layer was not measured directly, because the fibers of the PDOe implants remain visible below this layer this suggests this layer may be thinner around this implant compared to other patches (Figure 4.9).

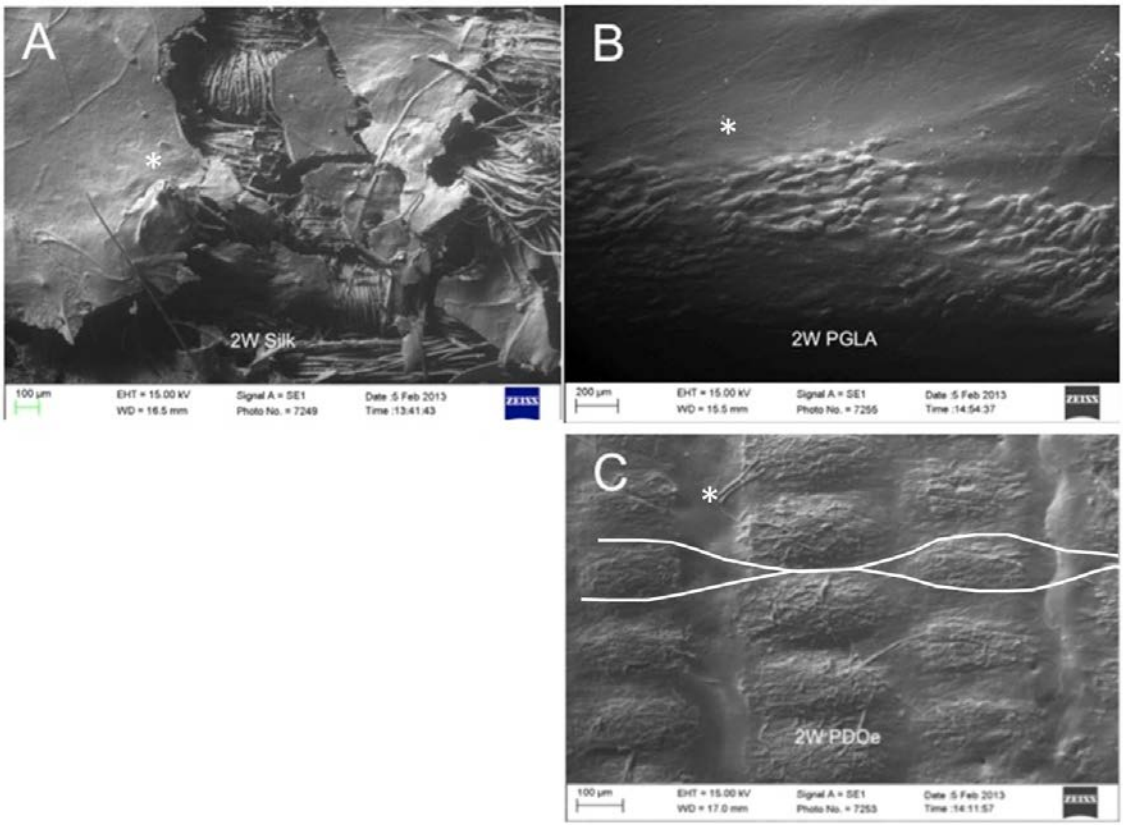

Figure 4.9 **Scanning electron microscopy (SEM) of the 3 patches (A) Silk, (B) PGLA and (C) PDOe at 2-week time-points. The layer of fibrous tissue surrounding the Silk and PGLA patches appears thicker compared to the PDOe where the fibres are identifiable below the tissue encapsulation (lines identify weave). The fiber weave of the other pathc materials are not identifiable until disruption of the patch material with tensile testing as seen in (A) suggesting a thinner layer of fibrous tissue in the PDOe group.**

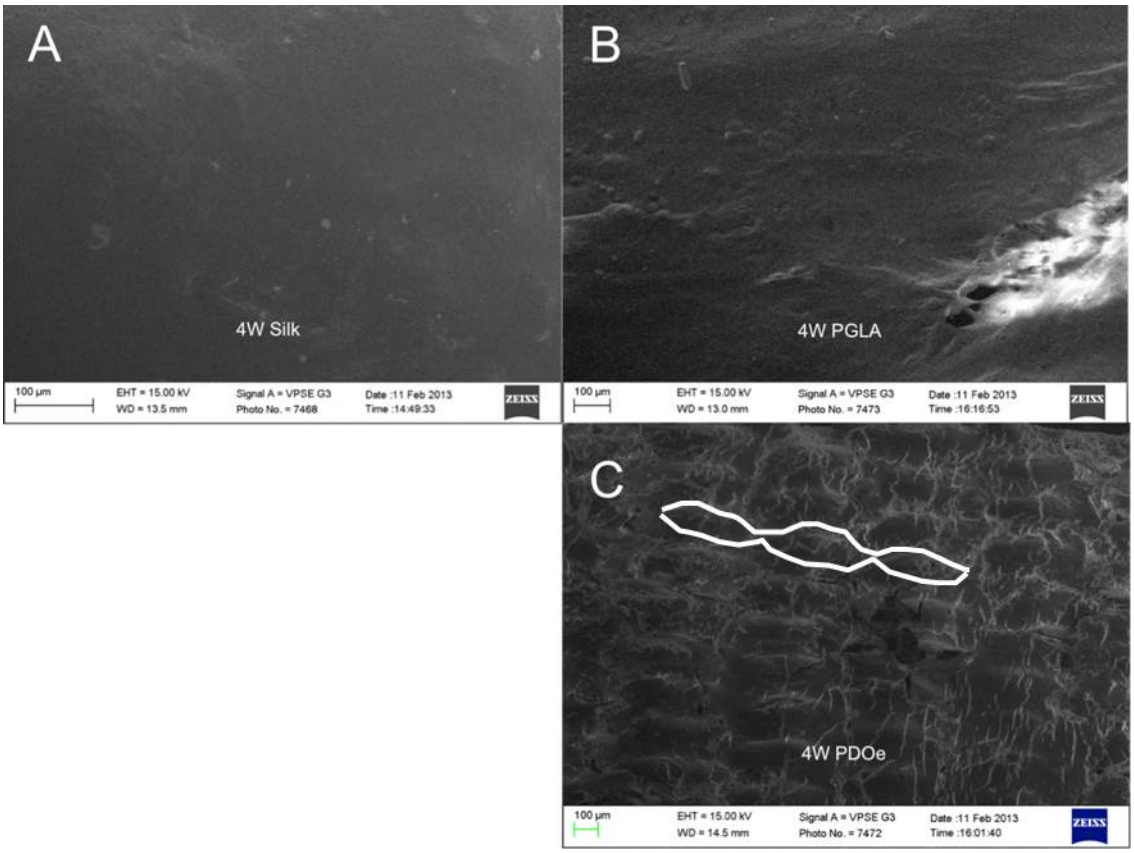

Figure 4.10 **Scanning electron microscopy (SEM) of the 3 patches (A) Silk, (B) PGLA and (C) PDOe at 4-week time-points. The layer of fibrous tissue surrounding the Silk and PGLA patches is even thicker at the 4-week time-point than the 2-week time-points. Again, the PDOe fibres remain visible below the tissue encapsulation (outlines).**

Articular Cartilage Response

There was no difference in the articular cartilage between the groups at any time-point (Figure 4.11).

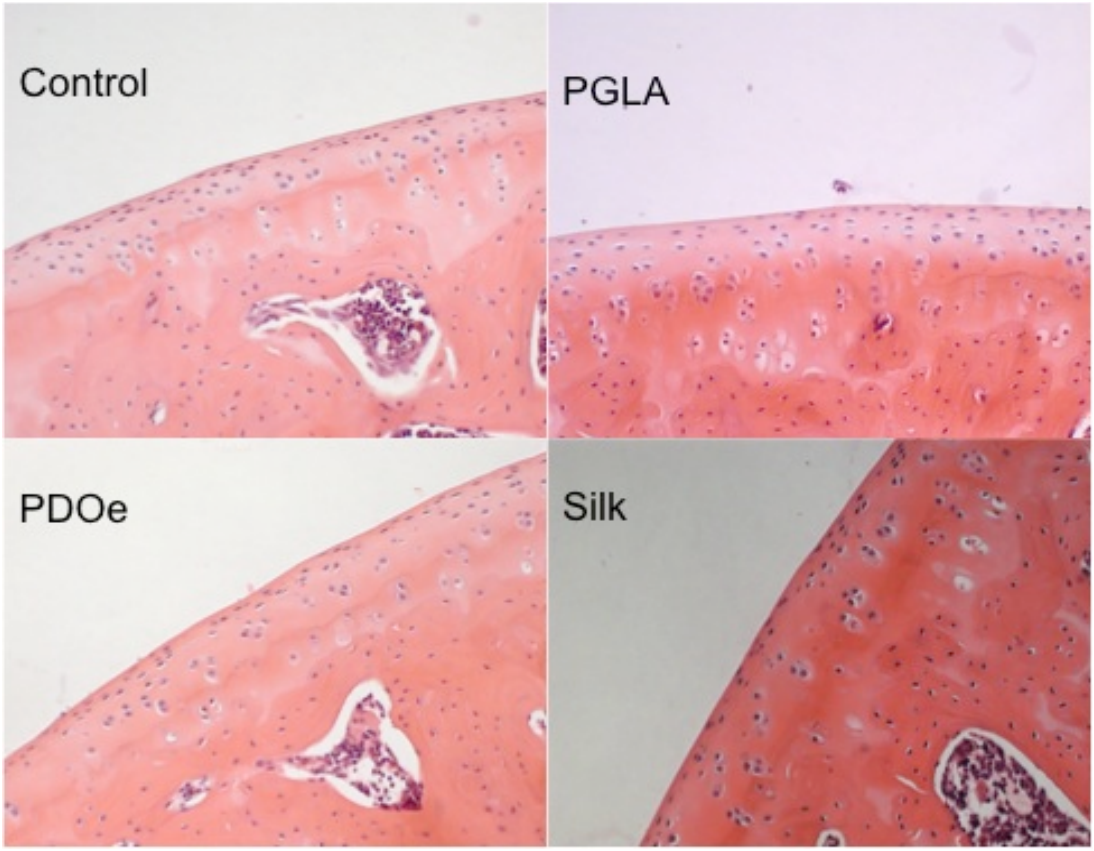

Figure 4.11- **12-week cartilage examination. Normal cartilage architecture and density with homogenously distributed, normal appearing chondrocytes and a smooth articular surface without erosions or pitting for each of the constructs tested.**

The articular cartilage was smooth and devoid of any thinning, pitting or other defects for all constructs tested. Chondrocytes were characteristically round and normal in appearance and there was no evidence of synovial thickening or lymphocytic infiltrate.

Foreign Body Giant Cell Response

1-Week Time-Point

At the 1-week time-point there was a mixed infiltrate of inflammatory neutrophils, macrophages, fibroblasts and eosinophils and few FBGC's (Figure 4.12).

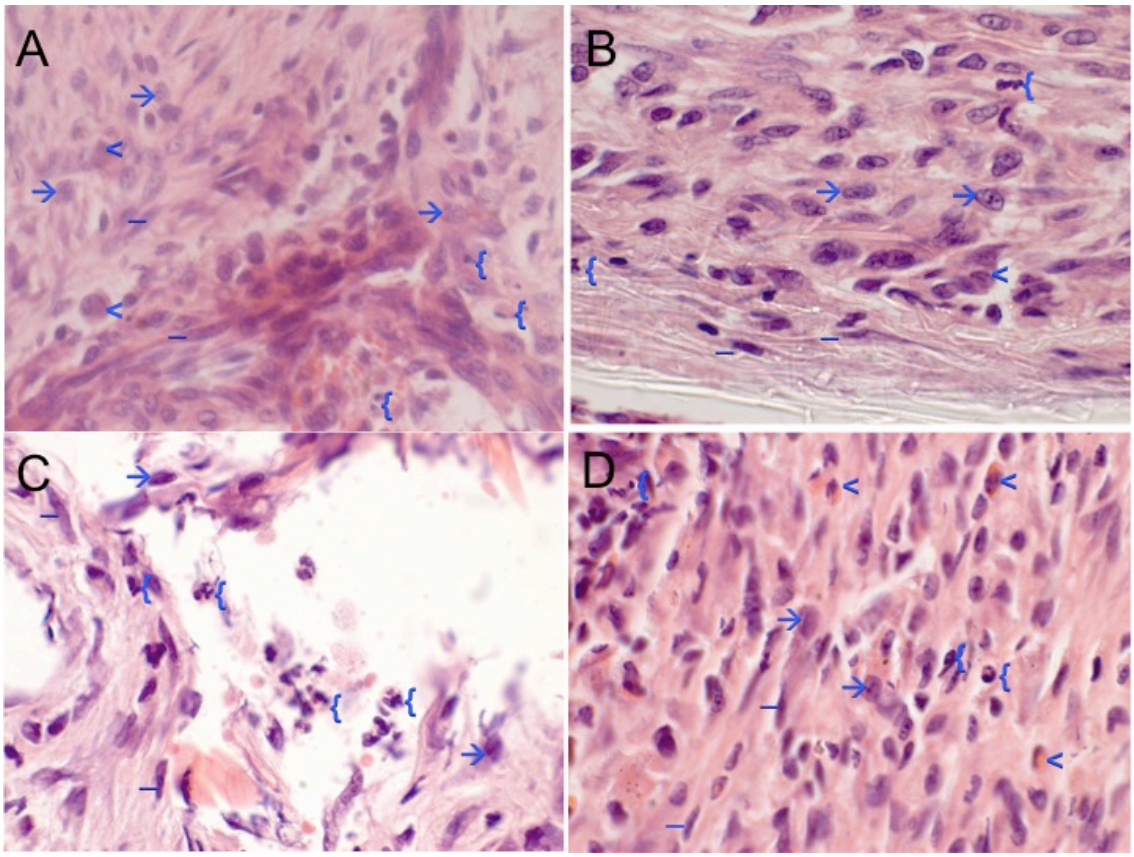

Figure 4.12 **Inflammatory infiltrate at 1 week post implantation at 100x magnification. (A) Control, (B) PDOe, (C) Silk, (D) PGLA patches. There are mixed cell types including eosinophils (<) identified by their eosinophilic cytoplasm and horseshoe shaped nuclei, macrophages (→) identified by their large nuclei and prominent nucleoli, neutrophils ({) identified by their multilobed nuclei and fibroblasts (-) identified by their elongated linear and sometimes wavy nuclei with cytoplasm that diffusely blends with background. Fibroblasts within the electrospun component of the PDOe patch (B) were elongated and phenotypically similar to tenocytes.**

These cells were present in all constructs and again were confirmed by a blinded independent histopathologist. The fibroblast cells next to the electrospun component of the PDOe patch took on a more elongated, fibroblast and/or tenocyte-like appearance, whereas cells not in contact with the electrospun component seemed to be predominantly rounded macrophages (Figure 4.13).

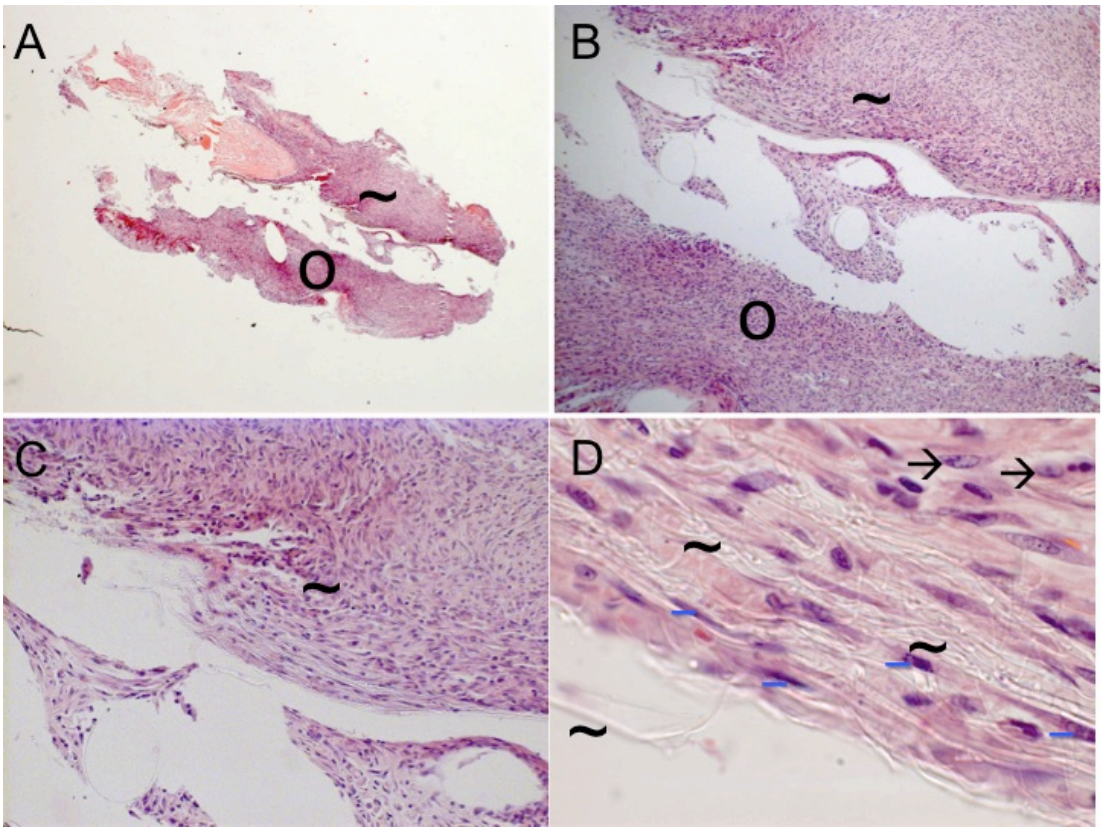

Figure 4.13 **PDOe patch at 1-week time-point with four different magnifications. (A) is a 2.5x magnification and shows the overall appearance of the patch in reference to the surrounding tissue. (B) is a 10x magnification. The woven structure becomes clearer. The electrospun side is labeled with a (~) and the woven side with a (o). (C) is a 20x magnification where the electrospun fibres are becoming more evident. The elongated fibroblasts (-) can be seen on the electrospun component (~) and rounded macrophages at the periphery (→). (D) 100x magnification reveals the electrospun fibres and the fibroblast cells (-)with a more elongated tenoctye-like appearance of cells within the electrospun component (~), whereas cells not in contact with the electrospun component are more round and phenotypically more similar to macrophages (→).**

2-Week Time-Point

Foreign body giant cells (FBGC's) were again observed independently by (MEM) and a blinded independent histopathologist for all constructs first becoming prominent at the two-week time-point (Figures 4.14-4.19). These cells are clearly identified even on low power by their characteristic multinucleated structure on H&E staining. For all patch constructs these FBGC were of the Langhans-type with peripherally arrange nuclei within the cytoplasm resembling a horseshoe and for controls were foreign-body-type with jumbled nuclei which do not assume a characteristic pattern within the nuclei (See figure 2.9 for structural differences)[192]. The

PDOe constructs again showed areas of organisation in the electrospun region of the patch with elongation and orientation of cells expressing tenocytic phenotype outside the area of cellular infiltrate. This region was thicker and appeared to have thicker, more pronounced orientation of what are possibly collagen bundles along the axis of the cells in this region.

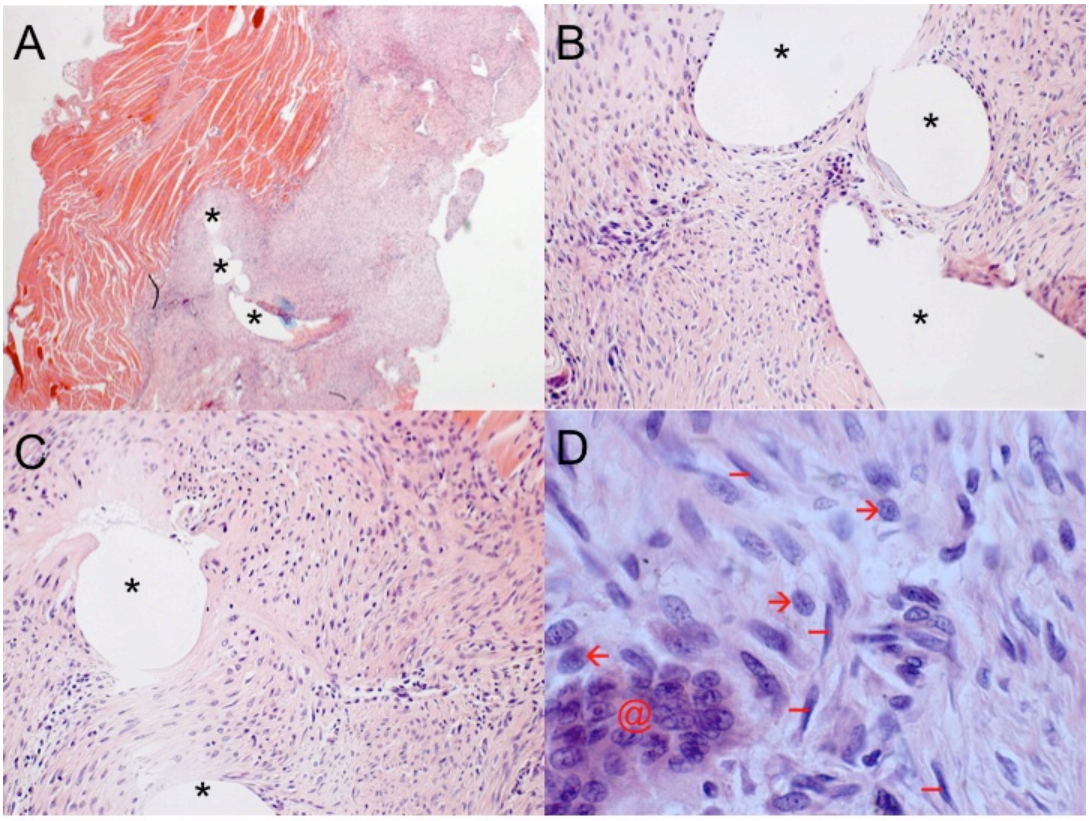

Figure 4.14 **Control at 2 weeks. (A) 2.5x magnification for overview. (B) and (C) show suture holes (*) and surrounding cellular stroma. (D) There was a dense population of cells consisting of mostly macrophages (→) and fibroblasts (-) within the area of repair. A FBGC (@) of the foreign-body-type can be seen in (D) at 100x magnification.**

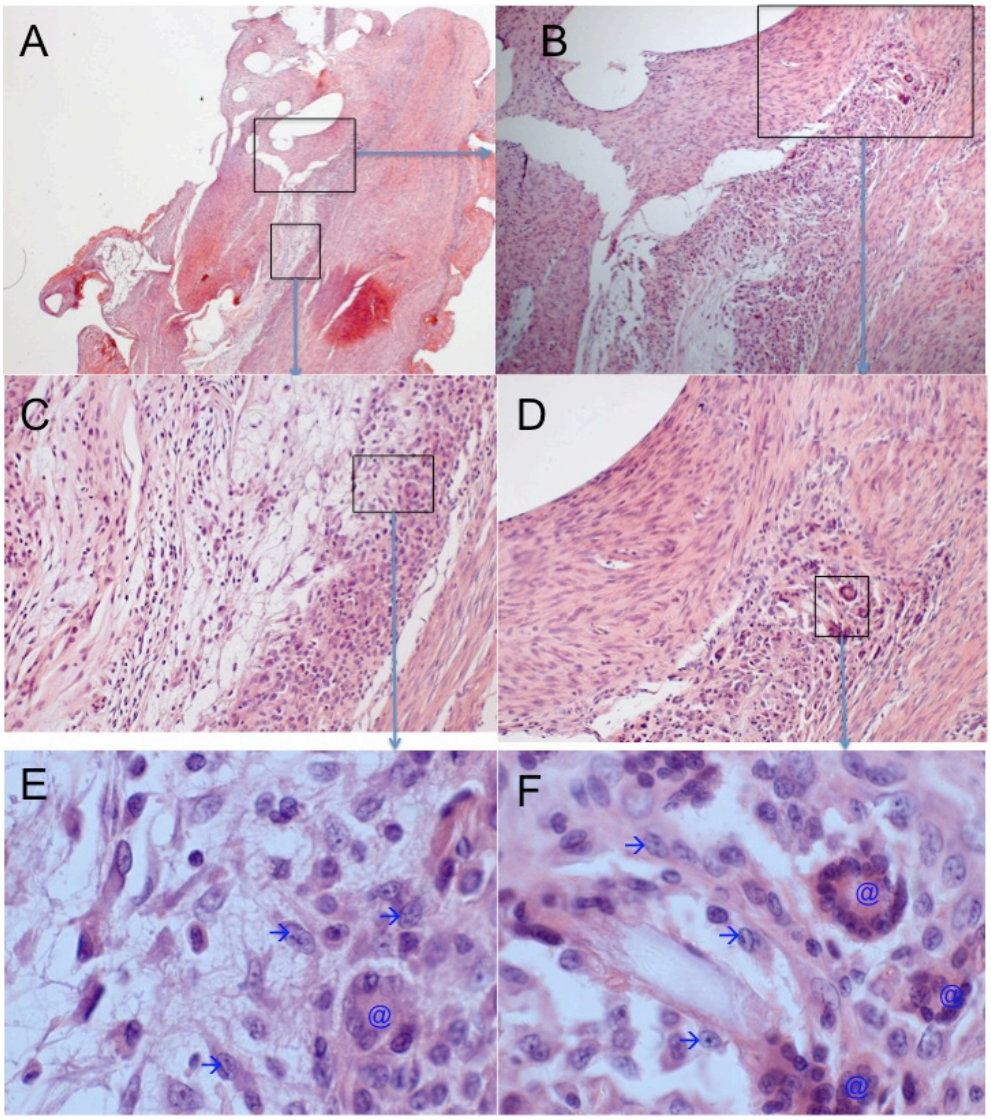

Figure 4.15 **PDOe at 2 weeks post-implantation in different regions next to the construct. (A) Shows overview of patch at 2.5x magnification. The rectangle regions correspond to 10X magnification in (B)and 20x's magnification in (C) and (D). (E) and (F) are 100x's magnification of the outlined rectangular areas and show dense areas of cellular infiltrate populated by Langhans-type FBGC's (@) and macrophages (→)**

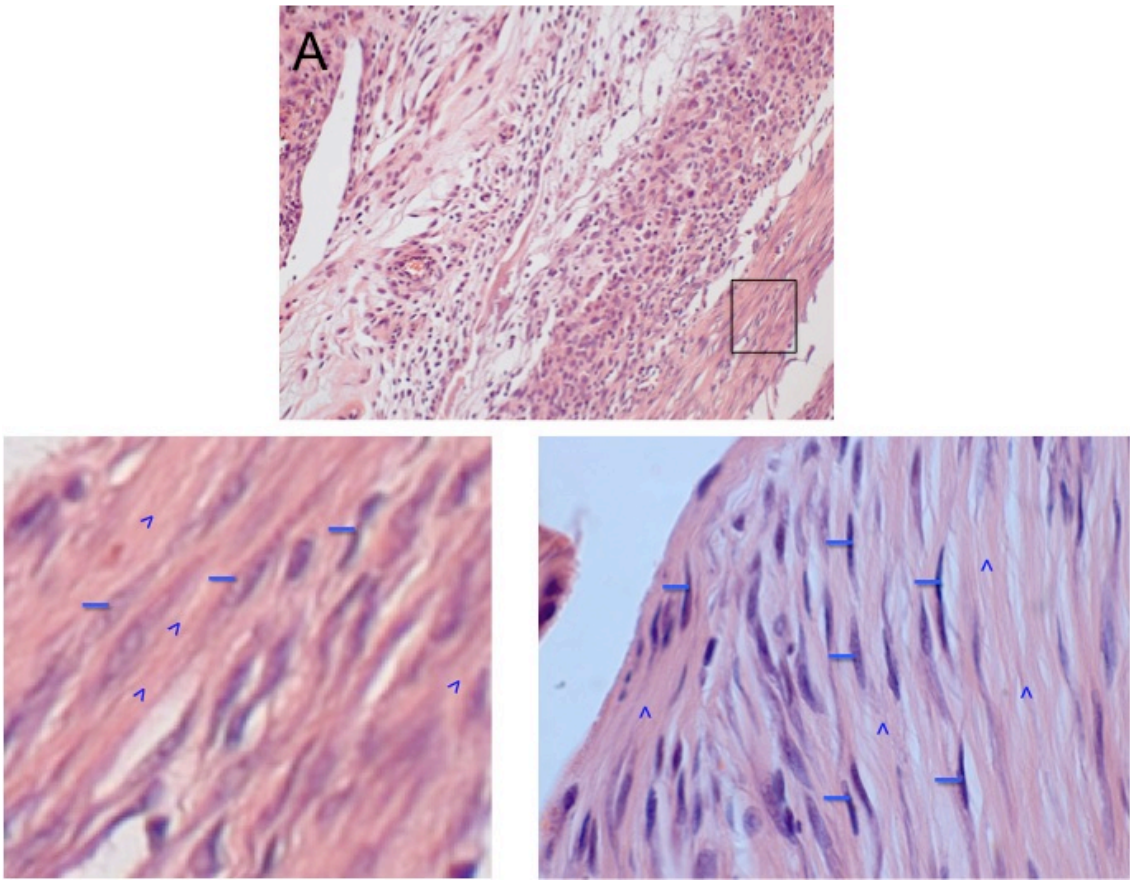

Figure 4.16 **Electrospun side of the PDOe scaffold at 2 weeks. (A) is a 20x magnification and shows the region of interest. (B) and (C) show fibroblasts (-) which are elongated and oriented in the same direction similar to tenocytes outside the area of cellular infiltrate and within the electrospun scaffold. Bundles, possible collagen (^), are oriented along the axis of the cells and are more pronounced than at the 1-week time-point.**

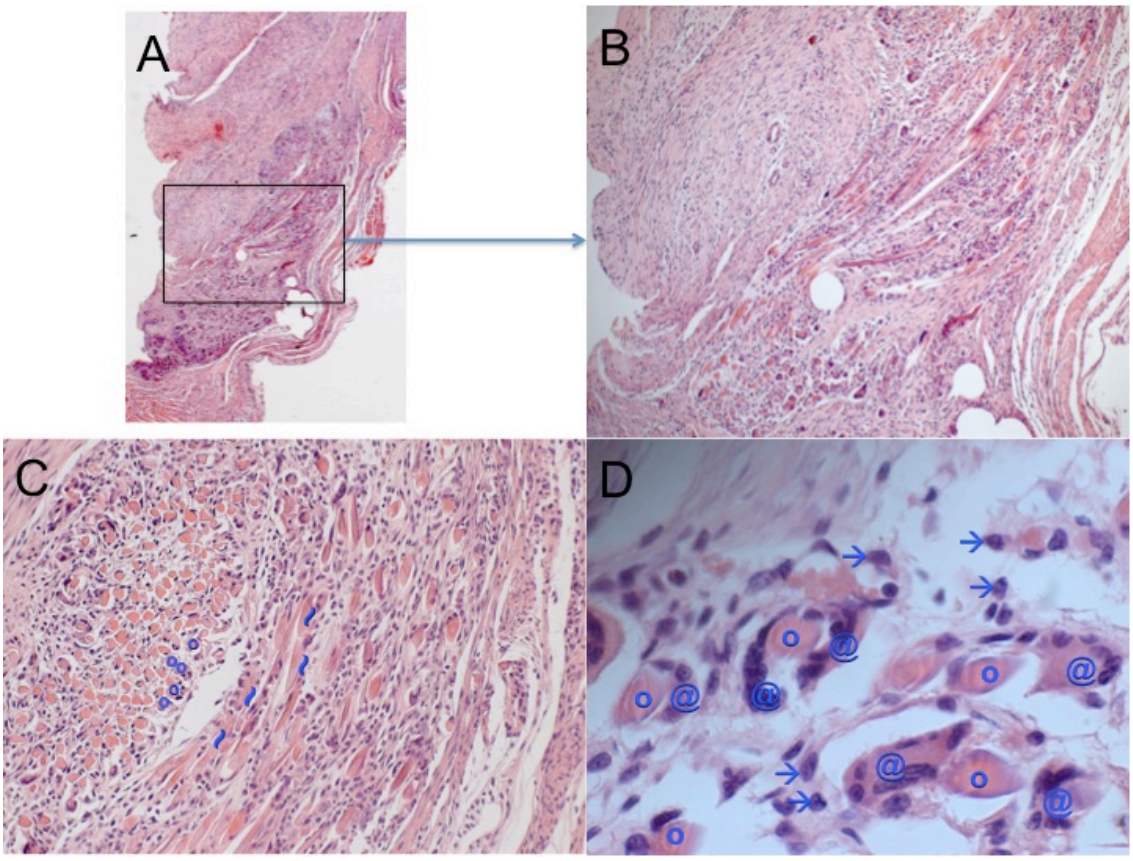

Figure 4.17 **2-week silk photomicrographs at different powers. (A) 2.5x magnification for overview. (B) 10x magnification of the rectangular area in (A). (C) At 20X power the silk fibre orientation becomes more noticeable and the weave pattern apparent. Longitudinal silk fibres (~) and axially arranged fibres marked with (o) juxtaposed with cells interspersed within the silk fibres. (D) 100x magnification shows numerous Langhans-type FBGC's (@) and scattered macrophages (→) which have not yet fused and are surrounding the silk fibres (o).**

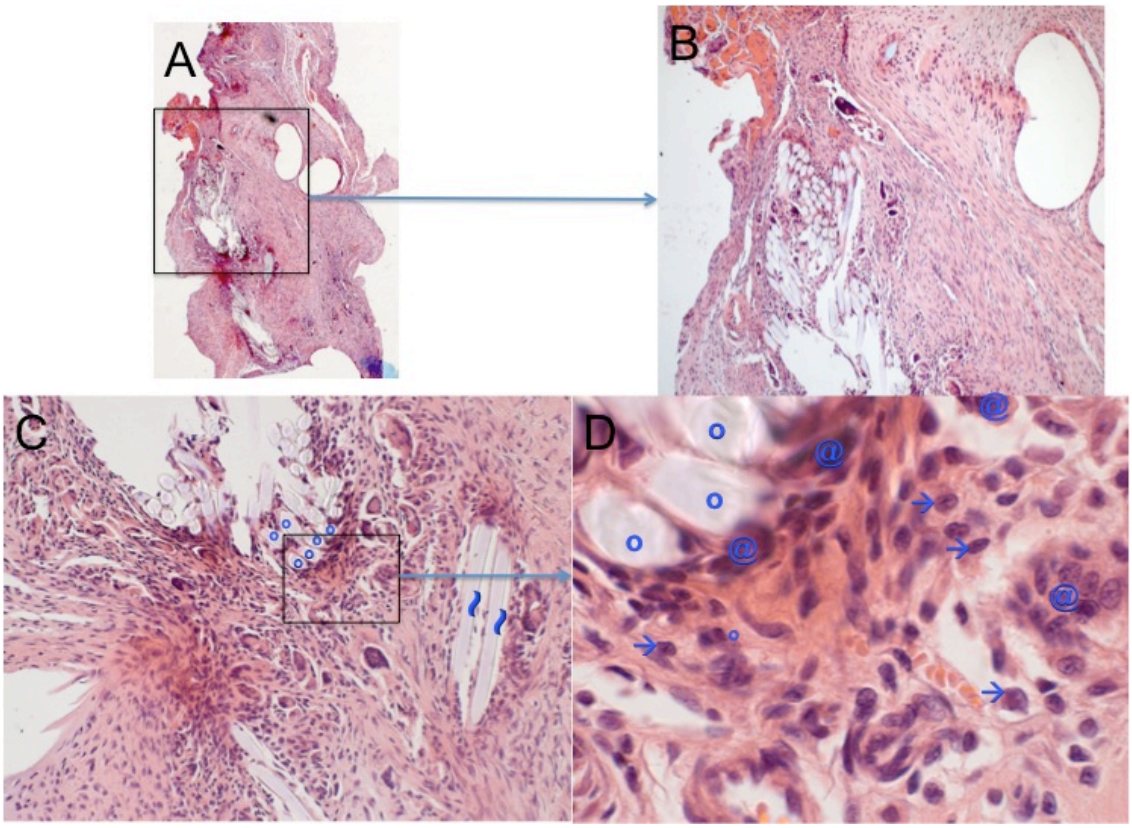

Figure 4.18 **2-week PGLA scaffolds. (A) 2.5x magnification for overview. (B) 10x magnification of the rectangular area in (A). (C) At 20X power the PGLA fibres are seen in axial orientation (o) and 2 in a longitudinal orientation (~) (D) 100x magnification and close up of the rectangular area in (C) shows numerous Langhans-type FBGC's (@) coalescing together around the fibres along with dense macrophages (→) also surrounding the PGLA fibres (o).**

.

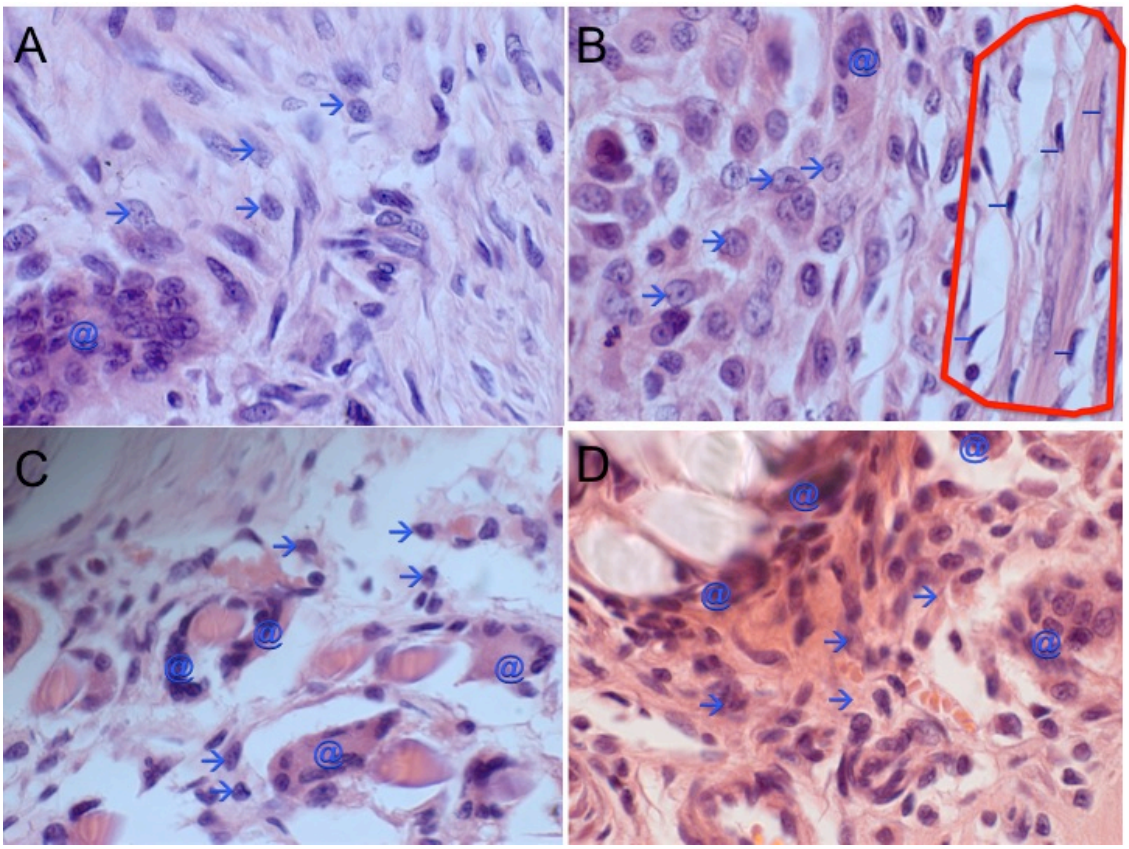

Figure 4.19 **2-week comparisons at 100x's magnification. (A) control, (B) PDOe, (C) silk, (D) PGLA constructs. Note the fibroblastic stroma [outlined in red and fibroblasts marked with (-)] near the electrospun component of the PDOe and the adjacent macrophage (→) infiltrate. For silk and PGLA macrophages (→) and FBGC's (@) predominate.**

4-Week Time-Point

The distribution and number of FBGC's was different between other constructs across all time-points with the exception of the 4-week time-point. FBGC's were sparse and remained consistent for the control repairs. For the PDOe constructs FBGC response seemed to peak at 4 weeks and then rapidly return to control levels. Again noted by blinded observers, (MEM and the independent histopathologist) was the aligned tendon-like regenerate near the patch (Figure 4.20).

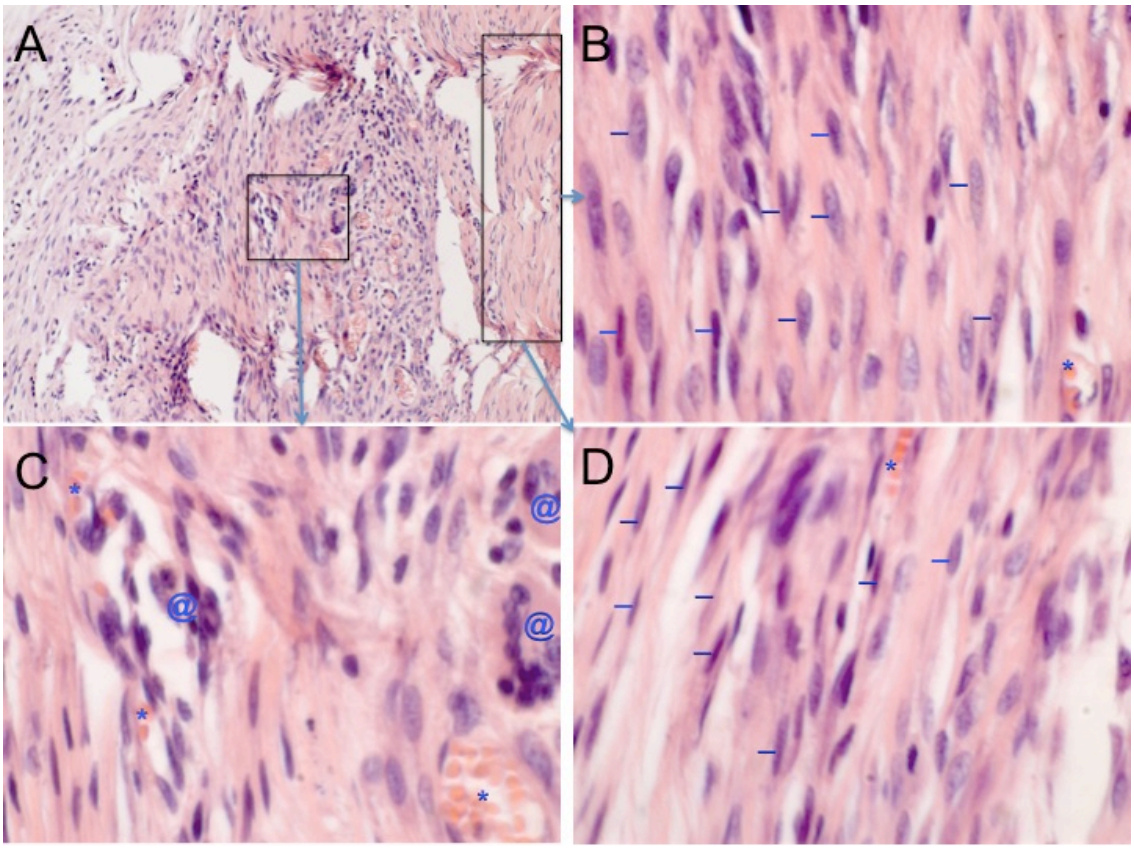

Figure 4.20 **PDOe scaffold at 4-weeks post implantation. (A) 20x's magnification shows clustering of FBGC's in the small rectangle next to aligned fibroblastic regions in the long rectangular area resembling tendon-like tissue which is shown again at 100x's magnification in (B) and (D). FGBC's in (C) are marked with (@). (B) and (D) show areas of more tendon-like fibroblastic cells (-). Also visible are areas of vascularisation (*) within the regenerate tissue.**

The 4-week time-point was the only time-point where there was no statistically significant difference between the constructs and the number of FBGC's (Figure 4.24). The FBGC's could be seen surrounding the foreign material of the polypropylene controls, PGLA and silk repairs as well (Figure 4.21-4.23). The FBGC's surrounding the silk fibres appeared to have more nuclei than other constructs. This remained the case at later time-points as well.

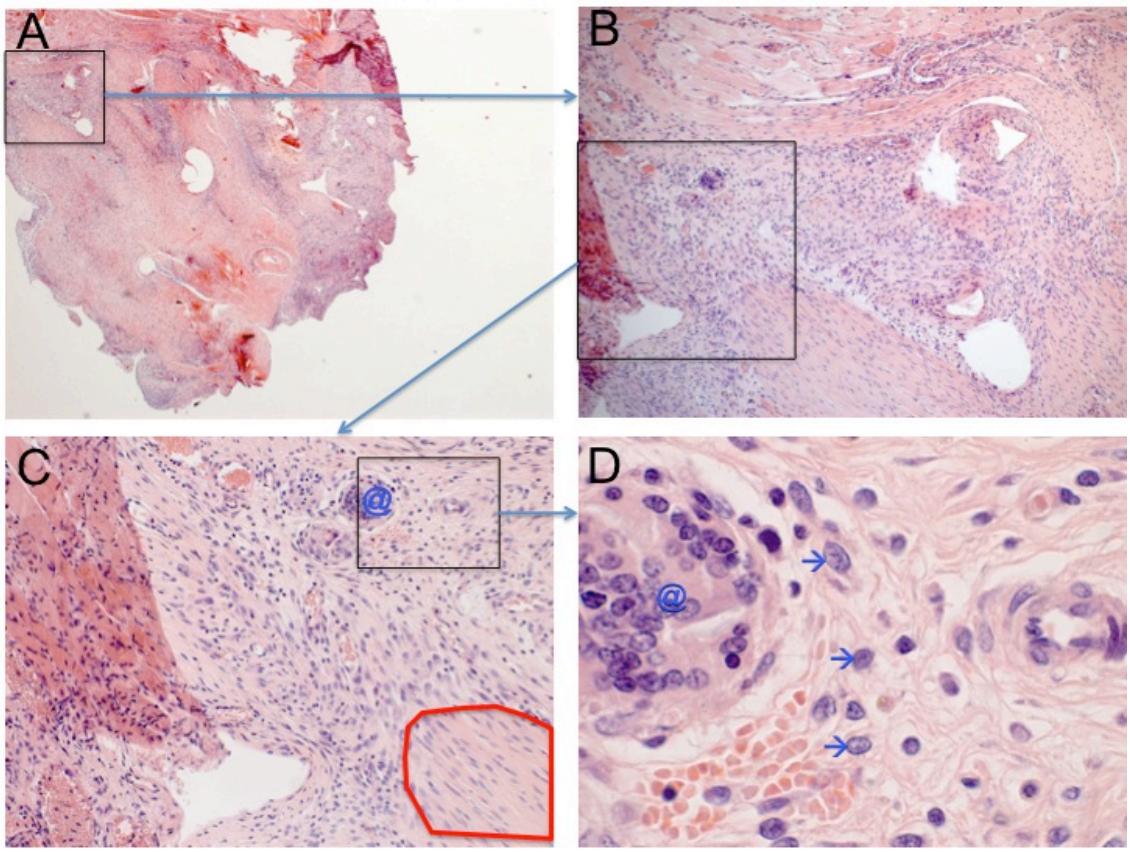

Figure 4.21 **4-week polypropylene control repairs. There are macrophages (→), fibroblasts (red outline) and FBGC (@) of the foreign body type near the suture hole.**

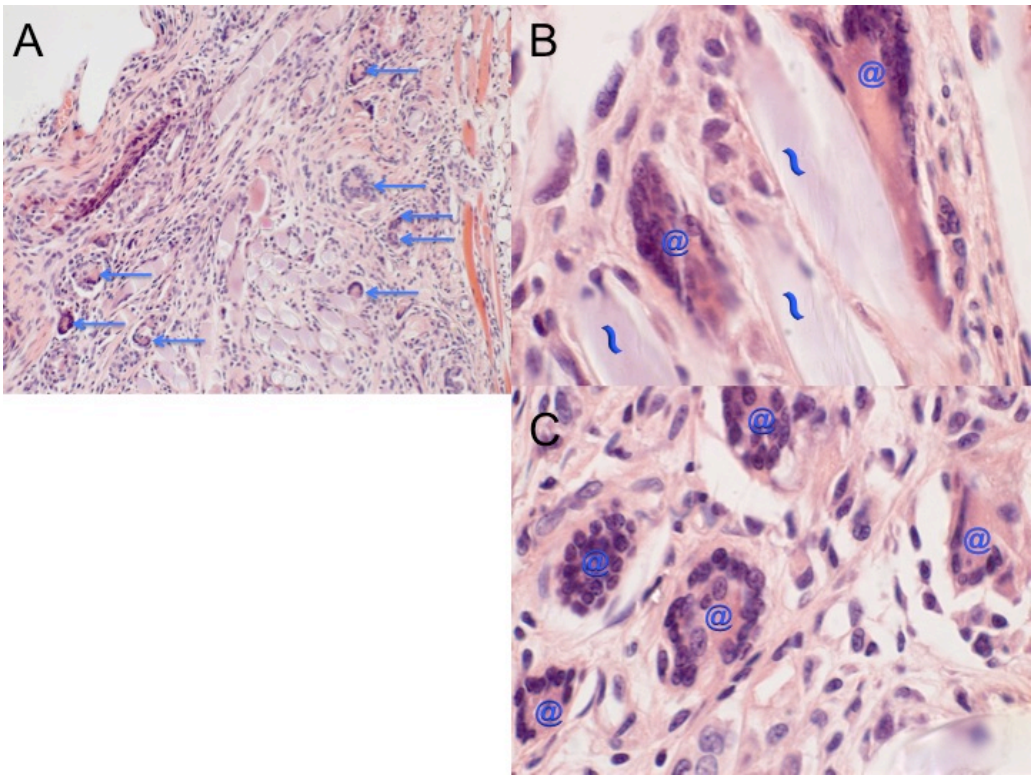

Figure 4.22 **PGLA constructs at 4-weeks. (A) 20x magnification shows FBGC's (→) throughout the construct. (B) and (C) are viewed at 100x's magnification and show a large number of Langhans-type FBGC's (@)surrounding, attached to and interspersed between the PGLA fibres (~).**

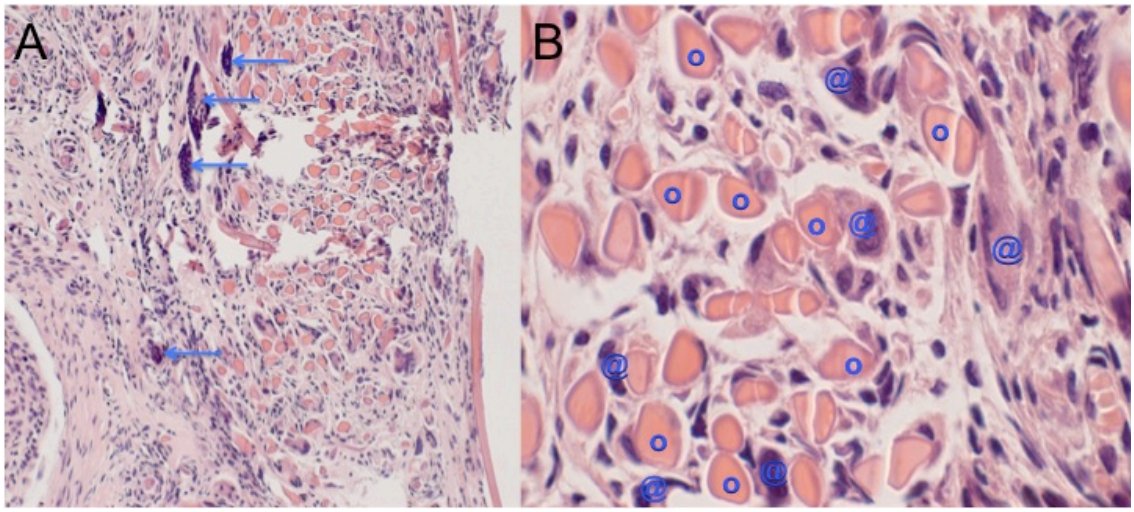

Figure 4.23 **Silk FBGC's at 4-weeks. (A) 20x magnification. Similar to PGLA constructs, there is a large number of Langhans-type FBGC's. There are more FBGC's which are larger and appear to have more nuclei within the FBGC's compared to other constructs (→). (B) 100x's magnification similar to PGLA constructs shows FBGC's (@)surrounding, attached to and interspersed between the silk fibres (o).**

The PDOe FBGC's seemed to take on a more peripheral role at 4-weeks (Figure 4.20). similar to earlier time points, there are long tenocytic-like cells in contact with the electrospun side of the material. The region of organisation was thicker and more pronounced at the 4 week time point and the electrospun component is harder to identify. While the numbers of FBGC on the PDOe implants peaked at 4-weeks, the silk FBGC response peaked at week 2, and although remaining high at 4, 6 and 12 weeks had a clear trend to reducing in number across these time points. The PGLA on the other hand peaked and remained elevated from 4 to 12 weeks. After statistical analysis significant differences between the constructs were seen at 1, 2, 6 and 12 weeks (Figure 4.24).

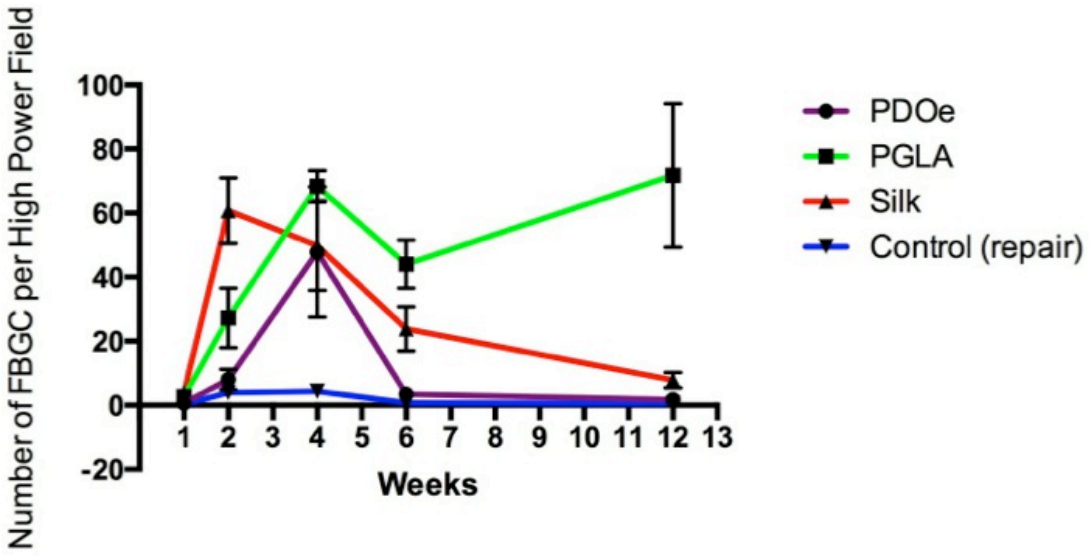

Figure 4.24 **The number of FBGC around the repair area over 12 weeks. Significant differences were seen between all constructs at all time-points with the exception of 4-weeks. PDOe had a spike of FBGC's at this time period but was not significantly different to controls at every other time-point. Error bars depict 95% confidence interval. Non-overlapping bars are statistically significant.**

The FBGC's surrounding each of the materials seemed to occur in a characteristic way. At 4-weeks when FBGC's were at their peak in the PDOe, they appeared in a characteristic ring at the periphery of the material followed by a layer of fibroblast-like cells at the patch-tissue

interface, in contrast to silk and PGLA where FBGC's were interwoven and appeared to be engulfing the fibre material.

The PDOe patch was not fixed to the slides, but the impression of the woven structure was clear with interdigitating cells. On the woven side of the PDOe patch, giant cells seem to prefer the valleys and crevices between two of the suture strands on the woven side of the construct.

At 6 and 12 weeks the FBGC response in the PDOe patch was negligible and similar to controls (Figure 4.25).

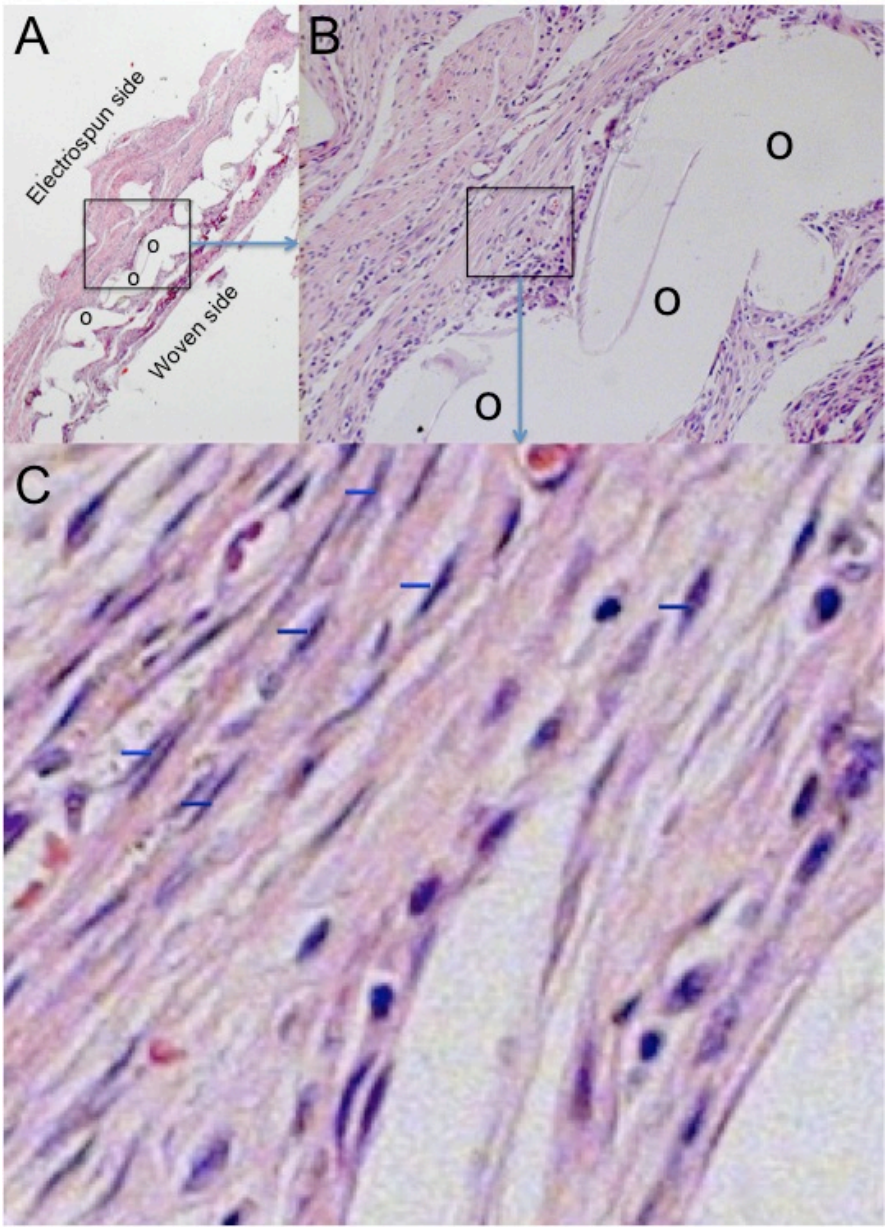

Figure 4.25 **PDOe at 6-weeks. (A) shows overview of patch at 2.5x's magnification with electrospun sides and woven sides labeled. The woven patch is marked with (o). (B) shows 20x's magnification of the rectangular area and (C) shows 100x's magnification of the rectangular area in (B). (B) and (C) show the alignment of the cells in reference to the patch and regenerate fibroblast cells (-) on the electrospun side of the patch. The electrospun component is not visible and was possibly resorbed at this time-point.**

A comparison between the slides and normal tendon at 6-and 12-weeks shows the stark contrast of the nature of the regenerate tissue and the cellular response to each construct and in comparison to normal tendon (Figure 4.26 and 4.27). Cells were aligned and elongated on the PDOe patches and disorganised and haphazard on other constructs. Control repairs at 12 weeks showed large areas of chondroid metaplasia (Figure 4.28).

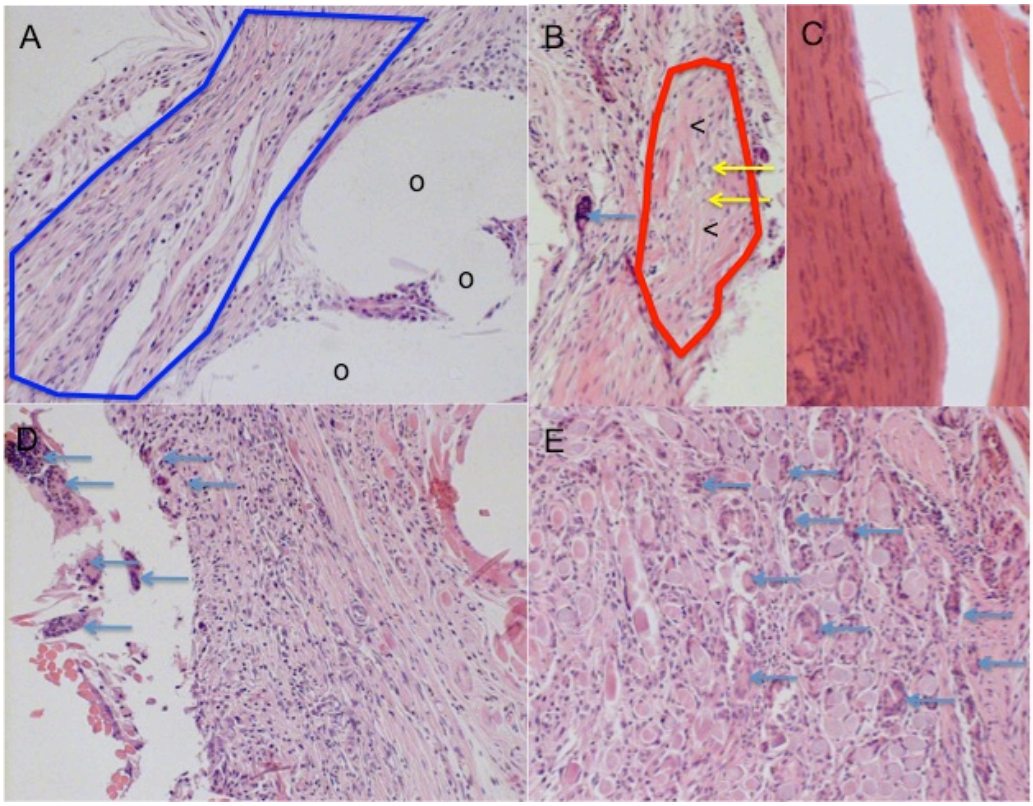

Figure 4.26 **Constructs of the patch at 6-weeks. (A) PDOe, (B) Control repair, (C) Normal tendon, (D) Silk, and (E) PGLA. The blue → denotes FBGC's and the (O) denotes where the woven structure of the PDOe patch has been cut out. Note the fibrous tissue with elongated cells (blue outline) remains on the electrospun part of the PDOe patch. Chondroid metaplasia (red outline) with round cells (yellow →)and abundant chondroid matrix (>) are evident on control repairs.**

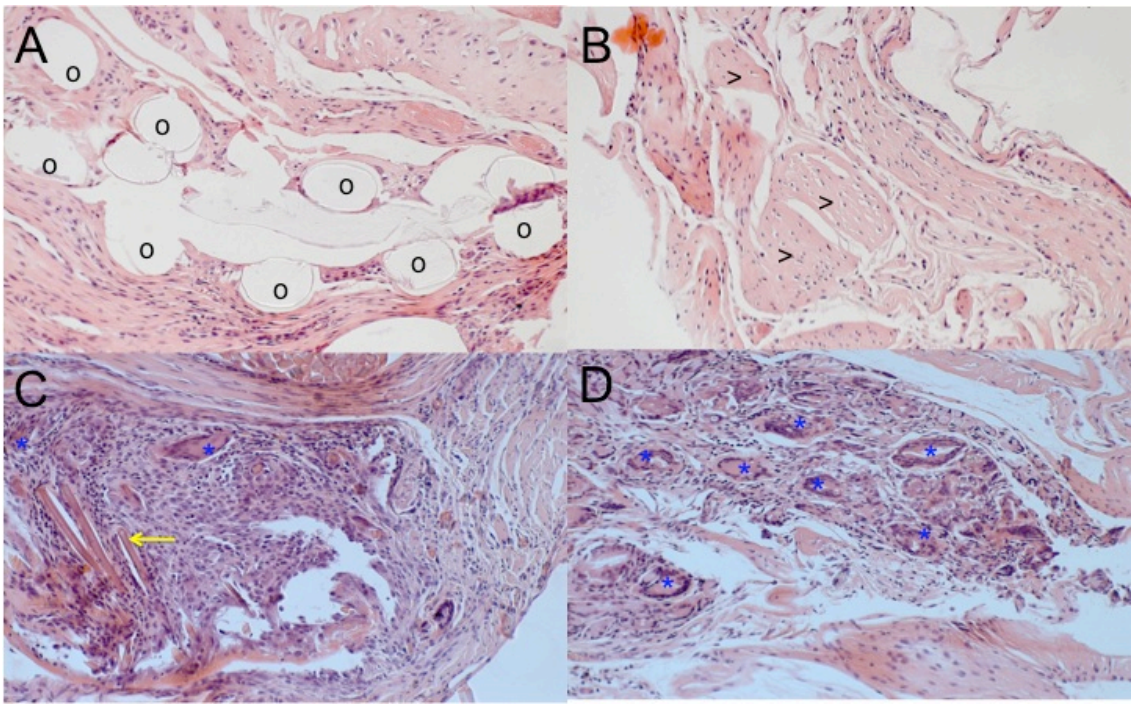

Figure 4.27 **Constructs of the patch at 12-weeks at 20x's magnification. (A) PDOe, (B) Control repair, (C) Silk, (D) PGLA patches. The (*) denotes FBGC's, the (O) denotes where the woven structure of the PDOe patch has been cut out, (>) depicts chondroid metaplasia of the control repairs with rounding of the cells in a chondroid matrix and (yellow ←) denotes visible silk fibres. Note the fibrous tissue with elongated cells remains on the electrospun part of the PDOe patch at the inferior portion of slide (A). The superior side reveals chondroid metaplasia. No giant cells are demonstrated on the PDOe image and very few were encountered at this time-point for all animals with PDOe implantations.**

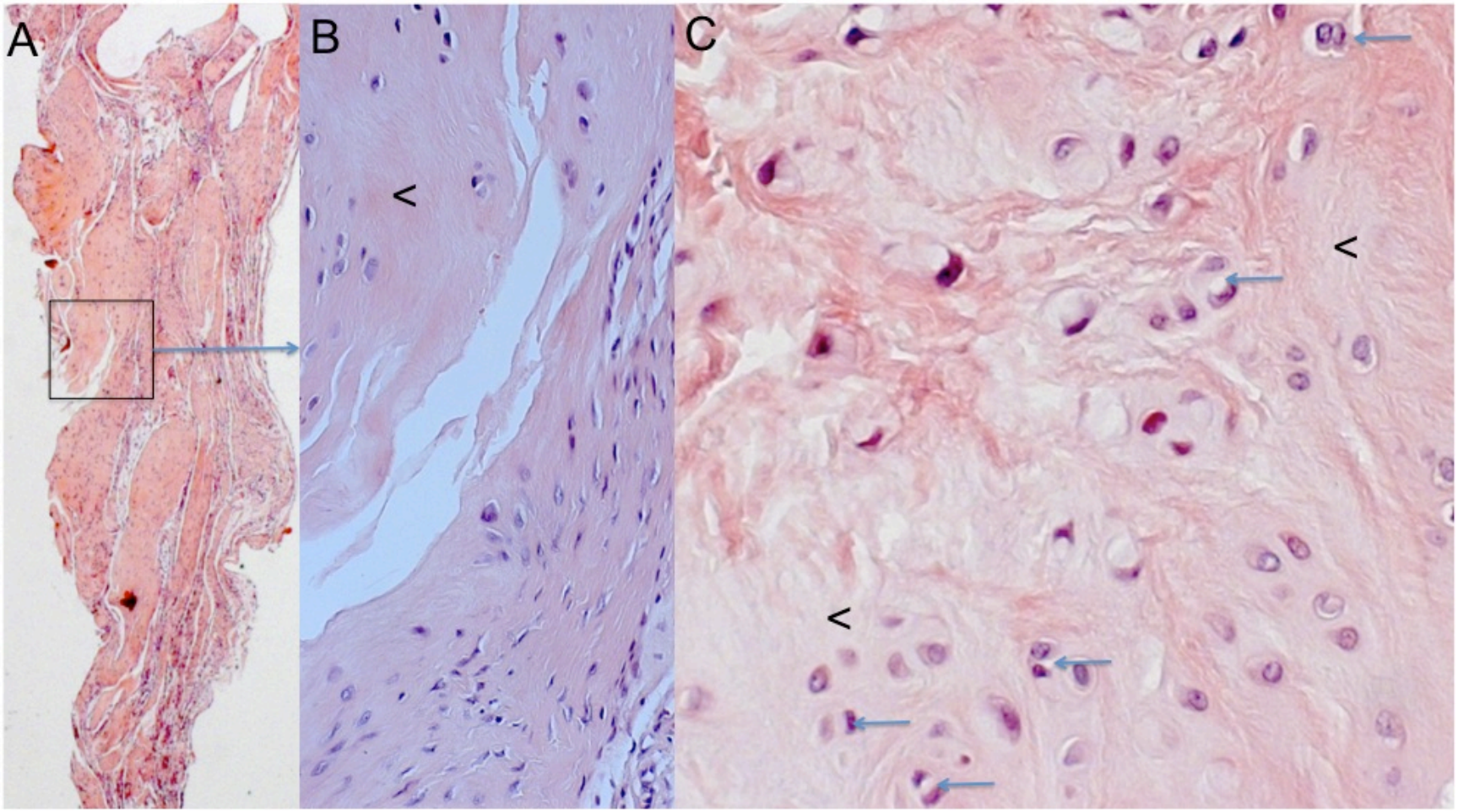

Figure 4.28 **Control repairs with chondroid metaplasia. (A) 2.5x's magnification (B) and (C) show areas at 20x and 100x's magnification. Chondroid metaplasia with round cells in doublets similar to cartilage cells (Blue →)and abundant chondroid matrix (>) is evident on control repairs.**

Macrophage Subtypes

To examine the macrophage subtypes, IHC was employed to stain for the inflammatory (M1) using iNOS or regenerative (M2) using mannose receptor (MR) stains. Representative histology images are shown in figure 4.29 for M1 macrophages, and in figure 4.30 for M2 macrophages at 6 weeks. The most heavily stained M1 macrophages were very prominent next to their respective patch constructs. M2 cells seemed to increase with time, however even FBGC's took up the MR stain as can be seen in figure 4.30 and which were also confirmed by a blinded independent histopathologist.

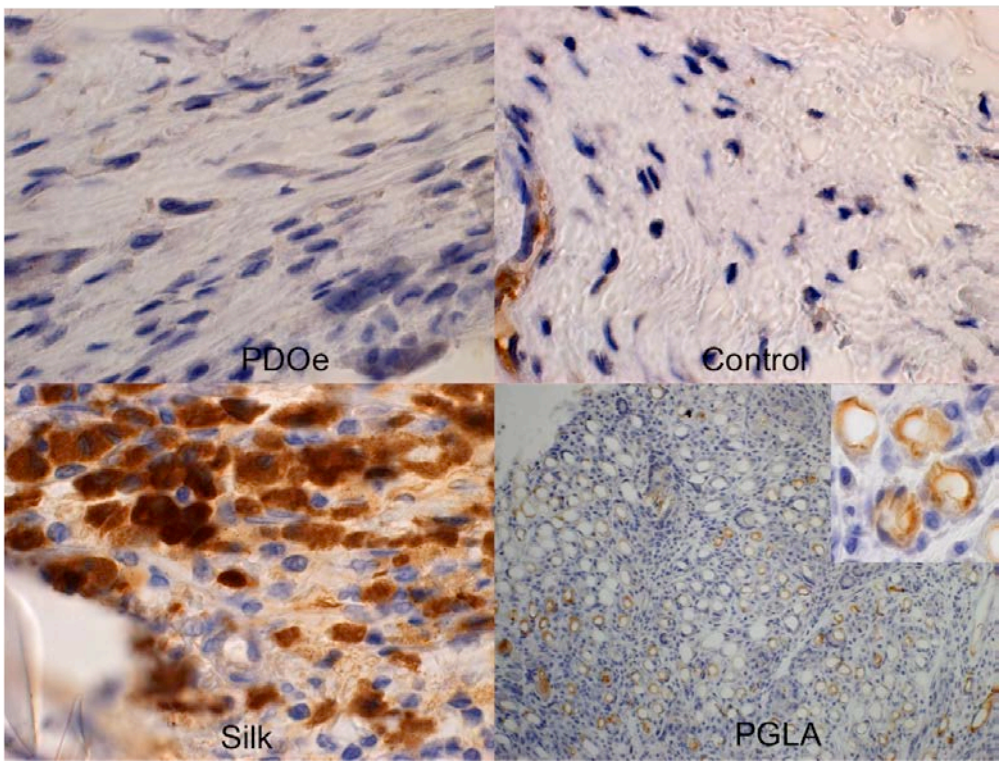

Figure 4.29 **IHC for M1 (inflammatory) macrophages at 6-weeks appears as dark brown blots. While PDOe and controls have limited staining, the PGLA (with inset) and Silk show heavy staining for this type of macrophage subset. These macrophages were clustered and very prominent directly adjacent to their patch fibres.**

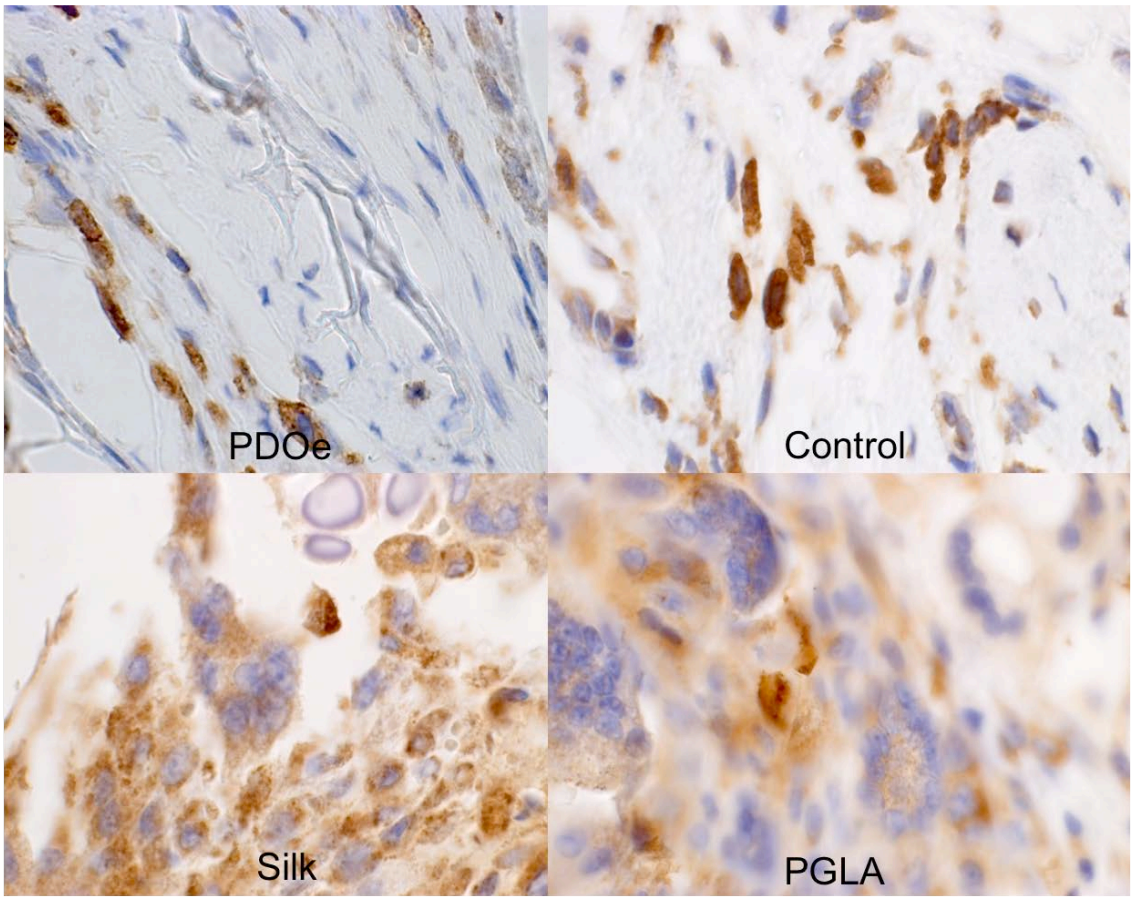

Figure 4.30 **M2 or regenerative macrophages at 6-weeks stained with… and appearing light brown. All constructs were heavily stained and increased numbers were found at later time-points. Even FBGC's appeared to take up the MR stain as shown for silk and PGLA constructs.**

The number of M1 or M2 macrophages over all time points are shown in figures 4.31 and 4.32. Ratios of M1 to total cells were significantly different for the PGLA and silk patch materials compared to controls and PDOe at all time-points again with the exception at 4 weeks. M2 cells to total cell ratios were similar between constructs at all of the time-points.

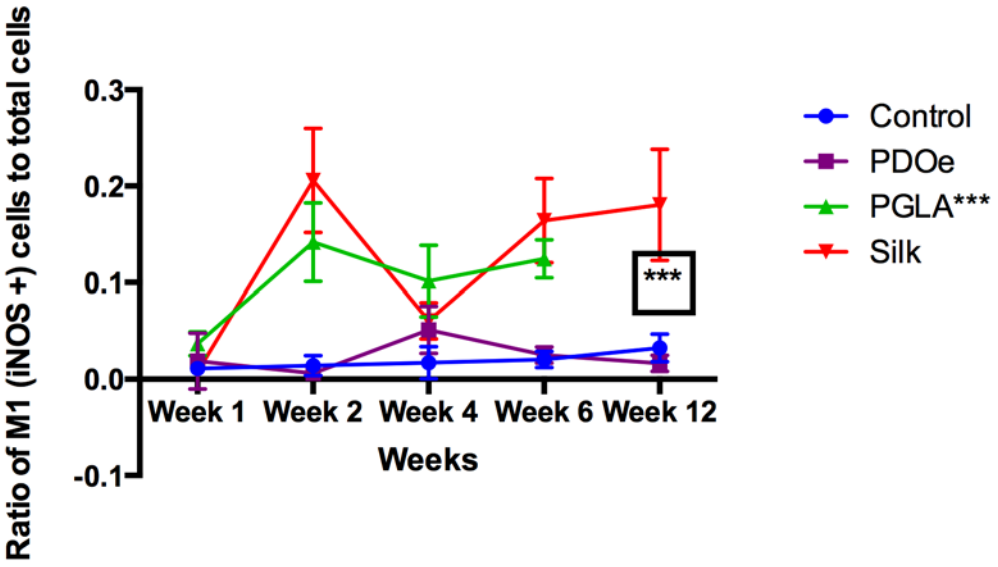

Figure 4.31 **Ratio of M1 cells to total cells at each time-point. Significant differences are noted at all-time points between silk and PGLA patch constructs compared to PDOe and controls with the exception of 4 weeks. *** FBGC's precluded the count for PGLA at 12 weeks.**

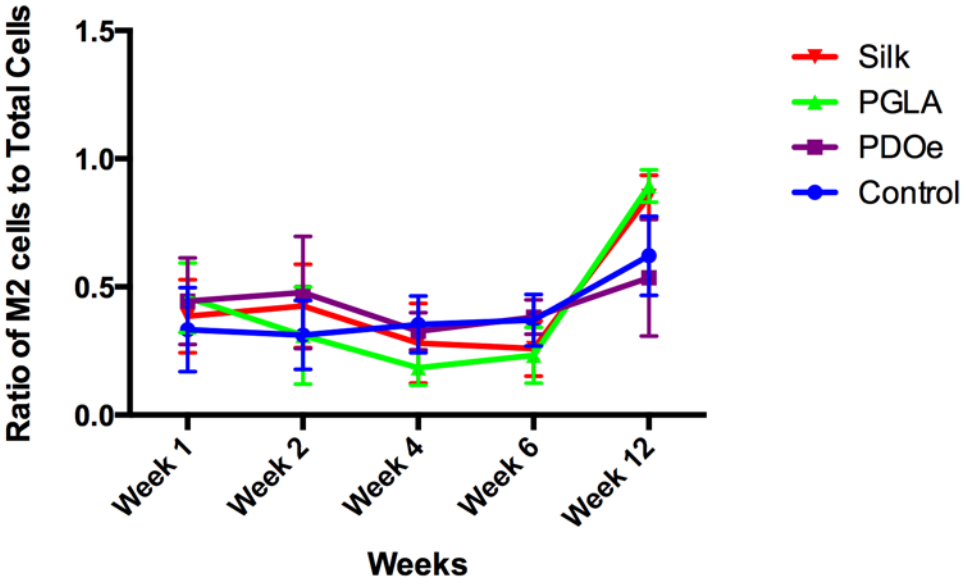

Figure 4.32 **M2 or tissue healing/regenerative macrophage ratio to total cells present with 95% confidence intervals. Massive amounts of M2+ cells were stained at 12 weeks. Note: There was no difference between constructs over time as evidenced by the overlapping 95% confidence intervals.**

Biomechanical tensile testing and electron microscopy

Tensile testing revealed that the PDOe patch maintained its original strength *in vivo* up to the 6-week time frame at around 20N (Figure 4.32).

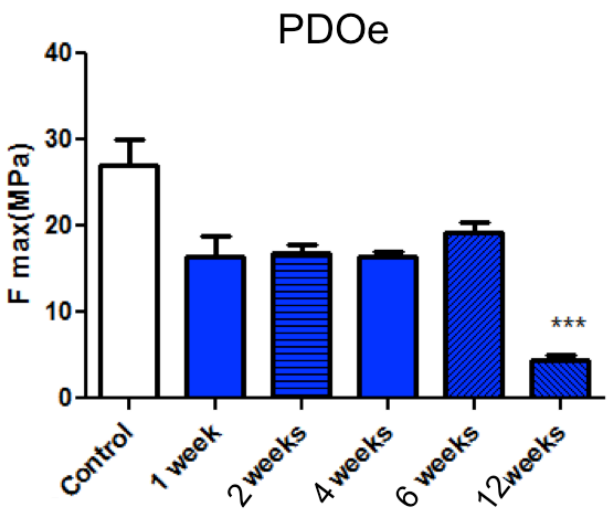

Figure 4.33 **PDOe strength to failure at different time points post implantation. The strength of the PDOe remained consistent until week 6. At 12 weeks there was a significant drop in tensile strength. Control was a dry patch which was not implanted.**

Although not statistically significant, the strength of the construct actually increased in the 1st 6-weeks slightly. Electron microscopy revealed a very adherent fibrous layer attached to all constructs over time. The woven component of the PDOe construct could be readily seen at 2- and 4-weeks, however it was less distinct as this fibrous layer thickened at weeks 6 and 12. (Figure 4.33).

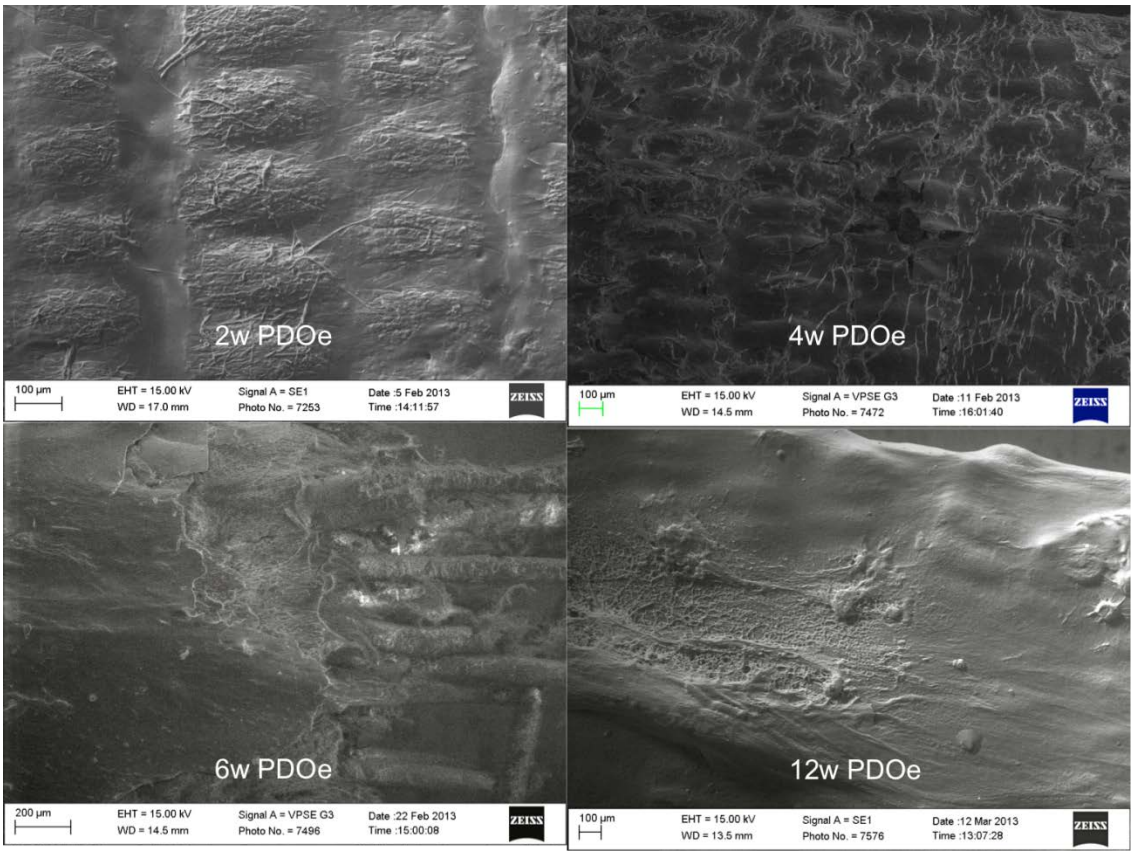

Figure 4.34 **Scanning electron microscopy images of the PDOe patch over the final four time-points as labeled. Note the matrix which has encased the material by 2 weeks and is even thicker by week 12. The week 6 image shows the depth of the encapsulating material most clearly on the left hand side of the photomicrograph as the right hand side shows how the material fails in tension. The micrograph was taken just at the point of failure.**

The electrospun side of the construct remained aligned and the fibrous material present coated it and remained intact even as the PDOe has appeared to be resorbed. Very little of the PDOe electrospun component was evident in 4-week H&E samples (Figure 4.34) and none was identifiable at the 6-week time-point. Nevertheless the cells remained aligned along the axis of the electrospun component and fibrous material likewise remained aligned over time in SEM images (Figure 4.35).

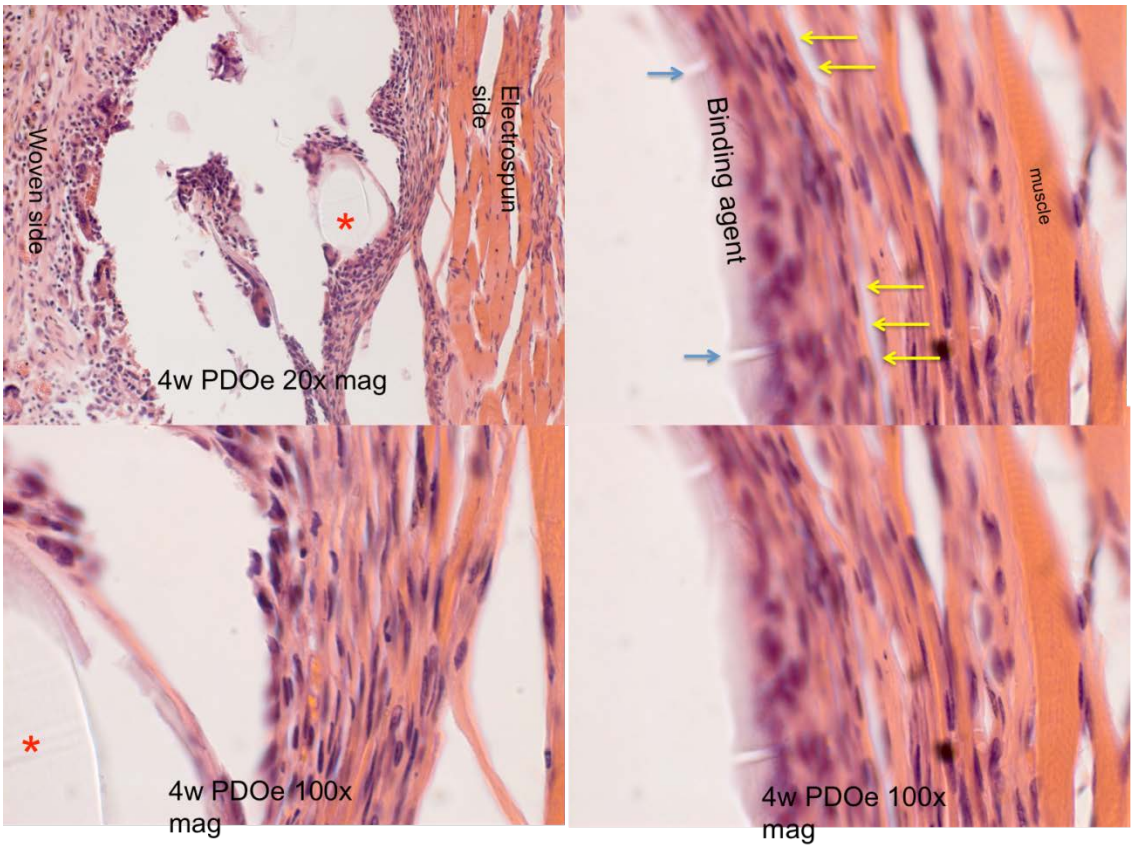

Figure 4.35 **Week 4 electrospun component (yellow ←) is barely visible as thin bluish lines within the fibroblastic stroma. Binding agent (Blue →) is visible along the interface between the woven (*) component and the electrospun component. Muscle is identified on the electrospun side of the patch deep to the regenerate tendon. Several FBGC's can be seen in the 20x mag micrograph, particularly on the woven side of the implant.**

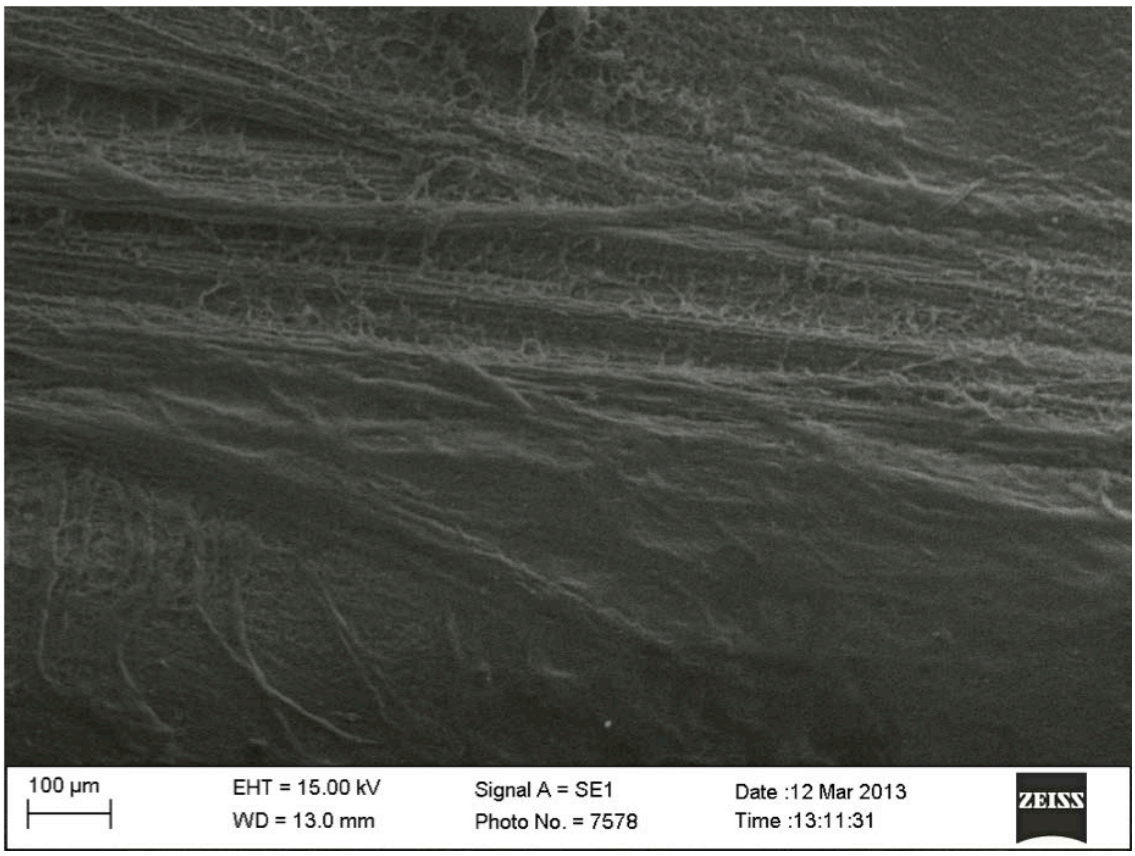

Figure 4.36 **An SEM image of the electrospun side of the construct at 12 weeks. Note the fibrous and aligned appearance of the encapsulating tissue.**

The other constructs tensile strength testing results are shown in figures 4.36 and 4.37.

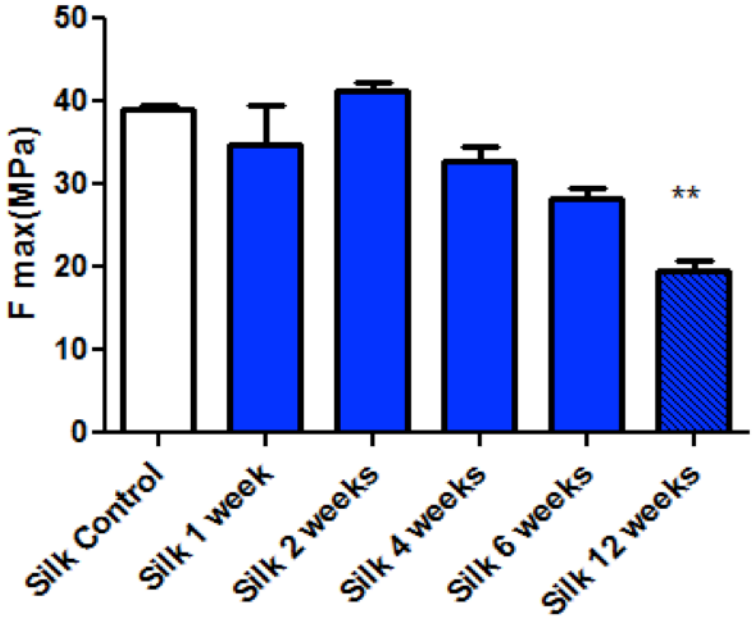

Figure 4.37 **Silk tensile testing over time. Again seen is a slight, but non-significant increase in strength between 1- and 2-weeks and a gradual reduction in tensile strength thereafter becoming significantly weaker at 12 weeks.**

The silk as a non-degradable polymer had the highest tensile strength with around 35N for the 1st 4 weeks and then decreasing to 20N at 12 weeks. PGLA, a more rapidly absorbable suture became weak in tension very quickly with significant differences noted between 2 and 4 weeks and across all time-points when compared to week-1 values (Figure 4.38). None of the PGLA material remained grossly identifiable by week-12 to perform tensile testing.

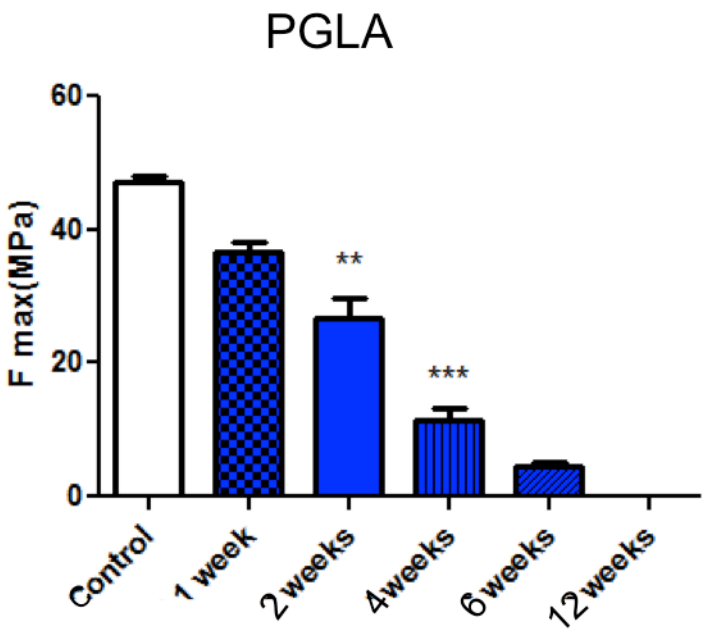

Figure 4.38 **PGLA (Vicryl) strength to failure at different time points post-implantation. A rapid and significant reduction in strength occurred over time. At 12 weeks there was no identifiable material present at the site of surgery in order to perform the tensile test.**

Chapter 5

5. Discussion

The ability to reliably heal RC lesions is of great importance to both orthopedists and their patients. Surgical management of RC tears continues to evolve and, although repair techniques have improved, failures or re-tears remain a substantial problem[23-30]. Because of the high failure rates, biologic solutions are increasingly sought to improve upon these results. Multiple strategies have been investigated including platelet rich plasma (PRP)[193-195], stem cells[184,196] and growth factors[197] and tendon 'patches'[104] or a combination thereof in an attempt to stimulate RC healing.

PRP has been used to try and encourage healing on the basis of increased growth factors present in the various formulations available. On the basis of promising case studies and case series, several randomised controlled trials have been instituted [193-195]. Unfortunately, the most recent randomised controlled trials were equivocal in terms of healing with one showing a benefit to PRP[193] and the others no difference[194,195]. Furthermore, the most recent trial with plasma rich in growth factors also failed to show a difference in healing rates[198] and these trials investigating PRP or growth factors to date have shown no functional improvement.

Bone marrow mononuclear cells have also been injected around the tendon after repair[196]. These investigators found that 14/14 patients demonstrated healing of the tendon at 1 year and 13/14 at two years. While this pilot case series seems to show promise, there was the potential for a significant bias with unblinded participants and surgeons. The authors rightly point out the need for more rigorous trials but were encouraged by the improvement in the

healing rates seen in their study.

While the concept of these therapies is appealing, based on the rationale that more growth factors should increase tendon healing, this has not born out in practice. Despite the increased interest and awareness of the need for biologic solutions for RC healing, the efficacy of RC repairs remains a challenge as between 20% to 94% are reported to fail[23-30]. In fact, the longer the time from operative intervention, the greater the likelihood that failure will occur. In the longest follow-up study of RC repairs to date, with a mean of 20 years follow-up, 94% had failed[30].

Tissue engineering strategies utilising scaffolds to influence the microenvironment of the healing tissue are one potential way of introducing biologic support to repairs. In previous studies, we developed and tested a novel polydioxanone (PDO) tendon patch *in vitro* and found that it had excellent biomimetic properties. Cellular ingrowth and degradation kinetics supported its role as a potential synthetic solution to increase the healing rates of torn tendons. The requisite final step to human trials is an *in vivo* safety and biocompatibility study. Despite the widespread use of PDO in sutures, the novel construction of the patch requires that it has extensive safety testing prior to its use in humans. Unfortunately, with previous commercial patches, incomplete or lack of biocompatibility testing has led to problems with inflammatory reactions and early failure for RC repairs. Walton reported a case series of 15 patients (16 shoulders) with large to massive RC tears who were treated by surgical repair with an intestinal submucosal implant (SIS) (Restore® De Puy) in Australia[139]. This implant primarily consists of a xenograft collagen scaffold obtained from porcine donors and processed for human implantation. Patients in Walton's study were originally enrolled in

a randomised controlled trial that was subsequently halted due to safety concerns about the inflammatory reactions in this group. The 16 patients who were treated by conventional surgical repair without the submucosal graft were used as a comparison group. Results from this study showed that, not only did a significant proportion of patients have inflammatory reactions (25%), they also had higher activity related pain scores at 3 months and less participation in sport.

Malcarney [138] similarly reported 4 cases of early inflammatory reaction after RC repair with the same implant among 25 patients. These reactions occurred at a mean of 13 days after surgery and were characterised by a response similar to infection with erythema and fluctuance. Two of the patients even had active drainage. All four patients underwent subsequent surgical debridement and irrigation of the RC and surrounding soft tissues. At the time of surgery a large amount of yellowish mucinous debris was found in the region of the repair. Infection was ruled out in all cases with negative cultures, yet histopathology revealed an acute inflammatory reaction to the implant. Importantly, there were no eosinophils to suggest an allergy or giant cells to suggest a typical foreign body reaction.

Corroborating an immune mediated reaction to the implant, Zheng *et al*.[199] examined the Restore patch and specifically analyzed it for cell and deoxyribonucleic acid (DNA) constituents. These researchers found that the SIS graft contained multiple layers of porcine cells including mast cells and PCR confirmed the presence of porcine DNA material. After implantation in both mice and rabbits, they showed that a massive inflammatory reaction ensued which was comprised of a lymphocytic infiltration. This study calls to question whether any allograft material is truly without biologic constituents that could react with the

hosts' immune system.

Furthermore, even synthetic mesh materials illicit a biologic response. Similar to some of the RC patches, synthetic mesh materials used in hernia and gynecologic surgery have had to be recalled due to high complications with erosion, rejection and infection[200]. These devices were approved through the FDA's 510K process. What this process entails is an approval of a device based on equivalence to an existing implant in terms of use, efficacy and safety. In the case of meshes used in hernia and gynecologic surgery, a specific device was recalled for the above safety concerns. Incredibly, prior to and after the recall 40 additional implants were approved based on the faulty implant's initial approval. This process has led to widespread criticism of the FDA, but more importantly a heightened awareness of the risks of all types of implantable devices whether they are biologic or synthetic. Because it has been shown that merely altering the size, porosity or architecture of scaffolds can have profound biologic consequences, it is necessary to test for biocompatibility with any change in the architecture of patch materials[107,115].

This thesis provides a potentially novel method for testing the biocompatibility of future implants. While efficacy of rotator cuff repairs in animal studies are often difficult to translate in animal models because of their ability to heal more robustly than humans [162], elements of biocompatibility can, and should be, tested given the similarities of the immune systems even between higher and lower species [181-183]. By examining both the responses of inflammatory cells in addition to the location of the implantation, as in this thesis, we believe a more comprehensive safety assessment can be achieved. Finally, in addition to traditionally studied response of neutrophils, macrophages and foreign body giant cells, others have begun

to analyze the lymphocytic response to biocompatibility[158]. Thus, future tissue scaffolds may also incorporate lymphocyte responses to biomaterial implantation as well. Certainly, it has been shown that T-lymphocytes cells in particular influence the formation of FBGC's by their release of interferon gamma[158]. By utilizing measures of immune response we believe that a higher margin of safety can be achieved prior to implantation, hopefully reducing the adverse reactions that have been seen with implants lacking such analysis.

While PDO sutures have a proven track record, by altering the physical topography, architecture, quantity of polymer in the joint and the manufacturing process (which includes electrospinning, which involves a harsh solvent), biocompatibility must be thoroughly tested. One of the goals of this thesis was therefore to characterise the biocompatibility of a novel laminated woven and electrospun PDO patch (PDOe). Our hypothesis was that the PDOe patch would be biocompatible and thus safe for implantation. Biocompatibility was measured through the foreign body response (FBR) including direct count and comparison of FBGC and macrophage subtypes with several different implantable biomaterials; a strategy often employed in other mesh studies[201]. We have shown in our *in vivo* experimentation that PDOe with its nanoscale electrospun component elicits very little FBR. Our model revealed that although a FBGC response is seen in all constructs, the PDOe construct FBGC response peaked at 4 weeks and returned to control levels at 6 and 12 weeks without rejection or infection of the implant. The Silk patch FBGC response peaked at 2 weeks and also decreased from this time point although remained significant up to 12 weeks. Silk patches had very thick fibrous tissue surrounding the implants rather than desired incorporation. Finally, PGLA FBGC's continued to increase even up to 12 weeks after surgery. Furthermore, although there was no

drainage from the wounds, the massive transudative reaction at one and two weeks to the PGLA was very concerning.

Our data supports a macrophage-mediated response to each of the constructs. With the PDOe the peak in FBGC's at four weeks may be due to the particulate debris as the implant degrades. In fact, because the implant degrades by hydrolysis which is dependent on surface area, the 4-week peak may occur more quickly for the electrospun component of the implant due to its higher surface area and near complete degradation at this time-point. Nevertheless, this response had completely resolved at the later time-points as evidenced by the absence of any FBGC's. Moreover, regenerate tissue, that is, organised scar tissue containing cells with a tenocytic appearance in a background of organised collagen appearing bundles, was present adjacent to the implant. It is possible that by creating the proper micro-environmental cues, such as shape, size and orientation of the electrospun component of the PDOe patch, the acceptance of the implant is facilitated[100]. Furthermore this orientation allows for a more tenocytic morphology of regenerate tissue as has been shown in our laboratory's *in vitro* studies.

In terms of tensile properties, there was no significant reduction in strength in the first six-weeks after implantation with the PDOe patch. The fact that no tensile differences were seen at 6 weeks suggests that, as predicted, the electrospun component has little contribution to the tensile strength of the implant, but rather acts merely as a scaffold to direct cell behavior.

Despite efforts to dissect off all tissue from the patch constructs, we noticed that all constructs had a fibrous material which was adhered tightly to the implants. Although, no specific assays were performed to identify the nature of this adherent tissue, this layer was

likely made up of fibrin in the early stages and of other adsorbed proteins later.

Our results revealed a statistically higher M1, or inflammatory, macrophage and FBGC response to the PGLA and silk patch materials compared to the PDOe patch and controls. The findings of macrophage counts are similar to those found in bone fixation devices for PDO [202]. These investigators found that macrophages increased at 3-weeks post-implantation and decreased steadily and were almost nonexistent at 12-weeks. This corresponds to the number of FBGC's seen in our experiment.

Interestingly, the peak for the M1 macrophages corresponded to the peak in the FBGC's also seen at the 4-week time-point for PDOe. The significance of this finding is unknown and requires more experimentation, but several possibilities may exist. One explanation would seem to be that the M1 macrophages directly or indirectly are producing a cytokine profile that is driving the fusion of macrophages into Langhans-type FBGC's. The cytokine profile recognised as responsible for fusion to Langhans-type FBGC's in most instances are INF-gamma in the presence of either IL-3, or macrophage colony stimulating factor (M-CSF) released from antigen presenting cells (APCs), mast cells and TH1 cells or even other macrophages[146,158]. It is interesting to note that M1 cells are TH1 mediated which may explain this characteristic FBGC response (Figure 5.1).

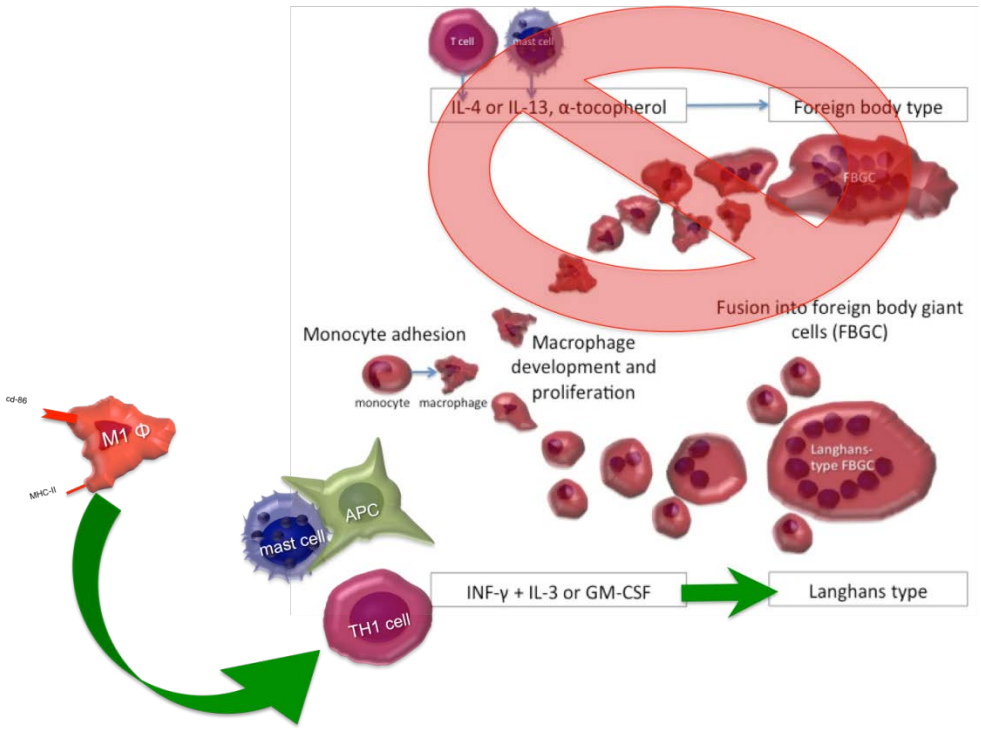

Figure 5.1 **One possible explanation for the large number of Langhans FBGC's seen in the responses to all biomaterials and the corresponding increase in M1 (inflammatory type) macrophages. M1 macrophages may signal TH1 cells which then release cytokines characteristic for fusion to the Langhans-type FBGC. Other possibilities for release of this type of cytokine profile includes mast cells, APC's and even other macrophages. Image modified and adapted from reference[158].**

As discussed previously, the interaction of the immune system with the implants, possibly driving the fusion of these cells may have important implications for future designs of biocompatible implants.

Although previous work showed cell necrosis to PGLA implants *in vitro*, cell death could not be quantified in this *in vivo* experiment. However, with such a large transudate and gross necrotic debris, this finding seems to, at least in part, corroborate the *in vitro* findings of Hakimi *et al*[134]. Both this fact and the massive FBGC response seen to PGLA seems to be in contrast to Aurora *et al*[169] who have published excellent biocompatibility to patches with components of PGLA. While their study examined a hybrid PLLA/PGLA patch (in a 66/34 ratio

by percent weight) (construct with fascia lata, only one representative histologic sample and no quantification of the responses were made. Using purely descriptive techniques may be appropriate in some instances, but when implantation into humans is the ultimate goal, a more robust examination of the response should be undertaken. Nevertheless there were other differences to our experiment including fibre diameter, which, as we have seen, plays a key role in inflammation as well as the ratio of PGLA to other polymers within constructs used in the Aurora study.

In addition to the FBR, equally important is whether or not juxta-articular implants cause any harm to the articular cartilage. This potential effect of patch materials, to our knowledge, has never been examined. This may be a critical oversight if, in fact, there is an inflammatory reaction that could be destructive in nature. There are many models of adjuvant-induced arthritis and a link between systemic inflammatory arthropathies and foreign antigens have been proposed[203]. Fortunately, in our experiment none of the materials produced any untoward effects not only to the local articular cartilage, but also systemically as judged by the lack of response in hind paw swelling and the normal articular cartilage seen in all animals implanted with biomaterials, which also confirmed our hypothesis. This is particularly encouraging as this animal was specifically chosen because of its propensity to develop adjuvant induced arthropathies[204].

Finally, it bears mentioning that even with the best biocompatibility testing, when a response is found in the animal, its true relevance to humans is still unknown [167]. Thus, clinical trials are paramount to discover the true effects of this material in humans. Nevertheless, in pre-clinical biocompatibility tests, it is normally assumed that humans will respond in a similar way

to animals, although this assumption can rarely be tested[167].

Limitations

There are several limitations to the experiments conducted. Despite our best efforts, there is always a question of adequate tissue sampling when conducting histologic studies. Sampling error and the fact that patch material was so difficult to cut, should result in caution when interpreting the results. Multiple slides needed to be examined to locate the electrospun component's orientation to the patch and any suggestion of efficacy should bear this in mind. In future studies, frozen section or resin embedded tissue sections may be attempted to alleviate this problem. However, this limitation was relevant to all the tested materials, and as biocompatibility was the main aim of the thesis, histological methods are considered the best estimate of this response.

Additionally, the response of the immune system is complex involving both innate and adaptive immunity. The foreign body response is largely an innate response. While FBGC response was used as a surrogate for the extent of tissue reaction, some doubt exists as to whether FBGC response is overall a negative component of tissue reaction to implants. For example several disease states including respiratory syncytial virus (RSV) infections require FBGC's in order to heal normally. The PGLA had a massive response due to its rapid and early degradation. This response may have totally abated at a later time-point when the phagocytic cells had cleared the foreign material similar to the resolution of RSV. Nevertheless, it has been accepted that for the most part when biomaterials are involved, a FBGC response is an attempt to wall off a foreign material. This response often causes excessive fibrosis, and contracture and ultimately poor performance of the implant. Therefore, as a surrogate to a

negative response to a biomaterial, this is an appropriate measure. Indeed, we found fewer FBGC's in the PDOe construct which would seem to support incorporation and acceptance rather than rejection of the material.

It has also been suggested that there is an additional peak of inflammatory cell action at the time of final degradation. For rapidly degrading implants this may appear to occur along a continuum, but for more slowly degrading implants there may be a bimodal peak- one at the time of implantation due to the inflammatory reaction to the surgery and one when the material ultimately degrades. This has been shown for silk, which can have adverse tissue reactions years after implantation[205]. To truly see whether or not the PDO remains benign, this portion of the experiment needs longer time-points after implantation to observe its effects at final degradation. Since PDO degrades slowly (180-190 days is the typical degradation profile for suture) it might be more appropriate to examine the tissue at this time-point. Interestingly however, 4-months have been shown to be a reliable degradation time-point in other PDO implants of larger bulk[202]. Regardless, studies following these materials out to longer time-points are currently underway.

One criticism of our thesis design may have been the controls utilised. While both PGLA and silk proved to be good positive controls for the FBR, another test which may have examined the effects of fibre size in addition to the chemical structures of the patches, on the immune response would have been to use electrospun silk and PGLA. This is something to consider for future studies, but does not diminish the positive biocompatibility of the PDOe patch, but rather highlights the fact that in the case of synthetic patches, structural topography may be of importance as well.

Another potential limitation is the fact that the sterilisation procedures utilised in these *in vivo* experiments were not ethylene oxide. Since ethylene oxide is the standard of sterilisation for these types of implants, there may have been some potential for contaminants to enter the system. Despite this, no contaminants or bacteria were seen on microscopy and ethanol is bactericidal. Nevertheless, prior to implantation into humans a validation of the relevant sterilisation procedures is requisite.

Finally, we did not stain for other inflammatory mediators or cells that may be important in the FBR. As helper T-cells (TH) TH1 are known to signal macrophages and be important for macrophage fusion to FBGC's by their elution of IL-3 with INF-ϒ to form Langhans-type FBGC's and TH2 cells elute IL-4 to promote fusion of traditional FBGC's, this may be an important connection. Certainly, the types of FBGC's seen were of the Langhans-type, which would suggest that the response to these materials is a TH2 mediated process. Nevertheless, this examination would be hypothesis generating and delving into the mechanisms of FBGC's formation in the response to these materials was not the intent of this body of work. Furthermore, with such a minimal response the biocompatibility of the PDOe implant, which was the main goal of the *in vivo* experimentation, was confirmed.

Chapter 6

6. Future Direction

In this thesis we demonstrated that the novel PDOe patch was biocompatible in the rat model of tendon repair. What remains, is to test not only the FBR response, but ultimately the efficacy and biocompatibility of the PDOe patch in humans. Initially, a small safety pilot study can and should be undertaken. If there are no adverse reactions, then a larger scale human trial to determine the efficacy of the patch material can be considered. Traditional patient reported outcome measures (PROMs) such as the Oxford Shoulder Score, which has been shown to have high sensitivity to change after shoulder surgery and been tested to provide reliable and valid measurements of shoulder symptoms and function should be utilized[206]. In addition to the PROMs objective strength testing should be entertained, as an intact cuff has been shown to have better functional outcomes in the long term[28-30,53,98]. MRI healing rates and ultimately biopsy of the reconstructed area should provide more objective criteria of healing rates.

On a mechanistic and molecular level, the macrophage subtype and FBGC response and the interaction of the adaptive immunity to biomaterials warrants further study. As discussed above, the fact that there was a characteristic Langhans-type FBGC suggests a signaling interaction between the adaptive and innate cell types and in particular the TH1 cells. The nature and significance of this interaction is unknown, however this possibility merits further exploration.

With regards to biomechanical testing prior to human implantation, further suture retention studies are warranted. While this experiment showed no decrease in tensile strength up to six weeks, failure mechanisms suggest that suture pullout may be more important than overall tensile strength of the implant. If the ultimate reason for scaffold failure is its attachment via sutures, this can and should be focused on prior to human implantation. This work is currently underway.

The ability of the body to recognise the microenvironmental cues seems to be supported by the different macrophage subpopulations seen in response to the different materials. If a characteristic response is seen, this can be used to assess the biocompatibility of implants. If this response is reproducible in humans, it gives validity to the model and will allow for other materials to be tested in a similar way. It is intriguing that by merely altering the shape or size of the implanted materials changes the host's response to the materials. A new paradigm is emerging in which biocompatibility testing should be done not only for alteration in the chemical makeup of the biomaterial, but also for topographical alterations in a material. This has been neglected in the past, but may have massive repercussions if implanted materials physical alteration leads to very different responses. Examples of this include metal on metal hip prosthesis and the "pre-coat" in total elbow arthroplasty implants. Both of these implants were approved without testing and both have had significant detrimental effects; the metal on metal inducing ALVAL and tumor-like responses and the pre-coat implants leading to massive osteolysis and implant loosening and failure[207-209]. We can now capitalise on the ability of implants to have different responses to implant architecture. Further study is being done on different prototypes with different woven and electrospun components of the PDOe implant and comparing these to other materials which have been implanted, but for which

biocompatibility data is unknown or has not been published by the manufacturers of these implants.

In conclusion, we have shown that this PDOe tendon scaffold is biocompatible and maintains its strength during the early, and probably critical, phase of healing. These findings should be corroborated in human clinical trials in the near future so that efficacy studies may ensue.

Appendix 1

ImageJ macro used for automated cell counts

The first cell count counts the entire number of cells and the second counts only those with immune staining. Thresholds were changed to ensure accuracy of counting by validating with hand counts. All slides were independently hand counted to ensure accuracy.

Cell count (blue nuclei-colour 1)

```
imgName=getTitle();
run("Colour Deconvolution", "vectors=[H DAB]");
selectWindow(imgName+"-(Colour_1)");
setAutoThreshold("Default");
//run("Threshold...");
setThreshold(0, 190);
run("Convert to Mask");
run("Fill Holes");
run("Despeckle");
run("Remove Outliers...", "radius=10 threshold=50 which=Dark");
run("Analyze Particles...", "size=10-Infinity circularity=0.00-1.00 show=Nothing display summarise");
```

HDAB stained cells (brown-colour 2)

```
imgName=getTitle();
run("Colour Deconvolution", "vectors=[H DAB]");
selectWindow(imgName+"-(Colour_2)");
```

```
setAutoThreshold("Default");
//run("Threshold...");
setThreshold(0, 80);
run("Convert to Mask");
run("Remove Outliers...", "radius=10  threshold=50 which=Dark");
run("Analyze Particles...", "size=10-Infinity circularity=0.00-1.00 show=Nothing
display summarise");
```

]

References

1. Oh LS, Wolf BR, Hall MP, Levy BA, Marx RG. Indications for rotator cuff repair: a systematic review. *Clin Orthop Relat Res* 2007;455:52-63.

2. Teefey SA. Shoulder sonography: why we do it. *J Ultrasound Med* 2012;31-9:1325-31.

3. Worland RL, Lee D, Orozco CG, SozaRex F, Keenan J. Correlation of age, acromial morphology, and rotator cuff tear pathology diagnosed by ultrasound in asymptomatic patients. *J South Orthop Assoc* 2003;12-1:23-6.

4. Moss EL, Jones PW, Newbould D, Luesley DM. The role of regional anaesthesia in the surgical management of vulval malignancy. *Journal of obstetrics and gynaecology : the journal of the Institute of Obstetrics and Gynaecology* 2014:1-5.

5. Vitale MA, Vitale MG, Zivin JG, Braman JP, Bigliani LU, Flatow EL. Rotator cuff repair: an analysis of utility scores and cost-effectiveness. *J Shoulder Elbow Surg* 2007;16-2:181-7.

6. Aurora A, McCarron J, Iannotti JP, Derwin K. Commercially available extracellular matrix materials for rotator cuff repairs: state of the art and future trends. *J Shoulder Elbow Surg* 2007;16-5 Suppl:S171-8.

7. Urwin M, Symmons D, Allison T, Brammah T, Busby H, Roxby M, Simmons A, Williams G. Estimating the burden of musculoskeletal disorders in the community: the comparative prevalence of symptoms at different anatomical sites, and the relation to social deprivation. *Ann Rheum Dis* 1998;57-11:649-55.

8. Linsell L, Dawson J, Zondervan K, Rose P, Randall T, Fitzpatrick R, Carr A. Prevalence and incidence of adults consulting for shoulder conditions in UK primary care; patterns of diagnosis and referral. *Rheumatology (Oxford)* 2006;45-2:215-21.

9. Mitchell C, Adebajo A, Hay E, Carr A. Shoulder pain: diagnosis and management in primary care. *BMJ* 2005;331-7525:1124-8.

10. Minagawa H, Itoi E, Abe H, Fukuta M, Yamamoto N, Seki N, Kikuchi K. Epidemiology of rotator cuff tears. *J Jpn Orthop Assoc.* 2006;80-s217.

11. Yamamoto A, Takagishi K, Osawa T, Yanagawa T, Nakajima D, Shitara H, Kobayashi T. Prevalence and risk factors of a rotator cuff tear in the general population. *J Shoulder Elbow Surg* 2010;19-1:116-20.

12. Itoi E. Rotator cuff tear: physical examination and conservative treatment. *J Orthop Sci* 2013;18-2:197-204.

13. van der Windt DA, Thomas E, Pope DP, de Winter AF, Macfarlane GJ, Bouter LM, Silman AJ. Occupational risk factors for shoulder pain: a systematic review. *Occup Environ Med* 2000;57-7:433-42.

14. Harkness EF, Macfarlane GJ, Nahit ES, Silman AJ, McBeth J. Mechanical and psychosocial factors predict new onset shoulder pain: a prospective cohort study of newly employed workers. *Occup Environ Med* 2003;60-11:850-7.

15. Ruotolo C, Penna J, Namkoong S, Meinhard BP. Shoulder pain and the overhand athlete. *Am J Orthop (Belle Mead NJ)* 2003;32-5:248-58.

16. van der Windt DA, Koes BW, Boeke AJ, Deville W, De Jong BA, Bouter LM. Shoulder disorders in general practice: prognostic indicators of outcome. *Br J Gen Pract* 1996;46-410:519-23.

17. Chaudhury S, Gwilym SE, Moser J, Carr AJ. Surgical options for patients with shoulder pain. *Nat Rev Rheumatol* 2010;6-4:217-26.

18. Franceschi F, Ruzzini L, Longo UG, Martina FM, Zobel BB, Maffulli N, Denaro V. Equivalent clinical results of arthroscopic single-row and double-row suture anchor repair for rotator cuff tears: a randomized controlled trial. *Am J Sports Med* 2007;35-8:1254-60.
19. Ide J, Maeda S, Takagi K. A comparison of arthroscopic and open rotator cuff repair. *Arthroscopy* 2005;21-9:1090-8.
20. Klintberg IH, Gunnarsson AC, Svantesson U, Styf J, Karlsson J. Early loading in physiotherapy treatment after full-thickness rotator cuff repair: a prospective randomized pilot-study with a two-year follow-up. *Clin Rehabil* 2009;23-7:622-38.
21. Koo SS, Burkhart SS. Rehabilitation following arthroscopic rotator cuff repair. *Clin Sports Med* 2010;29-2:203-11, vii.
22. Saridakis P, Jones G. Outcomes of single-row and double-row arthroscopic rotator cuff repair: a systematic review. *J Bone Joint Surg Am* 2010;92-3:732-42.
23. Accousti KJ, Flatow EL. Technical pearls on how to maximize healing of the rotator cuff. *Instr Course Lect* 2007;56:3-12.
24. Bishop J, Klepps S, Lo IK, Bird J, Gladstone JN, Flatow EL. Cuff integrity after arthroscopic versus open rotator cuff repair: a prospective study. *J Shoulder Elbow Surg* 2006;15-3:290-9.
25. Boileau P, Brassart N, Watkinson DJ, Carles M, Hatzidakis AM, Krishnan SG. Arthroscopic repair of full-thickness tears of the supraspinatus: does the tendon really heal? *J Bone Joint Surg Am* 2005;87-6:1229-40.
26. Galatz LM, Ball CM, Teefey SA, Middleton WD, Yamaguchi K. The outcome and repair integrity of completely arthroscopically repaired large and massive rotator cuff tears. *J Bone Joint Surg Am* 2004;86-A-2:219-24.
27. Gazielly DF, Gleyze P, Montagnon C. Functional and anatomical results after rotator cuff repair. *Clin Orthop Relat Res* 1994-304:43-53.
28. Gerber C, Fuchs B, Hodler J. The results of repair of massive tears of the rotator cuff. *J Bone Joint Surg Am* 2000;82-4:505-15.
29. Harryman DT, 2nd, Mack LA, Wang KY, Jackins SE, Richardson ML, Matsen FA, 3rd. Repairs of the rotator cuff. Correlation of functional results with integrity of the cuff. *J Bone Joint Surg Am* 1991;73-7:982-9.
30. Vastamaki M, Lohman M, Borgmastars N. Rotator cuff integrity correlates with clinical and functional results at a minimum 16 years after open repair. *Clin Orthop Relat Res* 2013;471-2:554-61.
31. Bartolozzi A, Andreychik D, Ahmad S. Determinants of outcome in the treatment of rotator cuff disease. *Clin Orthop Relat Res* 1994-308:90-7.
32. Cofield RH, Parvizi J, Hoffmeyer PJ, Lanzer WL, Ilstrup DM, Rowland CM. Surgical repair of chronic rotator cuff tears. A prospective long-term study. *J Bone Joint Surg Am* 2001;83-A-1:71-7.
33. Goutallier D, Postel JM, Lavau L, Bernageau J. [Influence of muscular degeneration of the supra- and infra-spinatus on the prognosis of surgical repair of the rotator cuff]. *Acta Orthop Belg* 1998;64 Suppl 2:42-5.
34. Thomopoulos S, Soslowsky LJ, Flanagan CL, Tun S, Keefer CC, Mastaw J, Carpenter JE. The effect of fibrin clot on healing rat supraspinatus tendon defects. *J Shoulder Elbow Surg* 2002;11-3:239-47.
35. Uhthoff HK, Matsumoto F, Trudel G, Himori K. Early reattachment does not reverse atrophy and fat accumulation of the supraspinatus--an experimental study in rabbits. *J Orthop Res* 2003;21-3:386-92.

36. Nho SJ, Adler RS, Tomlinson DP, Allen AA, Cordasco FA, Warren RF, Altchek DW, MacGillivray JD. Arthroscopic rotator cuff repair: prospective evaluation with sequential ultrasonography. *Am J Sports Med* 2009;37-10:1938-45.
37. Bartl C, Kouloumentas P, Holzapfel K, Eichhorn S, Wortler K, Imhoff A, Salzmann GM. Long-term outcome and structural integrity following open repair of massive rotator cuff tears. *Int J Shoulder Surg* 2012;6-1:1-8.
38. Bartl C, Senftl M, Eichhorn S, Holzapfel K, Imhoff A, Salzmann G. Combined tears of the subscapularis and supraspinatus tendon: clinical outcome, rotator cuff strength and structural integrity following open repair. *Arch Orthop Trauma Surg* 2012;132-1:41-50.
39. Cho NS, Rhee YG. The factors affecting the clinical outcome and integrity of arthroscopically repaired rotator cuff tears of the shoulder. *Clin Orthop Surg* 2009;1-2:96-104.
40. Cole BJ, McCarty LP, 3rd, Kang RW, Alford W, Lewis PB, Hayden JK. Arthroscopic rotator cuff repair: prospective functional outcome and repair integrity at minimum 2-year follow-up. *J Shoulder Elbow Surg* 2007;16-5:579-85.
41. Fuchs B, Gilbart MK, Hodler J, Gerber C. Clinical and structural results of open repair of an isolated one-tendon tear of the rotator cuff. *J Bone Joint Surg Am* 2006;88-2:309-16.
42. Galatz LM, Griggs S, Cameron BD, Iannotti JP. Prospective longitudinal analysis of postoperative shoulder function : a ten-year follow-up study of full-thickness rotator cuff tears. *J Bone Joint Surg Am* 2001;83-A-7:1052-6.
43. Gulotta LV, Nho SJ, Dodson CC, Adler RS, Altchek DW, MacGillivray JD. Prospective evaluation of arthroscopic rotator cuff repairs at 5 years: part II--prognostic factors for clinical and radiographic outcomes. *J Shoulder Elbow Surg* 2011;20-6:941-6.
44. Gulotta LV, Nho SJ, Dodson CC, Adler RS, Altchek DW, MacGillivray JD. Prospective evaluation of arthroscopic rotator cuff repairs at 5 years: part I--functional outcomes and radiographic healing rates. *J Shoulder Elbow Surg* 2011;20-6:934-40.
45. Jost B, Pfirrmann CW, Gerber C, Switzerland Z. Clinical outcome after structural failure of rotator cuff repairs. *J Bone Joint Surg Am* 2000;82-3:304-14.
46. Klepps S, Bishop J, Lin J, Cahlon O, Strauss A, Hayes P, Flatow EL. Prospective evaluation of the effect of rotator cuff integrity on the outcome of open rotator cuff repairs. *Am J Sports Med* 2004;32-7:1716-22.
47. Koh KH, Laddha MS, Lim TK, Park JH, Yoo JC. Serial structural and functional assessments of rotator cuff repairs: do they differ at 6 and 19 months postoperatively? *J Shoulder Elbow Surg* 2012;21-7:859-66.
48. Meyer M, Klouche S, Rousselin B, Boru B, Bauer T, Hardy P. Does arthroscopic rotator cuff repair actually heal? Anatomic evaluation with magnetic resonance arthrography at minimum 2 years follow-up. *J Shoulder Elbow Surg* 2012;21-4:531-6.
49. Zumstein MA, Jost B, Hempel J, Hodler J, Gerber C. The clinical and structural long-term results of open repair of massive tears of the rotator cuff. *J Bone Joint Surg Am* 2008;90-11:2423-31.
50. Buess E, Steuber KU, Waibl B. Open versus arthroscopic rotator cuff repair: a comparative view of 96 cases. *Arthroscopy* 2005;21-5:597-604.
51. Colegate-Stone T, Allom R, Tavakkolizadeh A, Sinha J. An analysis of outcome of arthroscopic versus mini-open rotator cuff repair using subjective and objective scoring tools. *Knee Surg Sports Traumatol Arthrosc* 2009;17-6:691-4.
52. Walch G, Marechal E, Maupas J, Liotard JP. [Surgical treatment of rotator cuff rupture. Prognostic factors]. *Rev Chir Orthop Reparatrice Appar Mot* 1992;78-6:379-88.
53. Thomazeau H, Boukobza E, Morcet N, Chaperon J, Langlais F. Prediction of rotator cuff repair results by magnetic resonance imaging. *Clin Orthop Relat Res* 1997-344:275-83.

54. Yoo JC, Ahn JH, Koh KH, Lim KS. Rotator cuff integrity after arthroscopic repair for large tears with less-than-optimal footprint coverage. *Arthroscopy* 2009;25-10:1093-100.
55. Nho SJ, Brown BS, Lyman S, Adler RS, Altchek DW, MacGillivray JD. Prospective analysis of arthroscopic rotator cuff repair: prognostic factors affecting clinical and ultrasound outcome. *J Shoulder Elbow Surg* 2009;18-1:13-20.
56. van de Sande MA, de Groot JH, Rozing PM. Clinical implications of rotator cuff degeneration in the rheumatic shoulder. *Arthritis Rheum* 2008;59-3:317-24.
57. Tempelhof S, Rupp S, Seil R. Age-related prevalence of rotator cuff tears in asymptomatic shoulders. *J Shoulder Elbow Surg* 1999;8-4:296-9.
58. Lehman C, Cuomo F, Kummer FJ, Zuckerman JD. The incidence of full thickness rotator cuff tears in a large cadaveric population. *Bull Hosp Jt Dis* 1995;54-1:30-1.
59. Yamaguchi K, Ditsios K, Middleton WD, Hildebolt CF, Galatz LM, Teefey SA. The demographic and morphological features of rotator cuff disease. A comparison of asymptomatic and symptomatic shoulders. *J Bone Joint Surg Am* 2006;88-8:1699-704.
60. Mall NA, Kim HM, Keener JD, Steger-May K, Teefey SA, Middleton WD, Stobbs G, Yamaguchi K. Symptomatic progression of asymptomatic rotator cuff tears: a prospective study of clinical and sonographic variables. *J Bone Joint Surg Am* 2010;92-16:2623-33.
61. Goutallier D, Postel JM, Lavau L, Bernageau J. [Impact of fatty degeneration of the suparspinatus and infraspinatus msucles on the prognosis of surgical repair of the rotator cuff]. *Rev Chir Orthop Reparatrice Appar Mot* 1999;85-7:668-76.
62. Fuchs B, Weishaupt D, Zanetti M, Hodler J, Gerber C. Fatty degeneration of the muscles of the rotator cuff: assessment by computed tomography versus magnetic resonance imaging. *J Shoulder Elbow Surg* 1999;8-6:599-605.
63. Yamaguchi H SN, Oizumi N, Hosokawa Y, Kanaya F. Will Preoperative Atrophy and Fatty Degeneration of the Shoulder Muscles Improve after Rotator Cuff Repair in Patients with Massive Rotator Cuff Tears? *Advancs in Orthopedics* 2012.
64. Melis B, Wall B, Walch G. Natural history of infraspinatus fatty infiltration in rotator cuff tears. *J Shoulder Elbow Surg* 2010;19-5:757-63.
65. Gerber C, Schneeberger AG, Hoppeler H, Meyer DC. Correlation of atrophy and fatty infiltration on strength and integrity of rotator cuff repairs: a study in thirteen patients. *J Shoulder Elbow Surg* 2007;16-6:691-6.
66. Gladstone JN, Bishop JY, Lo IK, Flatow EL. Fatty infiltration and atrophy of the rotator cuff do not improve after rotator cuff repair and correlate with poor functional outcome. *Am J Sports Med* 2007;35-5:719-28.
67. Goutallier D, Postel JM, Bernageau J, Lavau L, Voisin MC. Fatty infiltration of disrupted rotator cuff muscles. *Rev Rhum Engl Ed* 1995;62-6:415-22.
68. Liem D, Lichtenberg S, Magosch P, Habermeyer P. Magnetic resonance imaging of arthroscopic supraspinatus tendon repair. *J Bone Joint Surg Am* 2007;89-8:1770-6.
69. Cheung S, Dillon E, Tham SC, Feeley BT, Link TM, Steinbach L, Ma CB. The presence of fatty infiltration in the infraspinatus: its relation with the condition of the supraspinatus tendon. *Arthroscopy* 2011;27-4:463-70.
70. Barry JJ, Lansdown DA, Cheung S, Feeley BT, Ma CB. The relationship between tear severity, fatty infiltration, and muscle atrophy in the supraspinatus. *J Shoulder Elbow Surg* 2013;22-1:18-25.
71. Demirag B, Sarisozen B, Ozer O, Kaplan T, Ozturk C. Enhancement of tendon-bone healing of anterior cruciate ligament grafts by blockage of matrix metalloproteinases. *J Bone Joint Surg Am* 2005;87-11:2401-10.

72. Sun L, Zhou X, Wu B, Tian M. Inhibitory effect of synovial fluid on tendon-to-bone healing: an experimental study in rabbits. *Arthroscopy* 2012;28-9:1297-305.
73. Nassos JT, ElAttrache NS, Angel MJ, Tibone JE, Limpisvasti O, Lee TQ. A watertight construct in arthroscopic rotator cuff repair. *J Shoulder Elbow Surg* 2012;21-5:589-96.
74. Beason DP, Connizzo BK, Dourte LM, Mauck RL, Soslowsky LJ, Steinberg DR, Bernstein J. Fiber-aligned polymer scaffolds for rotator cuff repair in a rat model. *Journal of shoulder and elbow surgery / American Shoulder and Elbow Surgeons [et al]* 2012;21-2:245-50.
75. Nixon AJ, Watts AE, Schnabel LV. Cell- and gene-based approaches to tendon regeneration. *Journal of shoulder and elbow surgery / American Shoulder and Elbow Surgeons [et al]* 2012;21-2:278-94.
76. Fessel G, Gerber C, Snedeker JG. Potential of collagen cross-linking therapies to mediate tendon mechanical properties. *J Shoulder Elbow Surg* 2012;21-2:209-17.
77. Bedi A, Fox AJ, Harris PE, Deng XH, Ying L, Warren RF, Rodeo SA. Diabetes mellitus impairs tendon-bone healing after rotator cuff repair. *J Shoulder Elbow Surg* 2010;19-7:978-88.
78. Frank C, McDonald D, Wilson J, Eyre D, Shrive N. Rabbit medial collateral ligament scar weakness is associated with decreased collagen pyridinoline crosslink density. *J Orthop Res* 1995;13-2:157-65.
79. Avery NC, Bailey AJ. The effects of the Maillard reaction on the physical properties and cell interactions of collagen. *Pathol Biol (Paris)* 2006;54-7:387-95.
80. Avery NC, Bailey AJ. Enzymic and non-enzymic cross-linking mechanisms in relation to turnover of collagen: relevance to aging and exercise. *Scand J Med Sci Sports* 2005;15-4:231-40.
81. Dean BJF, Franklin SL, Carr AJ. A systematic review of the histological and molecular changes in rotator cuff disease. *Bone and Joint Research* 2012;1-7:158-66.
82. Riley G. The pathogenesis of tendinopathy. A molecular perspective. *Rheumatology (Oxford)* 2004;43-2:131-42.
83. Kannus P, Jozsa L. Histopathological changes preceding spontaneous rupture of a tendon. A controlled study of 891 patients. *J Bone Joint Surg Am* 1991;73-10:1507-25.
84. Cook JL, Feller JA, Bonar SF, Khan KM. Abnormal tenocyte morphology is more prevalent than collagen disruption in asymptomatic athletes' patellar tendons. *J Orthop Res* 2004;22-2:334-8.
85. Riley G. Tendinopathy--from basic science to treatment. *Nature clinical practice. Rheumatology* 2008;4-2:82-9.
86. Jones GC, Corps AN, Pennington CJ, Clark IM, Edwards DR, Bradley MM, Hazleman BL, Riley GP. Expression profiling of metalloproteinases and tissue inhibitors of metalloproteinases in normal and degenerate human achilles tendon. *Arthritis and rheumatism* 2006;54-3:832-42.
87. Rees JD, Stride M, Scott A. Tendons - time to revisit inflammation. *Br J Sports Med* 2013.
88. Millar NL, Hueber AJ, Reilly JH, Xu Y, Fazzi UG, Murrell GA, McInnes IB. Inflammation is present in early human tendinopathy. *Am J Sports Med* 2010;38-10:2085-91.
89. Molloy TJ, Kemp MW, Wang Y, Murrell GA. Microarray analysis of the tendinopathic rat supraspinatus tendon: glutamate signaling and its potential role in tendon degeneration. *J Appl Physiol* 2006;101-6:1702-9.
90. Millar NL, Hueber AJ, Reilly JH, Xu Y, Fazzi UG, Murrell GAC, McInnes IB. Inflammation is present in early human tendinopathy. *The American journal of sports medicine* 2010;38-10:2085-91.

91. Millar NL, Wei AQ, Molloy TJ, Bonar F, Murrell GA. Cytokines and apoptosis in supraspinatus tendinopathy. *J Bone Joint Surg Br* 2009;91-3:417-24.
92. Matthews TJ, Hand GC, Rees JL, Athanasou NA, Carr AJ. Pathology of the torn rotator cuff tendon. Reduction in potential for repair as tear size increases. *J Bone Joint Surg Br* 2006;88-4:489-95.
93. Abrahams Y, Laguette MJ, Prince S, Collins M. Polymorphisms within the COL5A1 3'-UTR That Alters mRNA Structure and the MIR608 Gene are Associated with Achilles Tendinopathy. *Ann Hum Genet* 2013.
94. El Khoury L, Posthumus M, Collins M, Handley CJ, Cook J, Raleigh SM. Polymorphic variation within the ADAMTS2, ADAMTS14, ADAMTS5, ADAM12 and TIMP2 genes and the risk of Achilles tendon pathology: A genetic association study. *Journal of science and medicine in sport / Sports Medicine Australia* 2013.
95. Jarvinen TA, Kannus P, Maffulli N, Khan KM. Achilles tendon disorders: etiology and epidemiology. *Foot Ankle Clin* 2005;10-2:255-66.
96. Bavan L, Midwood K, Nanchahal J. MicroRNA epigenetics: a new avenue for wound healing research. *BioDrugs* 2011;25-1:27-41.
97. Knudsen HB, Gelineck J, Sojbjerg JO, Olsen BS, Johannsen HV, Sneppen O. Functional and magnetic resonance imaging evaluation after single-tendon rotator cuff reconstruction. *J Shoulder Elbow Surg* 1999;8-3:242-6.
98. Borgmastars N, Paavola M, Remes V, Lohman M, Vastamaki M. Pain relief, motion, and function after rotator cuff repair or reconstruction may not persist after 16 years. *Clin Orthop Relat Res* 2010;468-10:2678-89.
99. Wall ME, Banes AJ. Early responses to mechanical load in tendon: role for calcium signaling, gap junctions and intercellular communication. *J Musculoskelet Neuronal Interact* 2005;5-1:70-84.
100. Henry JA, Burugapalli K, Neuenschwander P, Pandit A. Structural variants of biodegradable polyesterurethane in vivo evoke a cellular and angiogenic response that is dictated by architecture. *Acta biomaterialia* 2009;5-1:29-42.
101. Scott A, Cook JL, Hart DA, Walker DC, Duronio V, Khan KM. Tenocyte responses to mechanical loading in vivo: a role for local insulin-like growth factor 1 signaling in early tendinosis in rats. *Arthritis Rheum* 2007;56-3:871-81.
102. Heinemeier KM, Kjaer M. In vivo investigation of tendon responses to mechanical loading. *J Musculoskelet Neuronal Interact* 2011;11-2:115-23.
103. Thornton GM, Hart DA. The interface of mechanical loading and biological variables as they pertain to the development of tendinosis. *J Musculoskelet Neuronal Interact* 2011;11-2:94-105.
104. Ricchetti ET, Aurora A, Iannotti JP, Derwin KA. Scaffold devices for rotator cuff repair. *Journal of shoulder and elbow surgery / American Shoulder and Elbow Surgeons [et al]* 2012;21-2:251-65.
105. Zhang X, Bogdanowicz D, Erisken C, Lee NM, Lu HH. Biomimetic scaffold design for functional and integrative tendon repair. *J Shoulder Elbow Surg* 2012;21-2:266-77.
106. Jayaraman K, Kotaki M, Zhang Y, Mo X, Ramakrishna S. Recent advances in polymer nanofibers. *J Nanosci Nanotechnol* 2004;4-1-2:52-65.
107. Bryers JD, Giachelli CM, Ratner BD. Engineering biomaterials to integrate and heal: the biocompatibility paradigm shifts. *Biotechnology and bioengineering* 2012;109-8:1898-911.
108. Chew SY, Wen Y, Dzenis Y, Leong KW. The role of electrospinning in the emerging field of nanomedicine. *Curr Pharm Des* 2006;12-36:4751-70.

109. Focarete ML, Gualandi C, Scandola M, Govoni M, Giordano E, Foroni L, Valente S, Pasquinelli G, Gao W, Gross RA. Electrospun scaffolds of a polyhydroxyalkanoate consisting of omega-hydroxylpentadecanoate repeat units: fabrication and in vitro biocompatibility studies. *J Biomater Sci Polym Ed* 2010;21-10:1283-96.
110. Huang D, Balian G, Chhabra AB. Tendon tissue engineering and gene transfer: the future of surgical treatment. *J Hand Surg Am* 2006;31-5:693-704.
111. Yin A, Zhang K, McClure MJ, Huang C, Wu J, Fang J, Mo X, Bowlin GL, Al-Deyab SS, El-Newehy M. Electrospinning collagen/chitosan/poly(L-lactic acid-co-epsilon-caprolactone) to form a vascular graft: mechanical and biological characterization. *J Biomed Mater Res A* 2013;101-5:1292-301.
112. Ayres CE, Jha BS, Sell SA, Bowlin GL, Simpson DG. Nanotechnology in the design of soft tissue scaffolds: innovations in structure and function. *Wiley Interdiscip Rev Nanomed Nanobiotechnol* 2010;2-1:20-34.
113. Barnes CP, Sell SA, Boland ED, Simpson DG, Bowlin GL. Nanofiber technology: designing the next generation of tissue engineering scaffolds. *Adv Drug Deliv Rev* 2007;59-14:1413-33.
114. Matthews JA, Wnek GE, Simpson DG, Bowlin GL. Electrospinning of collagen nanofibers. *Biomacromolecules* 2002;3-2:232-8.
115. Saino E, Focarete ML, Gualandi C, Emanuele E, Cornaglia AI, Imbriani M, Visai L. Effect of electrospun fiber diameter and alignment on macrophage activation and secretion of proinflammatory cytokines and chemokines. *Biomacromolecules* 2011;12-5:1900-11.
116. Hakimi O, Murphy R, Stachewicz U, Hislop S, Carr AJ. An electrospun polydioxanone patch for the localisation of biological therapies during tendon repair. *European cells & materials* 2012;24:344-57.
117. Chen JP, Chiang Y. Bioactive electrospun silver nanoparticles-containing polyurethane nanofibers as wound dressings. *J Nanosci Nanotechnol* 2010;10-11:7560-4.
118. Zhou Y, Yang H, Liu X, Mao J, Gu S, Xu W. Electrospinning of carboxyethyl chitosan/poly(vinyl alcohol)/silk fibroin nanoparticles for wound dressings. *Int J Biol Macromol* 2013;53:88-92.
119. Cao H, Marcy G, Goh EL, Wang F, Wang J, Chew SY. The effects of nanofiber topography on astrocyte behavior and gene silencing efficiency. *Macromol Biosci* 2012;12-5:666-74.
120. Jang JH, Castano O, Kim HW. Electrospun materials as potential platforms for bone tissue engineering. *Adv Drug Deliv Rev* 2009;61-12:1065-83.
121. Sell SA, McClure MJ, Ayres CE, Simpson DG, Bowlin GL. Preliminary Investigation of Airgap Electrospun Silk-Fibroin-Based Structures for Ligament Analogue Engineering. *J Biomater Sci Polym Ed* 2010.
122. Chainani A, Hippensteel KJ, Kishan A, Garrigues NW, Ruch DS, Guilak F, Little D. Multi-Layered Electrospun Scaffolds for Tendon Tissue Engineering. *Tissue Eng Part A* 2013.
123. Irie T, Majima T, Sawaguchi N, Funakoshi T, Nishimura S, Minami A. Biomechanical and histologic evaluation of tissue engineered ligaments using chitosan and hyaluronan hybrid polymer fibers: a rabbit medial collateral ligament reconstruction model. *J Biomed Mater Res A* 2011;97-2:111-7.
124. Majima T, Irie T, Sawaguchi N, Funakoshi T, Iwasaki N, Harada K, Minami A, Nishimura SI. Chitosan-based hyaluronan hybrid polymer fibre scaffold for ligament and tendon tissue engineering. *Proc Inst Mech Eng H* 2007;221-5:537-46.
125. Funakoshi T, Majima T, Iwasaki N, Suenaga N, Sawaguchi N, Shimode K, Minami A, Harada K, Nishimura S. Application of tissue engineering techniques for rotator cuff regeneration using a chitosan-based hyaluronan hybrid fiber scaffold. *Am J Sports Med* 2005;33-8:1193-201.

126. Mehta P, Patel P, Olver JM. Functional results and complications of Mersilene mesh use for frontalis suspension ptosis surgery. *Br J Ophthalmol* 2004;88-3:361-4.
127. Nada AN, Debnath UK, Robinson DA, Jordan C. Treatment of massive rotator-cuff tears with a polyester ligament (Dacron) augmentation: clinical outcome. *J Bone Joint Surg Br* 2010;92-10:1397-402.
128. Masata J, Martan A, Poislova M, Kobilkova J, Masatova D, Jedlickova A, Svabik K, Hubka P, Zvara K. A Comparison of the Incidence of Early Postoperative Infections between Patients Using Synthetic Mesh and Those Undergoing Traditional Pelvic Reconstructive Surgical Procedures. *Prague Med Rep* 2013;114-2:81-91.
129. Williams DF. On the mechanisms of biocompatibility. *Biomaterials* 2008;29-20:2941-53.
130. Milleret V, Simona B, Neuenschwander P, Hall H. Tuning electrospinning parameters for production of 3D-fiber-fleeces with increased porosity for soft tissue engineering applications. *Eur Cell Mater* 2011;21:286-303.
131. Sanders JE, Cassisi DV, Neumann T, Golledge SL, Zachariah SG, Ratner BD, Bale SD. Relative influence of polymer fiber diameter and surface charge on fibrous capsule thickness and vessel density for single-fiber implants. *J Biomed Mater Res A* 2003;65-4:462-7.
132. Sanders JE, Stiles CE, Hayes CL. Tissue response to single-polymer fibers of varying diameters: evaluation of fibrous encapsulation and macrophage density. *J Biomed Mater Res* 2000;52-1:231-7.
133. Garg K, Bowlin GL. Electrospinning jets and nanofibrous structures. *Biomicrofluidics* 2011;5-1:13403.
134. Hakimi O, Chaudhury S, Murphy R, Carr A. Differential growth on sutures of tendon cells derived from torn human rotator cuff. *Journal of Biomedical Materials Research Part B: Applied Biomaterials* 2012;100-3:685-92.
135. Yoon SJ, Kim SH, Ha HJ, Ko YK, So JW, Kim MS, Yang YI, Khang G, Rhee JM, Lee HB. Reduction of inflammatory reaction of poly(d,l-lactic-co-glycolic Acid) using demineralized bone particles. *Tissue Eng Part A* 2008;14-4:539-47.
136. Lendlein A, Langer R. Biodegradable, elastic shape-memory polymers for potential biomedical applications. *Science* 2002;296-5573:1673-6.
137. Blakney AK, Swartzlander MD, Bryant SJ. The effects of substrate stiffness on the in vitro activation of macrophages and in vivo host response to poly(ethylene glycol)-based hydrogels. *Journal of biomedical materials research. Part A* 2012;100-6:1375-86.
138. Malcarney HL, Bonar F, Murrell GA. Early inflammatory reaction after rotator cuff repair with a porcine small intestine submucosal implant: a report of 4 cases. *Am J Sports Med* 2005;33-6:907-11.
139. Walton JR, Bowman NK, Khatib Y, Linklater J, Murrell GAC. Restore orthobiologic implant: not recommended for augmentation of rotator cuff repairs. *The Journal of bone and joint surgery American volume* 2007;89-4:786-91.
140. Bostman O, Pihlajamaki H. Clinical biocompatibility of biodegradable orthopaedic implants for internal fixation: a review. *Biomaterials* 2000;21-24:2615-21.
141. Krishnan A, Siedlecki CA, Vogler EA. Mixology of protein solutions and the Vroman effect. *Langmuir* 2004;20-12:5071-8.
142. Krishnan A, Cha P, Liu YH, Allara D, Vogler EA. Interfacial energetics of blood plasma and serum adsorption to a hydrophobic self-assembled monolayer surface. *Biomaterials* 2006;27-17:3187-94.
143. Wilson CJ, Clegg RE, Leavesley DI, Pearcy MJ. Mediation of biomaterial-cell interactions by adsorbed proteins: a review. *Tissue Eng* 2005;11-1-2:1-18.

144. Wilson CJ, Clegg RE, Leavesley DI, Pearcy MJ. Mediation of Biomaterial–Cell Interactions by Adsorbed Proteins: A Review. *Tissue Engineering* 2005;11-1-2:1-18.
145. McNally AK, Jones JA, Macewan SR, Colton E, Anderson JM. Vitronectin is a critical protein adhesion substrate for IL-4-induced foreign body giant cell formation. *J Biomed Mater Res A* 2008;86-2:535-43.
146. Anderson JM, Rodriguez A, Chang DT. Foreign body reaction to biomaterials. *Seminars in immunology* 2008;20-2:86-100.
147. Smith MJ, Smith DC, White Jr KL, Bowlin GL. Immune response testing of electrospun polymers: an important consideration in the evaluation of biomaterials. *J Eng Fibers Fabrics* 2007.
148. Robbins Ca, ed. *Pathologic Basis of Disease.* 7 ed. Philadelphia: Elsevier Inc., 2005.
149. Broughton G, 2nd, Janis JE, Attinger CE. The basic science of wound healing. *Plast Reconstr Surg* 2006;117-7 Suppl:12S-34S.
150. Mantovani A, Sica A, Sozzani S, Allavena P, Vecchi A, Locati M. The chemokine system in diverse forms of macrophage activation and polarization. *Trends Immunol* 2004;25-12:677-86.
151. Mosser DM, Edwards JP. Exploring the full spectrum of macrophage activation. *Nat Rev Immunol* 2008;8-12:958-69.
152. Franz S, Rammelt S, Scharnweber D, Simon JC. Immune responses to implants - a review of the implications for the design of immunomodulatory biomaterials. *Biomaterials* 2011;32-28:6692-709.
153. Martinez FO. Regulators of macrophage activation. *Eur J Immunol* 2011;41-6:1531-4.
154. Martinez FO, Sica A, Mantovani A, Locati M. Macrophage activation and polarization. *Front Biosci* 2008;13:453-61.
155. Brown BN, Ratner BD, Goodman SB, Amar S, Badylak SF. Macrophage polarization: an opportunity for improved outcomes in biomaterials and regenerative medicine. *Biomaterials* 2012;33-15:3792-802.
156. Mitchell RN, ed. *Biomaterials Science: An Introduction to Materials in Medicine.* San Diego, CA: Elsevier Academic Press, 2004.
157. Kyriakides TR, Bornstein P. Matricellular proteins as modulators of wound healing and the foreign body response. *Thrombosis and haemostasis* 2003;90-6:986-92.
158. Anderson JM, McNally AK. Biocompatibility of implants: lymphocyte/macrophage interactions. *Semin Immunopathol* 2011;33-3:221-33.
159. Garg K, Pullen NA, Oskeritzian CA, Ryan JJ, Bowlin GL. Macrophage functional polarization (M1/M2) in response to varying fiber and pore dimensions of electrospun scaffolds. *Biomaterials* 2013;34-18:4439-51.
160. Seok J, Warren HS, Cuenca AG, Mindrinos MN, Baker HV, Xu W, Richards DR, McDonald-Smith GP, Gao H, Hennessy L, Finnerty CC, Lopez CM, Honari S, Moore EE, Minei JP, Cuschieri J, Bankey PE, Johnson JL, Sperry J, Nathens AB, Billiar TR, West MA, Jeschke MG, Klein MB, Gamelli RL, Gibran NS, Brownstein BH, Miller-Graziano C, Calvano SE, Mason PH, Cobb JP, Rahme LG, Lowry SF, Maier RV, Moldawer LL, Herndon DN, Davis RW, Xiao W, Tompkins RG. Genomic responses in mouse models poorly mimic human inflammatory diseases. *Proc Natl Acad Sci U S A* 2013;110-9:3507-12.
161. van der Worp HB, Howells DW, Sena ES, Porritt MJ, Rewell S, O'Collins V, Macleod MR. Can animal models of disease reliably inform human studies? *PLoS Med* 2010;7-3:e1000245.
162. Derwin KA, Baker AR, Iannotti JP, McCarron JA. Preclinical models for translating regenerative medicine therapies for rotator cuff repair. *Tissue engineering. Part B, Reviews* 2010;16-1:21-30.

163. Ni M, Lui PP, Rui YF, Lee YW, Lee YW, Tan Q, Wong YM, Kong SK, Lau PM, Li G, Chan KM. Tendon-derived stem cells (TDSCs) promote tendon repair in a rat patellar tendon window defect model. *J Orthop Res* 2012;30-4:613-9.
164. Funauchi M, Shimadsu H, Tamaki C, Yamagata T, Nozaki Y, Sugiyama M, Ikoma S, Kinoshita K. Role of endothelial damage in the pathogenesis of interstitial pneumonitis in patients with polymyositis and dermatomyositis. *J Rheumatol* 2006;33-5:903-6.
165. Holmdahl R, Lorentzen JC, Lu S, Olofsson P, Wester L, Holmberg J, Pettersson U. Arthritis induced in rats with nonimmunogenic adjuvants as models for rheumatoid arthritis. *Immunol Rev* 2001;184:184-202.
166. Nawabi DH, Gold S, Lyman S, Fields K, Padgett DE, Potter HG. MRI Predicts ALVAL and Tissue Damage in Metal-on-Metal Hip Arthroplasty. *Clin Orthop Relat Res* 2013.
167. Festing MF, Altman DG. Guidelines for the design and statistical analysis of experiments using laboratory animals. *ILAR J* 2002;43-4:244-58.
168. Festing MF. Inbred strains should replace outbred stocks in toxicology, safety testing, and drug development. *Toxicol Pathol* 2010;38-5:681-90.
169. Aurora A, Mesiha M, Tan CD, Walker E, Sahoo S, Iannotti JP, McCarron JA, Derwin KA. Mechanical characterization and biocompatibility of a novel reinforced fascia patch for rotator cuff repair. *Journal of biomedical materials research. Part A* 2011;99-2:221-30.
170. Zhou J, Yang Y, Yin X, Xu Y, Cao Y, Xu Q. The compatibility of swine BMDC-derived bile duct endothelial cells with a nanostructured electrospun PLGA material. *Int J Artif Organs* 2013;36-2:121-30.
171. Festing MF. Is the use of animals in biomedical research still necessary in 2002? Unfortunately, "yes". *Altern Lab Anim* 2004;32 Suppl 1B:733-9.
172. Festing MF. Improving toxicity screening and drug development by using genetically defined strains. *Methods Mol Biol* 2010;602:1-21.
173. Festing MF. Refinement and reduction through the control of variation. *Altern Lab Anim* 2004;32 Suppl 1A:259-63.
174. Festing MF. The choice of animal model and reduction. *Altern Lab Anim* 2004;32 Suppl 2:59-64.
175. Shaw R, Festing MF, Peers I, Furlong L. Use of factorial designs to optimize animal experiments and reduce animal use. *ILAR J* 2002;43-4:223-32.
176. Festing MF. The design and statistical analysis of animal experiments. *ILAR J* 2002;43-4:191-3.
177. Festing MF. Reduction in animal use in the production and testing of biologicals. *Dev Biol Stand* 1999;101:195-200.
178. Chen LE, Seaber AV, Urbaniak JR. Comparison of 10-0 polypropylene and 10-0 nylon sutures in rat arterial anastomosis. *Microsurgery* 1993;14-5:328-33.
179. Saxena S, Ray AR, Kapil A, Pavon-Djavid G, Letourneur D, Gupta B, Meddahi-Pelle A. Development of a new polypropylene-based suture: plasma grafting, surface treatment, characterization, and biocompatibility studies. *Macromol Biosci* 2011;11-3:373-82.
180. Festing MF. The choice of animals in toxicological screening: inbred strains and the factorial design of experiment. *Acta Zool Pathol Antverp* 1980-75:117-31.
181. Levine S, Sowinski R. Allergic inflammation, infarction and induced localization in the testis. *Am J Pathol* 1970;59-3:437-51.
182. Linington C, Berger T, Perry L, Weerth S, Hinze-Selch D, Zhang Y, Lu HC, Lassmann H, Wekerle H. T cells specific for the myelin oligodendrocyte glycoprotein mediate an unusual autoimmune inflammatory response in the central nervous system. *Eur J Immunol* 1993;23-6:1364-72.

183. Fournie GJ, Cautain B, Xystrakis E, Damoiseaux J, Mas M, Lagrange D, Bernard I, Subra JF, Pelletier L, Druet P, Saoudi A. Cellular and genetic factors involved in the difference between Brown Norway and Lewis rats to develop respectively type-2 and type-1 immune-mediated diseases. *Immunol Rev* 2001*;*184:145-60.
184. Gulotta LV, Kovacevic D, Packer JD, Deng X-H, Rodeo SA. Bone marrow-derived mesenchymal stem cells transduced with scleraxis improve rotator cuff healing in a rat model. *The American journal of sports medicine* 2011*;*39-6:1282-9.
185. Corona BT, Wu X, Ward CL, McDaniel JS, Rathbone CR, Walters TJ. The promotion of a functional fibrosis in skeletal muscle with volumetric muscle loss injury following the transplantation of muscle-ECM. *Biomaterials* 2013*;*34-13:3324-35.
186. Leigh DR, Mesiha M, Baker AR, Walker E, Derwin KA. Host response to xenograft ECM implantation is not different between the shoulder and body wall sites in the rat model. *Journal of orthopaedic research : official publication of the Orthopaedic Research Society* 2012.
187. Perlik F, Zidek Z. The susceptibility of several inbred strains of rats to adjuvant-induced arthritis and experimental allergic encephalomyelitis. *Z Immunitatsforsch Exp Klin Immunol* 1974*;*147-2:191-3.
188. Hu Y, Cheng W, Cai W, Yue Y, Li J, Zhang P. Advances in research on animal models of rheumatoid arthritis. *Clinical Rheumatology* 2012.
189. Gerwin N, Bendele AM, Glasson S, Carlson CS. The OARSI histopathology initiative - recommendations for histological assessments of osteoarthritis in the rat. *Osteoarthritis and cartilage / OARS, Osteoarthritis Research Society.* Vol. 18 Suppl 3, 2010:S24-34.
190. Derwin KA, Baker AR, Spragg RK, Leigh DR, Iannotti JP. Commercial extracellular matrix scaffolds for rotator cuff tendon repair. Biomechanical, biochemical, and cellular properties. *J Bone Joint Surg Am* 2006*;*88-12:2665-72.
191. Chaudhury S, Holland C, Thompson MS, Vollrath F, Carr AJ. Tensile and shear mechanical properties of rotator cuff repair patches. *J Shoulder Elbow Surg* 2012*;*21-9:1168-76.
192. Mescher AL, ed. *Junqueira's Basic Histology.* 13 ed: McGraw-Hill Companies

193. Gumina S, Campagna V, Ferrazza G, Giannicola G, Fratalocchi F, Milani A, Postacchini F. Use of platelet-leukocyte membrane in arthroscopic repair of large rotator cuff tears: a prospective randomized study. *J Bone Joint Surg Am* 2012*;*94-15:1345-52.
194. Antuna S, Barco R, Martinez Diez JM, Sanchez Marquez JM. Platelet-rich fibrin in arthroscopic repair of massive rotator cuff tears: a prospective randomized pilot clinical trial. *Acta Orthop Belg* 2013*;*79-1:25-30.
195. Weber SC, Kauffman JI, Parise C, Weber SJ, Katz SD. Platelet-rich fibrin matrix in the management of arthroscopic repair of the rotator cuff: a prospective, randomized, double-blinded study. *Am J Sports Med* 2013*;*41-2:263-70.
196. Ellera Gomes JL, da Silva RC, Silla LM, Abreu MR, Pellanda R. Conventional rotator cuff repair complemented by the aid of mononuclear autologous stem cells. *Knee Surg Sports Traumatol Arthrosc* 2012*;*20-2:373-7.
197. Gulotta LV, Rodeo SA. Growth factors for rotator cuff repair. *Clin Sports Med* 2009*;*28-1:13-23.
198. Ruiz-Moneo P, Molano-Munoz J, Prieto E, Algorta J. Plasma rich in growth factors in arthroscopic rotator cuff repair: a randomized, double-blind, controlled clinical trial. *Arthroscopy* 2013*;*29-1:2-9.

199. Zheng MH, Chen J, Kirilak Y, Willers C, Xu J, Wood D. Porcine small intestine submucosa (SIS) is not an acellular collagenous matrix and contains porcine DNA: possible implications in human implantation. *Journal of Biomedical Materials Research Part B: Applied Biomaterials* 2005;73-1:61-7.

200. Transvaginal Mesh Recall. Drugwatch, 2013.

201. Junge K, Rosch R, Krones CJ, Klinge U, Mertens PR, Lynen P, Schumpelick V, Klosterhalfen B. Influence of polyglecaprone 25 (Monocryl) supplementation on the biocompatibility of a polypropylene mesh for hernia repair. *Hernia* 2005;9-3:212-7.

202. Pihlajamaki H, Salminen S, Laitinen O, Tynninen O, Bostman O. Tissue response to polyglycolide, polydioxanone, polylevolactide, and metallic pins in cancellous bone: An experimental study on rabbits. *J Orthop Res* 2006;24-8:1597-606.

203. Wooley PH. The usefulness and the limitations of animal models in identifying targets for therapy in arthritis. *Best Pract Res Clin Rheumatol* 2004;18-1:47-58.

204. Perlik F, Zidek Z, Elis J. Adjuvant arthritis in Lewis and AVN inbred strain of rats. *Physiol Bohemoslov* 1975;24-6:555-7.

205. Postlethwait RW, Willigan DA, Ulin AW. Human tissue reaction to sutures. *Annals of surgery* 1975;181-2:144-50.

206. Dawson J, Fitzpatrick R, Carr A. Questionnaire on the perceptions of patients about shoulder surgery. *J Bone Joint Surg Br* 1996;78-4:593-600.

207. Jeon IH, Morrey BF, Sanchez-Sotelo J. Ulnar component surface finish influenced the outcome of primary Coonrad-Morrey total elbow arthroplasty. *Journal of shoulder and elbow surgery / American Shoulder and Elbow Surgeons ... [et al.]* 2012;21-9:1229-35.

208. Wiley KF, Ding K, Stoner JA, Teague DC, Yousuf KM. Incidence of pseudotumor and acute lymphocytic vasculitis associated lesion (ALVAL) reactions in metal-on-metal hip articulations: a meta-analysis. *The Journal of arthroplasty* 2013;28-7:1238-45.

209. Rajpura A, Porter ML, Gambhir AK, Freemont AJ, Board TN. Clinical experience of revision of metal on metal hip arthroplasty for aseptic lymphocyte dominated vasculitis associated lesions (ALVAL). *Hip international : the journal of clinical and experimental research on hip pathology and therapy* 2011;21-1:43-51.